NITROUS OXIDE PRODUCTION IN THE GRAND RIVER, ONTARIO, CANADA: NEW INSIGHTS FROM STABLE ISOTOPE ANALYSIS OF DISSOLVED NITROUS OXIDE

by

Simon J. Thuss

A thesis
presented to the University of Waterloo
in fulfilment of the thesis requirement for the degree of
Master of Science
in
Earth Sciences

Waterloo, Ontario, Canada, 2008

AUTHOR’S DECLARATION

I hereby declare that I am the sole author of this thesis. This is a true copy of the thesis, including any required final revisions, as accepted by my examiners.

I understand that my thesis may be made electronically available to the public.

ABSTRACT

Nitrous oxide (N_2O) is a powerful greenhouse gas, and its atmospheric concentration is increasing dramatically. N_2O is produced through the microbially-mediated processes of nitrification and denitrification. Since these processes have difference substrates and isotopic enrichment factors, stable isotope analysis ($\delta^{15}N$ and $\delta^{18}O$) of N_2O can be used to study the production of this important greenhouse gas.

Although production in rivers accounts for a significant portion of the global N_2O budget, the isotopic composition of N_2O from this source is poorly characterized. Most of the previous work using stable isotopes of N_2O has been conducted in terrestrial or oceanic environments, and only one published study has measured $\delta^{15}N$ and $\delta^{18}O$ of N_2O produced in a riverine environment. The purpose of this research project was to use stable isotope analysis to characterize the processes responsible for N_2O production in the Grand River, Ontario, Canada, and to determine the spatial and temporal variability of the isotopic composition of the N_2O flux.

To meet the study objectives, an offline "purge and trap" method was developed to collect and purify dissolved N_2O for stable isotope analysis. Using this method, $\delta^{15}N$ and $\delta^{18}O$ analysis of dissolved N_2O is possible for samples with concentrations as low as 6 nmol N_2O/L.

Due to the isotopic effects of gas exchange and the back flux of tropospheric N_2O, there is a complex relationship between the $\delta^{15}N$ and the $\delta^{18}O$ of source, dissolved, and emitted N_2O in aquatic environments. A simple box model (SIDNO – **S**table **I**sotopes of **D**issolved **N**itrous **O**xide) was developed to properly interpret isotopic data for dissolved N_2O. Using this model, it was determined that the isotopic composition of emitted N_2O is much more representative of N_2O production in aquatic environments than the isotopic composition of dissolved N_2O. If the concentration, $\delta^{15}N$ and $\delta^{18}O$ of dissolved N_2O are measured, the magnitude and isotopic composition of the N_2O flux can be calculated.

Sampling downstream of the major wastewater treatment plants (WWTPs) on the Grand River indicates that nitrification and denitrification in the river are strongly tied to diel changes in dissolved oxygen (DO) concentration. During the day, when DO concentrations are high, nitrification or nitrifier-denitrification is the dominant N_2O production pathway, with sediment denitrification also contributing to N_2O production. At night, when DO concentrations are low, denitrification in the sediments and at the sediment / water interface is the dominant production pathway. Using the SIDNO model, N_2O produced during the day was found to have a $\delta^{15}N$ of -22‰ and a $\delta^{18}O$ of 43‰. N_2O produced at night had a $\delta^{15}N$ of -30‰ and a $\delta^{18}O$ of 30‰. The isotopic composition of N_2O emitted from the Grand River is dominated by night-time production downstream of the Waterloo and Kitchener WWTPs during the summer. The flux and time weighted annual average isotopic composition of N_2O emitted from the Grand River is -18.5‰ and 32.7‰ for $\delta^{15}N$ and $\delta^{18}O$ respectively. These values are significantly more depleted than the only other published data for riverine N_2O production. If the Grand River is representative of global riverine N_2O production, these results will have significant implications for the global isotopic budget for atmospheric N_2O.

ACKNOWLEDGEMENTS

Thank you to Sherry Schiff for the great opportunity to be involved in this project, and for the valuable support and guidance that allowed me to successfully complete my degree.

Thank you to my thesis committee, Dr. Sherry Schiff, Dr. John Spoelstra, Dr. Ramon Aravena, and Dr. Bill Taylor, for their valuable critique and suggestions.

Thank you to John Spoelstra, Helen Baulch, Richard Elgood, Dave Snider, Maddy Rosamond, Heather Loomer, Krista Chomicki and Jason Venkiteswaran for the many stimulating theoretical and technical discussions which generated ideas to form the foundation of this project.

I am very grateful for the field and laboratory assistance provided by Richard Elgood, Maddy Rosamond, Marlin Rempel, Eric Thuss, Marilla Murray, Dave Snider, Krista Chomicki, Jason Venkiteswaran, Clarence Lo, Ryan Hutchins, Sandra Timsic, Silvia Adao, Sharon Joseph, Bonnie DeBaets, Jun Choo, Lisa Erven, Gao Chen and Tim Kuntz. Special thanks to Justin Harbin, whose help I neglected to mention during my defense.

I also thank the Grand River Conservation Authority and the Region of Waterloo for site and wastewater treatment plant access.

I would like to thank my wife Sarah, as well as my family and friends for everything they have done to support me throughout my educational career.

Funding for this project was provided by the Natural Sciences and Engineering Research Council of Canada (NSERC) through a Strategic grant to Dr. Sherry Schiff and a Canadian Graduate Scholarship (CGS) to Simon Thuss. This project was also supported through Environment Canada's Science Horizons Internship Program and the UW Work Placement program.

TABLE OF CONTENTS

TABLE OF CONTENTS (cont'd)

TABLE OF CONTENTS (cont'd)

LIST OF TABLES

LIST OF TABLES (Cont'd)

LIST OF TABLES (Cont'd)

LIST OF FIGURES

LIST OF FIGURES (Cont'd)

LIST OF FIGURES (Cont'd)

LIST OF FIGURES (Cont'd)

LIST OF FIGURES (Cont'd)

LIST OF FIGURES (Cont'd)

Chapter 1:
Introduction

1.1 Introduction

Global climate change is becoming a great concern. Anthropogenic emissions of greenhouse gases absorb long wave radiation reflected by the surface of the earth, trapping heat in the atmosphere (Harrington 1987). Nitrous oxide (N_2O) is a very potent greenhouse gas, with a global warming potential 310 times that of CO_2 over a 100 year timescale (Denman et al. 2007). N_2O is also a concern because it is destructive to stratospheric ozone and it has a 114 year lifetime in the atmosphere (Montzka et al. 1999).

The concentration of N_2O in the atmosphere has been steadily increasing over the last 250 years, from a pre-industrial concentration of 270 to 320 ppbv today, an increase of approximately 50 ppbv (Denman et al. 2007). Recently, the increase in N_2O concentration has been directly observed by GAGE/AGAGE atmospheric monitoring stations around the globe (Figure 1.1 – Prinn et al. 1990, Prinn et al. 2000). Tropospheric N_2O concentrations have been increasing linearly over the last three decades at a rate of approximately 0.26%/year (Denman et al. 2007).

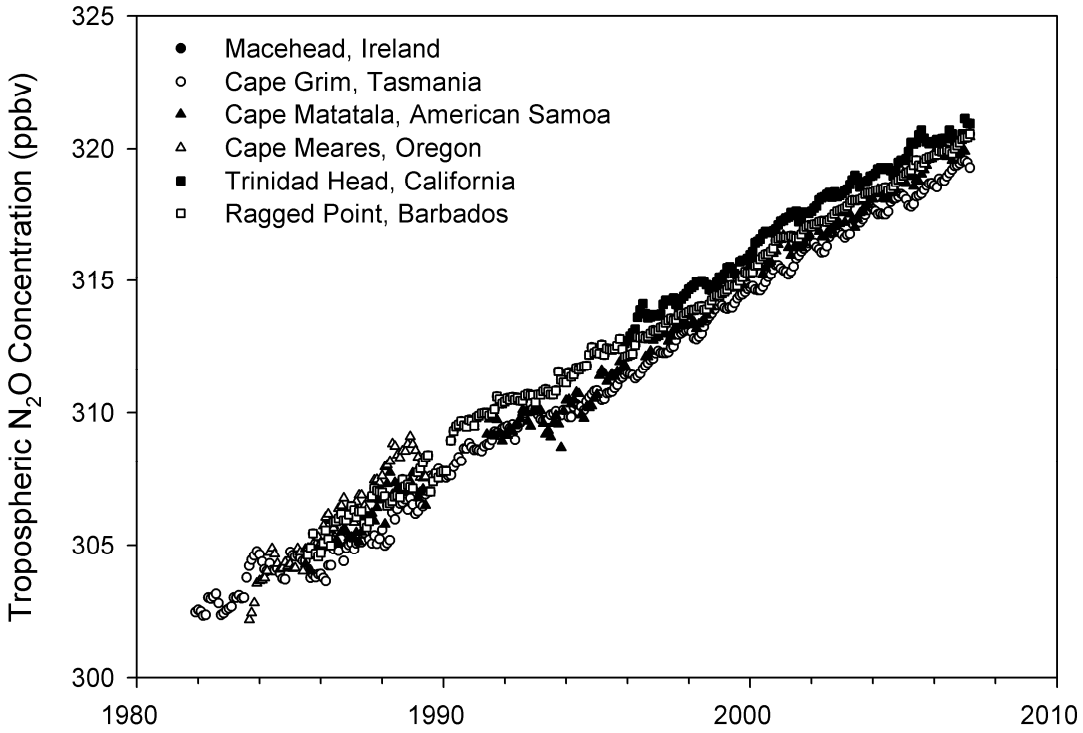

Figure 1.1: Average monthly tropospheric N_2O concentrations measured at GAGE/AGAGE stations, indicating an average annual increase of 0.26% yr^{-1} (Prinn et al 1990, Prinn et al 2000).

Globally, anthropogenic sources account for 6.7 Tg N/ year of the total 17.7 Tg N/year of N_2O emissions to the atmosphere. Currently, best estimates indicate that emissions from rivers, estuaries, and near shore marine environments account for 25% of the total anthropogenic source to the atmosphere (Denman et al. 2007). However, the uncertainty of this estimate is high, and the true value may range between 7% to 61% (Denman et al. 2007). Therefore, aquatic systems are quite important for the production of N_2O on a global scale. However, very little research has been done to study the processes responsible for N_2O production in these systems.

1.2 N_2O Production in the Nitrogen Cycle

Globally, approximately 65% of N_2O emissions are produced through microbial processes in soils (Bouwman 1990). Generally, these processes fall into two main categories, nitrification and denitrification. N_2O production during nitrification and denitrification was first described by a "leaky pipe" model (Firestone & Davidson 1989, Zafiriou 1990), where N_2O is a by-product (in the case of nitrification) or an intermediate (in the case of denitrification) of the major processes (Figure 1.2). This leaky pipe model may be an oversimplification of N_2O production in natural systems but it is a useful conceptual model.

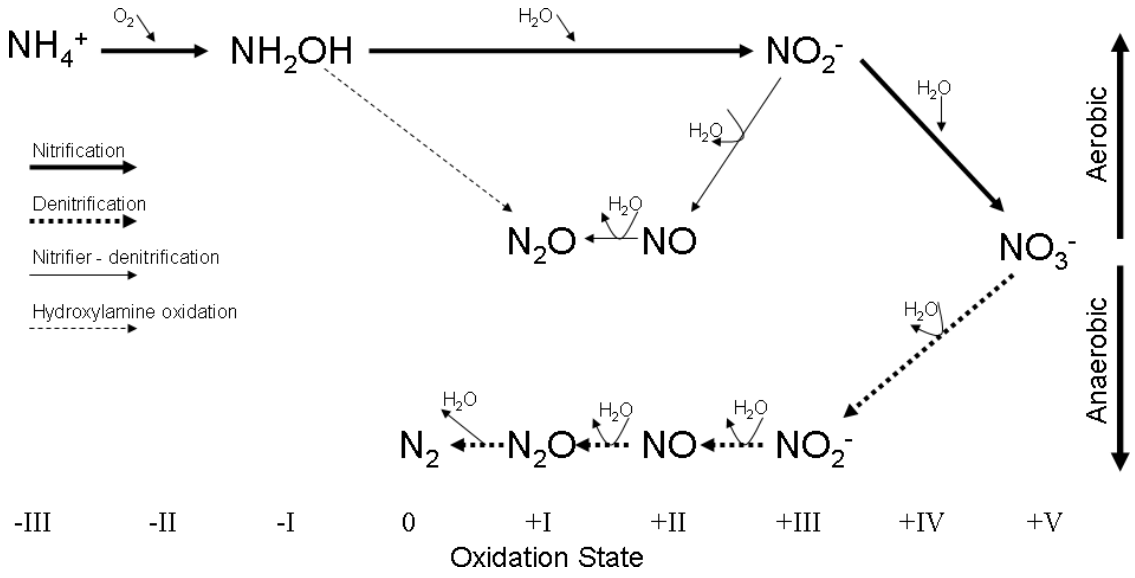

Figure 1.2: N_2O production in the nitrogen cycle. N_2O can be produced through both nitrification and denitrification. Oxygen isotopic exchange with water can occur at multiple locations in the cycle. The oxidation state of nitrogen throughout the cycle is shown on the bottom scale.

1.2.1 Nitrification

Nitrification is the aerobic oxidation of ammonium (NH_4^+) to produce nitrate (NO_3^-). The first part of nitrification is termed nitrosification, where NH_4^+ is oxidized to

form nitrite (NO_2^-) through a hydroxylamine (NH_2OH) intermediate. The NO_2^- is then excreted by the nitrosifying microorganisms and further oxidized by other microorganisms to produce NO_3^- in a process termed nitrite oxidation.

In most environments, nitrification is conducted by chemolithotrophic ammonium oxidizing bacteria and nitrite oxidizing bacteria (Hayatsu et al 2008) in order to provide energy for cell growth and metabolism. The ammonium oxidizing bacteria consist of three main genera (*Nitrosomonas, Nitrosopira, and Nitrosococcus*), while the major nitrite oxidizing bacteria belong to four genera (*Nitrobacter, Nitrospina, Nitrococcus, Nitrospira*).

Recently, research has shown that nitrification is carried out by a much more diverse set of microorganisms than previously thought. The enzyme necessary for nitrification (ammonia monooxygenase) has recently been discovered in archaeal microorganisms (Hayatsu et al 2008). For example Crenarchaeota have been shown to play a major role in oceanic nitrification (Venter et al. 2004). *Nitrosopumilus maritimus*, a chemolithoautotrophic species of Crenarchaeota, has been shown to use NH_4^+ as its sole energy source while maintaining a similar growth rate to nitrifying bacteria (Hayatsu et al. 2008). Additionally, nitrification may be carried out by heterotrophic bacteria and fungi, though in heterotrophic organisms nitrification does not yield energy and does not contribute to cell growth.

Although nitrifying microorganisms are generally slow growing, they have the ability to process large quantities of nitrogen in the environment, due to the high energy requirements for CO_2 fixation. For example, *Nitrosomonas* species process approximately 35 moles of NH_4^+ for every mole of CO_2 fixed (Sprent 1987).

N_2O is produced as a by-product of nitrification through two possible pathways. The first is through the oxidation of the NH_2OH intermediate. NH_2OH is the first reaction product during the oxidation of NH_4^+. During nitrification, most of the NH_2OH is further oxidized to produce NO_2^-. However, some of the NH_2OH is oxidized through a side reaction to produce N_2O. It is likely that N_2O is formed through the spontaneous decomposition of an unstable intermediate (HNO) during the oxidation of NH_2OH to form NO_2^- (Hayatsu et al 2008).

A second possible nitrification N_2O production pathway during nitrification has been termed "nitrifier – denitrification" in the literature. In this pathway, NH_4^+ is oxidized to form NO_2^-, but before it is excreted from the microbial cell, the NO_2^- is reduced to form N_2O. There is evidence that this reaction becomes favourable when the oxygen supply for nitrification becomes limited. Nitrifier –denitrification may also be used by microorganisms as a method to remove toxic NO_2^- from the cell (Cho et al 2006).

Nitrification can take place in a variety of environments, provided there is an adequate supply of NH_4^+ substrate and oxygen. Nitrification has been shown to increase in agricultural soils in response to fertilization events (Perez et al 2001). Nitrification also occurs in aquatic systems such as rivers, especially when stimulated by inputs of NH_4^+ from sources such as agriculture or municipal wastewater effluent (Garnier et al 2006, Garnier et al 2007). In most cases, nitrification can only take place when pH is greater than 6, however, some species of *Nitrosospira* may have adapted to grow in acidic soils, down to pH 3 (Hayatsu et al 2008).

1.2.2 Denitrification

Denitrification is the step-wise reduction of NO_3^- through NO_2^-, NO, N_2O and finally to N_2. N_2O is an obligate intermediate during this process, and therefore, denitrification has the potential to produce large quantities of N_2O (Bremner 1997).

As with nitrification, a diverse group of organisms have the ability to perform denitrification. Heterotrophic bacteria, including *Pseudomonas*, *Bacillus and Paracoccous* species, are responsible for much of the denitrification activity in soils (Bouman 1990). Many of these bacterial species are facultative aerobes, and only denitrify when oxygen becomes depleted (Bremner 1997). Often, the lack of oxygen triggers the production of denitrification enzymes in these microbes (Sprent 1987).

Many fungi species also contribute significantly to denitrification in nature, both aerobically and anaerobically (Hayatsu et al. 2008). These fungal species contain many of the same denitrifying enzymes that have been studied extensively in the heterotrophic denitrifying bacteria. For example, the fungal species *Fusarium oxysporum* and *Fusarium solani* have been shown to reduce nitrate and produce N_2O in cultures with low O_2 concentration (Hayatsu et al 2008).

Recently, it has been discovered that several archaea species, such as *Pyrobaculum aerophilum* and *Haloferax denitrificans* have the ability to denitrify (Cabello et al. 2004). However, there are differences between the archaea and bacteria species in terms of the structure and regulation of the denitrifying enzymes (Hayatsu et al 2008). The importance of archaeal microorganisms for denitrification in most natural systems is currently unknown (Hayatsu et al 2008).

Denitrifying bacteria and fungi are widely distributed in nature, and present in large numbers in most soils (Bremner 1997). As a result, denitrification nearly always takes place in NO_3^- containing soils when O_2 becomes limited (Bremner 1997).

During denitrification, the ratio of N_2:N_2O produced can vary widely depending on several factors, including soil pH, soil moisture content, redox potential, temperature, and NO_3^- and organic carbon concentration (Bouman 1990). Additionally, higher N_2:N_2O ratios can result from denitrification in soils if the N_2O is unable to escape from the system before it is reduced by other microbes (Bremner 1997). Some microbial organisms lack the ability to reduce N_2O to N_2; as a result more N_2O can be produced by such microbial communities (Bouman 1990). High levels of nitrate in the soil have been shown to inhibit the reduction of N_2O to N_2 (Bremner 1997). Therefore, the N_2:N_2O ratio is related to the overall level of anoxia in the system, with highly anoxic, low nitrate systems producing less N_2O than environments containing more oxygen and nitrate.

1.2.3 Abiotic Sources of N_2O in Soils.

Biological processes are by far the largest source of N_2O in nature; however, it is possible that some N_2O is produced through abiotic chemical reactions (Bouman 1990). One such reaction is the chemical decomposition of NH_2OH. As mentioned previously, NH_2OH is an intermediate species in the process of nitrification. Laboratory experiments have indicated that NH_2OH undergoes rapid decomposition in sterile soil to form N_2O and N_2 (Bremner 1997). However, there is no evidence that NH_2OH is released from microbial cells during nitrification, and it has not been measured in significant concentrations in natural soils. Therefore it is unlikely that chemical decomposition of NH_2OH is a significant source of N_2O in the environment (Bremner 1997).

A second abiotic process that produces N_2O is termed chemo-denitrification. This process occurs when NO_3^- in the soil reacts with organic compounds, in particular lignin and its breakdown products (Sprent 1987). This reaction forms unstable compounds that can abiotically decompose to form N_2O and other nitrogen compounds (Bouman 1990). The amount of N_2O that is produced through chemo-denitrification is small compared to the other products of this reaction, such as N_2 and NO (Bremner 1997). Also, it is unlikely that NO_3^- is present in sufficient concentrations for this reaction to be significant (Sprent 1987). If the rates of chemo-denitrification are high, it would be expected that the N_2:N_2O ratio would be much greater than in systems where the chemo-denitrification rate is insignificant. Since chemo-denitrification is a relatively slow process compared to biological denitrification, and the major products of this reaction are N_2 and NO, it is unlikely that chemo-denitrification contributes significantly to N_2O production in the environment.

1.3 Stable Isotope Fractionation Associated with N_2O Production

Stable isotope ratio analysis of N_2O provides insights into the processes responsible for its production. Stable isotope ratios can be determined for both nitrogen and oxygen atoms in the N_2O molecule. Nitrogen has two stable isotopes, ^{15}N and ^{14}N. ^{14}N is much more abundant and accounts for 99.632% of the nitrogen atoms in atmospheric N_2 (Kaiser 2002). Oxygen has three stable isotopes (^{18}O, ^{17}O, and ^{16}O). The relative abundances of these stable isotopes in ocean water are 0.201%, 0.038% and 99.761% respectively (Kaiser 2002).

Nitrogen and oxygen form N_2O molecules with different combinations of stable isotopes. The most common isotopologues of N_2O are: $^{14}N^{14}N^{16}O$, $^{15}N^{14}N^{16}O$, $^{14}N^{15}N^{16}O$, and $^{14}N^{14}N^{18}O$. The other isotopic combinations are statistically rare (Kaiser 2002).

Stable isotope data is usually expressed in delta (δ) notation in units of per mil (‰) according to Equation 1.1, where:

$$\delta = (R_{sample}/R_{standard} - 1) * 1000 \quad (1.1)$$

R_{sample} and $R_{standard}$ are the stable isotope ratios of the sample and standard, respectively. N_2O is introduced into an isotope ratio mass spectrometer (IRMS) under a vacuum and given a positive charge through ionization. The N_2O^+ is then focused into a beam and accelerated by an electric field. The beam is redirected by a magnetic field, causing it to split into several beams based on the mass/charge (m/z) ratio of the ions. The relative intensity of these beams is measured by Faraday cup detectors, with the intensity being a function of the abundance of the various isotopologues in the sample.

Both nitrogen and oxygen isotope ratios are changed during many important biological processes. Isotopic fractionation occurs when a particular elemental isotope is favoured in the products of a reaction (Kendall and Aravena 2000). Isotopic fractionation occurs in both reversible equilibrium and irreversible kinetic reactions. The fractionation associated with irreversible kinetic reactions is generally more important during low temperature biological reactions, and therefore dominates during the production of N_2O (Kendall and Aravena 2000). Kinetic fractionation factors are much more variable than equilibrium fractionation factors and depend heavily on the environmental conditions under which the reaction takes place (Kendall and Aravena 2000).

Generally speaking, for biologically facilitated kinetic reactions, compounds containing the lighter isotope react faster, and therefore the products of the reaction tend to have less of the heavy isotopes compared to the reactants (Kendall and Aravena 2000). For example, during the denitrification of nitrate to form N_2O, the $\delta^{15}N$ value of the N_2O that is formed is more negative than the original nitrate. For kinetic isotopic fractionation, an isotopic fractionation factor between the reaction product and substrate ($\alpha_{p\text{-}s}$) can be defined (Equation 1.2) (Kendall & Aravena 2000), where

$$\alpha_{p\text{-}s} = R_p/R_s \tag{1.2}$$

R_p and R_s are the stable isotope ratios of the reaction product and substrate, respectively.

Isotopic fractionation can also be expressed as a kinetic isotope enrichment factor ($\varepsilon_{p\text{-}s}$), (Equation 1.3) (Kendall & Aravena 2000).

$$\varepsilon_{p\text{-}s} = 1000 \text{ x } (\alpha_{p\text{-}s} - 1) \tag{1.3}$$

While the fractionation factor ($\alpha_{p\text{-}s}$) and the enrichment factor ($\varepsilon_{p\text{-}s}$) are the most accurate ways to express isotopic fractionation, occasionally in the published literature, these terms are approximated using Equation 1.4 (Kendall & Aravena 2000), where

$$\varepsilon_{p\text{-}s} \sim \Delta = \delta_p - \delta_s \tag{1.4}$$

δ_p and δ_s are the isotopic delta values in the product and substrate, respectively. When isotopic fractionation is small, Δ is a good approximation for ε, but the error associated with Δ increases when fractionation is large.

Many studies have reported isotopic fractionation factors associated with N_2O production through nitrification and denitrification (Table 1.1). In many cases, it is not clear whether the isotopic fractionation is reported as Δ or ε, therefore, a distinction is not made between the two in Table 1.1.

Organism or Community	Substrate	Product	ε or Δ (product - substrate) (‰) ^{15}N	^{18}O	Reference
Mineralization					
-	Organic N	NH_4^+	+/-1	-	Kendall 1998
Nitrification					
(observed range in field studies)	NH_4^+	NO_3^-	-12 to -29	-	Shearer and Kohl 1986, Kendall 1998
Nitrosomonas europaea	NH_4^+	NO_2^-	-32 to -37 -25 to -32	- -	Mariotti et al. 1981 Yoshida 1988
N_2O Production (Nitrifier - denitrification pathway)					
soil microbial community	NH_4^+	N_2O	-102 to -112	-	Perez et al. 2006
Nitrosomonas europaea	NH_4^+	N_2O	-47 -35 to -36	- -	Sutka et al. 2006 Yoshida 1988
Nitrosomonas europaea	NO_2^-	N_2O	-32 to -38	-	Sutka et al. 2003, 2004
Nitrosomonas multiformis	NO_2^-	N_2O	-24 to -25	-	Sutka et al. 2006
N_2O Production (Hydroxylamine oxidation pathway)					
Methylococcus capsulatus	NH_2OH	N_2O	0 to -3	-	Sutka et al. 2003, 2004
Methylosinus trichosporium	NH_2OH	N_2O	+4 to +8	-	Sutka et al. 2006
Nitrosomonas europaea	NH_2OH	N_2O	-20 to -32 -3 to +7	- -	Sutka et al. 2003, 2004 Sutka et al. 2006
Nitrosomonas multiformis	NH_2OH	N_2O	-1 to +5	-	Sutka et al. 2006
Denitrification					
soil microbial community	NO_3^-	N_2	-38 -14 to -23	- -	Tilsner et al. 2003 Blackmer and Bremner 1977
N_2O Production					
soil microbial community	NO_3^-	N_2O	-10 to -45 -24 to -29 -27 -16 -24 to -35	- -34 to -54 - -8 -	Perez et al. 2006 Menyailo and Hungate 2006 Wada et al. 1991 Schumidt and Voekelius 1989 Mariotti et al. 1981, 1982
soil microbial community	NO_2^-	N_2O	-9 to -37	-	Mariotti et al. 1982
Paracoccous denitrificans	NO_3^-	N_2O	-10 to -22 -24 to -33	+4 to +23 -	Toyoda et al. 2005 Barford et al. 1999
Pseudomonas aureofaciens	NO_3^-	N_2O	-37 -	- +40	Sutka et al. 2006 Casciotti et al. 2002
Pseudomonas chlororaphis	NO_3^-	N_2O	-13	-	Sutka et al. 2006
Pseudomonas fluorescens	NO_3^-	N_2O	-17 to -39 -33 to -37	-1 to +32 -	Toyoda et al. 2005 Yoshida 1988
N_2O Consumption					
soil microbial community	N_2O	N_2	-9 -6 to -10 -2 -4	-26 -13 to -25 -5 -11	Vieten et al. 2007 Menyailo and Hungate 2006 Mandernack et al. 2000 Schumidt and Voekelius 1989
Paracoccous denitrificans	N_2O	N_2	-7 to -19 -1 to -27	- -	Barford et al. 1999 Yoshida 1984
Pseudomonas aeruginosa	N_2O	N_2	-	-37 to -42	Wahlen and Yoshinari 1985a

Table 1.1: Isotopic fractionation factors for ^{15}N and ^{18}O available in the published literature.

1.3.1 Nitrification

All of the published data on isotopic fractionation associated with N_2O production through nitrification was obtained from laboratory incubation experiments using pure culture organisms (e.g. Sutka et al 2003, 2004, 2006), or soil microbial communities (Perez et al 2006). Therefore, since these are the only data available, researchers have attempted to apply these fractionation factors to observations made in field environments.

N_2O produced through nitrification tends to be very depleted in ^{15}N. Nitrogen enrichment factors for nitrification typically range from -47‰ to -20‰ (Table 1.1). However, Perez et al (2006) observed a very large fractionation (-112‰ to -102‰) in lab incubations of soils collected from the Brazilian Amazon. These very large nitrogen enrichment factors were obtained by mass balance calculations from various experimental treatments (where nitrification was inhibited or not inhibited). These extreme nitrogen enrichment factors for nitrification have not yet been confirmed by other lab or field studies.

Observed nitrogen enrichment factors for nitrifier-denitrification are generally greater than those observed for the hydroxylamine oxidation pathway (Table 1.1). In fact, several studies by Sutka et al (2003, 2004, 2006) have observed near zero or positive fractionation associated with the hydroxylamine oxidation pathway. The nitrogen fractionation factors associated with nitrification can be highly variable, depending largely on the metabolic pathway and the particular microorganisms involved.

There are very few data available on the oxygen isotopic composition of N_2O produced through nitrification. Historically, laboratory incubation studies have not reported the $\delta^{18}O$ of N_2O produced through nitrification. However, several field based

studies have measured and reported the $\delta^{18}O$-N_2O values. Wahlen & Yoshinari (1985a) observed a $\delta^{18}O$ of 24‰ for N_2O produced through nitrification in a manure-fertilized field. These same authors measured $\delta^{18}O$ of 23, 22, and 36‰ in N_2O produced through nitrification at a sewage treatment plant (Wahlen & Yoshinari 1985b). Perez et al (2001) measured $\delta^{18}O$ of N_2O ranging from 20.5 to 28.5‰ produced during nitrification in a Mexican agricultural field fertilized with 150 kg N/ha as urea. These published results indicate that the $\delta^{18}O$ of N_2O produced through nitrification is typically close to that of atmospheric oxygen ($\delta^{18}O - O_2 = 23.5‰$).

During nitrification of NH_4^+, the first oxygen atom added to form NH_2OH is obtained from atmospheric O_2 (Hollocher et al. 1981, Andersson & Hooper 1983). The two additional oxygen atoms needed to form NO_3^- are obtained from ambient water (Aleem et al. 1965, Andersson & Hooper 1983, Kumar et al. 1983, Hollocher 1984). Therefore, it is expected that NO_3^- produced through nitrification should have a $\delta^{18}O$ value that reflects a 1/3 contribution from atmospheric O_2 and a 2/3 contribution from ambient water. Given this relationship, the $\delta^{18}O$ of N_2O produced through nitrification should be different depending on whether the N_2O was produced through the hydroxylamine oxidation or nitrifier-denitrification pathway. The fact that the observed $\delta^{18}O - N_2O$ is typically similar to atmospheric O_2 during nitrification might suggest that hydroxylamine oxidation is the dominant pathway. However, there are several complicating factors. First, fractionation could occur during the cellular uptake of O_2 from the environment, and the $\delta^{18}O$ of NH_2OH should actually be greater than that of atmospheric O_2. Fractionation of O_2 during cellular uptake has been used as an indicator of respiration in aquatic environments (Venkiteswaran et al. 2007). Secondly, although

N_2O produced through the nitrifier-denitrification pathway incorporates some oxygen from ambient water (which would have a $\delta^{18}O$ much less than atmospheric O_2), a significant positive enrichment would be expected for ^{18}O as oxygen atoms are removed from NO_2^- to produce N_2O. This could theoretically produce N_2O that has a $\delta^{18}O$ value that is similar to atmospheric O_2 merely through coincidence. Lastly, recent research has shown that significant isotopic exchange of oxygen occurs between N_2O precursors and ambient water during nitrification and denitrification (Kool et al 2007). This exchange of oxygen atoms would alter the ^{18}O signature of the resulting N_2O, and make it very difficult to accurately determine the origin of the oxygen atoms.

1.3.2 Denitrification

As is the case with nitrification, all of the studies used to determine the isotopic fractionation effects associated with N_2O production through denitrification have been conducted using laboratory incubation experiments. Most of these studies have used pure cultures; however, several studies have used incubated soils containing natural microbial communities (Table 1.1), and thus may be more representative of the isotopic fractionation expected in the natural environment.

Generally, the nitrogen fractionation factors for N_2O produced through denitrification are less than those for nitrification. Typical values range from -30 to -9‰, though recently a few studies have observed values that fall outside this range (-45‰ Perez et al. 2006; -39‰, Toyoda et al. 2005; -37‰ Sutka et al. 2006). There is a great amount of variability in the nitrogen fractionation factors observed between different species in the pure culture incubation experiments. Therefore, the isotopic fractionation

associated with denitrification is highly dependent on the microbial species involved. Several recent studies (Hayatsu et al 2008, Irabar et al. 2008) have shown that the microbial communities responsible for denitrification in natural undisturbed environments are much more complex than previously thought, and that only a small fraction of the microorganisms present are able to be grown in laboratory cultures. This has implications for applying fractionation factors obtained through laboratory incubation studies to the field environment.

An additional complicating factor associated with laboratory incubation experiments is the fact that most of these studies used acetylene (C_2H_2) to inhibit nitrification and N_2O reduction to N_2. Although, in theory, the use of C_2H_2 should allow researchers to isolate N_2O production through denitrification, this situation is not representative of the natural environment and the effect on the observed isotopic fractionation is unknown. Also, the presence of C_2H_2 has been shown to enhance the chemical oxidation of NO ($2NO + O_2 \rightarrow NO_{2(g)}$) by at least three orders of magnitude when O_2 is present in trace concentrations (Bollmann & Conrad 1997a, Bollmann & Conrad 1997b, McKenney et al 1997). If this chemical oxidation artificially removes a significant amount of NO from the denitrification sequence, it could have a significant effect on the $\delta^{15}N$ and $\delta^{18}O$ of the N_2O produced.

In comparison to nitrogen fractionation, very little is known about oxygen fractionation effects during denitrification. Denitrification should have a very strong ^{18}O enrichment effect, because five oxygen atoms are removed for every molecule of N_2O produced. This should leave the remaining oxygen atoms very enriched in ^{18}O; however, for the few studies that have reported oxygen fractionation factors for denitrification, the

range in values is tremendous (-54 to +40‰ Table 1.1). The disparity between what is expected and the observed values can be explained by isotopic exchange of oxygen atoms between ambient water and N_2O precursors during denitrification (Kool et al 2007). Isotopic exchange of oxygen can readily occur during the NO_2^- to NO and NO to N_2O reduction steps, with exchange rates ranging from <10 to 100% (Kool et al. 2007). The isotopic exchange of oxygen alters the $^{18}O/^{16}O$ ratio in the N_2O that is produced, making it very difficult to use the $\delta^{18}O$ values to determine the source and processes involved in N_2O production. The degree of oxygen isotopic exchange has been shown to vary greatly depending on the microorganism and the type of denitrifying enzymes used (Kool et al 2007). Different microbial communities would likely facilitate different oxygen isotopic exchange rates, and produce N_2O with differing $\delta^{18}O$ values, even given identical environmental conditions and initial substrate compositions.

1.3.3 N_2O Consumption

Extracellular N_2O consumption (reduction to N_2), causes the $\delta^{15}N$ and $\delta^{18}O$ of N_2O produced by denitrification to become more enriched than that observed during laboratory incubation studies. Several published studies have attempted to quantify the isotopic fractionation associated with N_2O consumption using laboratory incubations (Table 1.1). Typically these experiments involve providing the microbial organisms with a N_2O substrate in the absence of oxygen, while monitoring the isotopic composition of the residual N_2O as it is reduced to N_2. The nitrogen and oxygen fractionation factors for N_2O consumption range from -27‰ to -1‰ and -5‰ to -42‰ respectively (Table 1.1). Although the range for these fractionation factors is quite large, several studies have

observed a relatively constant ratio of 1:2.5 for $\delta^{15}N$:$\delta^{18}O$ evolution during N_2O consumption (Vieten et al. 2007, Menyailo & Hungate 2006, Mandernack et al. 2000). This effect is analogous to the characteristic 2:1 enrichment observed for $\delta^{15}N$:$\delta^{18}O$ of residual NO_3^- during reduction by denitrification (Mariotti et al 1988, Böttcher et al 1990, Smith et al. 1991, Aravena & Robertson 1998, Cey et al. 1999, Mengis et al. 1999). Therefore, this relationship could potentially be used as a characteristic indicator of N_2O consumption in a natural system. Furthermore, since the characteristic ratios are different between N_2O consumption and NO_3^- substrate consumption, $\delta^{15}N$ and $\delta^{18}O$ values can be used to distinguish between these two processes, both of which can affect measured N_2O isotope ratios.

1.4 Field Studies using $\delta^{15}N$ and $\delta^{18}O$ of N_2O

There is a tremendous amount of scatter in the $\delta^{15}N$ and $\delta^{18}O$ values that have been measured for N_2O from various field environments (Figure 1.3). However, some generalizations can be made about the data. Most of the N_2O collected from terrestrial environments is more depleted with respect to ^{15}N and ^{18}O compared to the isotopic signature of tropospheric N_2O. Generally, the terrestrial N_2O isotopic data falls between -40‰ and +5‰ for $\delta^{15}N$ and +20‰ and +45‰ for $\delta^{18}O$, compared to the tropospheric N_2O composition of 6.72 (+/- 0.12)‰ and 44.62 (+/- 0.21)‰ for $\delta^{15}N$ and $\delta^{18}O$, respectively (Kaiser et al 2003). Most of the studies conducted in terrestrial environments have been in fertilized agricultural systems (Kim & Craig 1993, Well et al 2005, Yamulki et al 2001, Perez et al. 2001, Bol et al 2003, Tilsner 2003, Van Groenigen et al. 2005, Rock et al 2007), though some data has also been collected from natural forest soils (Kim

& Craig 1993, Perez et al 2000). There is not a clear distinction in the $\delta^{15}N$ and $\delta^{18}O$ values between samples collected from agricultural and natural soils.

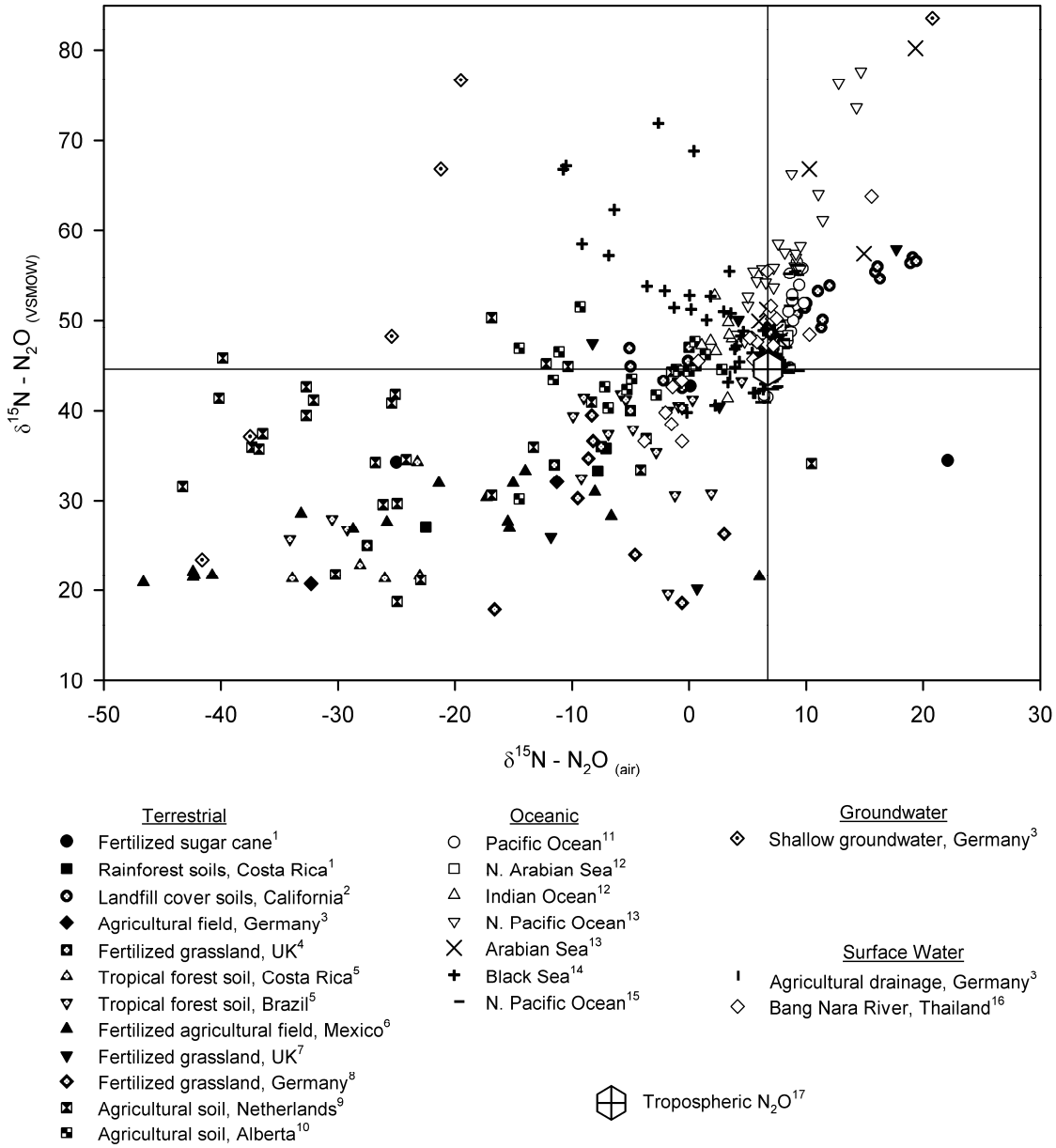

Figure 1.3: Summary of N_2O stable isotope data collected by various studies in terrestrial and aquatic environments. One point is an outlier, and did not fit on the scales of this plot (Shallow Groundwater, Germany[3] $\delta^{15}N$ = 86.1‰, $\delta^{18}O$ = 89.8‰). References: 1 – Kim & Craig (1993), 2 – Mandernack et al. (2000), 3 – Well et al. (2005), 4 – Yamulki et al. (2001), 5 – Perez et al. (2000), 6 – Perez et al. (2001), 7 – Bol et al. (2003), 8 – Tilsner et al (2003), 9 - Van Groenigen et al. (2005), 10 – Rock et al. (2007), 11 – Kim & Craig (1990), 12 – Naqvi et al (1998), 13 - Yoshanari et al (1997), 14 – Westley et al (2006), 15 - Dore et al. (1998), 16 – Boontanon et al. (2000), 17 – Kaiser et al. (2003)

In contrast, N_2O stable isotope data collected from aquatic environments tends to be enriched with respect to ^{15}N and ^{18}O compared to the values for tropospheric N_2O (Kaiser et al 2003). Again, there is a great amount of scatter in the aquatic N_2O data, with $\delta^{15}N$ generally ranging between -5‰ and +20‰, and $\delta^{18}O$ generally ranging between +40‰ and +80‰. Most of the aquatic N_2O studies have been conducted in marine environments (Kim & Craig 1990, Naqvi et al 1998, Yoshanari et al 1997, Westley et al 2006, Dore et al 1998). Most of the data from marine samples have $\delta^{15}N$ and $\delta^{18}O$ values that are very similar to the values for tropospheric N_2O (Kaiser et al 2003). This is likely due to the isotopic effects of gas exchange with the atmosphere and low ambient N_2O concentrations in near surface ocean samples (e.g. 118% saturation in the Black Sea, Westley et al. 2006).

The one study that measured $\delta^{15}N$ and $\delta^{18}O$ of N_2O dissolved in groundwater reported very wide ranging values. Well et al (2005) measured the stable isotope composition of N_2O dissolved in shallow groundwater beneath an experimental agricultural plot in Germany. The researchers observed $\delta^{15}N$ values ranging between -41.6‰ and +86.1‰, and $\delta^{18}O$ values ranging between 23.4‰ and 89.8‰. This extremely wide data range has not been observed in any other field sites.

There is currently only one published study that measured the isotopic ratios of dissolved N_2O produced in a river (Boontanon et al 2000). These researchers measured the $\delta^{15}N$ and $\delta^{18}O$ of N_2O in the Bang Nara River in Thailand on several occasions between November 1997 and January 1998. They observed $\delta^{15}N$ values ranging between -3.8‰ and 15.6‰ and $\delta^{18}O$ values ranging between 36.6‰ and 63.8 ‰. Boontanon et al (2000) observed a change in both $\delta^{15}N$ and $\delta^{18}O$ values with time in their study. Initially,

the values were enriched in to ^{15}N and ^{18}O compared to tropospheric N_2O. However, partway through the study the values became more depleted, before returning to the enriched values. The authors attributed this change in $\delta^{15}N$ and $\delta^{18}O$ to a change from N_2O production through denitrification to production through nitrification. However, this conclusion is not consistent with other studies (Perez et al 2001, Bol et al 2003), which have shown that the $\delta^{15}N$ and $\delta^{18}O$ values of N_2O produced through nitrification are usually much lower than the values observed by Boontanon et al. (2000).

Several studies have also used $\delta^{15}N$ and $\delta^{18}O$ of N_2O to distinguish between nitrification and denitrification in field environments. For example, Perez et al (2001) measured the $\delta^{15}N$ and $\delta^{18}O$ of N_2O, NH_4^+ and NO_3^- in agricultural soils following fertilization and irrigation. These researchers found that the observed instantaneous ^{15}N enrichment factor between N_2O and its precursors (NH_4^+ and NO_3^-) was a good indicator of nitrification and denitrification, and closely matched values obtained from laboratory studies (Table 1.1). Bol et al (2003) measured the $\delta^{15}N$ and $\delta^{18}O$ of N_2O produced from a grassland soil in the UK after an application of fertilizer. The authors of this study also measured the N_2O/N_2 production ratio, and used this data to identify three phases of N_2O production (phase 1, nitrification > denitrification; phase 2 denitrification > nitrification; phase 3, denitrification >> nitrification). Bol et al. (2003) found that the $\delta^{15}N$ and $\delta^{18}O$ data independently confirmed this conclusion, as the $\delta^{15}N$ and $\delta^{18}O$ values increased as N_2O production became dominated by denitrification rather than nitrification.

Although some studies have had success in distinguishing nitrification from denitrification using $\delta^{15}N$ and $\delta^{18}O$ of N_2O, the large range in ^{15}N and ^{18}O enrichment factors for nitrification and denitrification (Table 1.1) can lead to ambiguous results. For

example Tilsner et al. (2003) measured N_2O produced by grassland soils in Bavaria, Germany, both before and after application of organic and mineral fertilizers. These authors observed a large amount of scatter in the $\delta^{15}N$ and $\delta^{18}O$ values, and were not able to use the isotopic data to determine the dominant N_2O production process. The authors attributed scatter in the data to a high spatial heterogeneity in N_2O production processes in the soil. However, using laboratory incubations of the same soil, Tilsner et al. (2003) were able to determine that denitrification was likely the dominant N_2O production process at the site.

1.5 Research Objectives

The primary goal of this thesis project was to characterize N_2O production in the Grand River, Ontario, Canada, in terms of dominant production pathways and isotopic composition of the N_2O produced. This was achieved through the stable isotope analysis of dissolved N_2O, NO_3^- and NH_4^+. To achieve this goal, four main objectives were addressed.

The first objective was to develop a method to measure the stable isotope ratio of dissolved N_2O. Although there are several online methods available in the literature (e.g. Ostrom et al 2000, Westley et al 2006), these methods were not practical for this study due to the large sample processing time and the requirement for a dedicated mass spectrometer. Therefore, a new offline method was developed and tested to ensure accuracy for isotopic analysis of dissolved N_2O.

The second objective was to develop a computer model to simulate the stable isotope dynamics of dissolved N_2O in systems that are open to gas exchange with the

atmosphere. Since N_2O is highly soluble, the invasion of N_2O from the atmosphere has a significant effect on the $\delta^{15}N$ and $\delta^{18}O$ of dissolved N_2O, especially when the dissolved concentrations approach equilibrium saturated conditions. Additionally, there are kinetic and equilibrium fractionation factors for nitrogen and oxygen during N_2O gas exchange with the atmosphere. As a result, the relationship between the $\delta^{15}N$ and $\delta^{18}O$ values of dissolved N_2O, produced N_2O, and emitted N_2O is not simple. A box model was created using Stella modeling software to elucidate this relationship.

The third objective was to determine the dominant N_2O production processes in the Grand River, making use of stable isotope analysis of N_2O, NO_3^- and NH_4^+. From previous work and continuous monitoring by the Grand River Conservation Authority (GRCA), it was known that the concentration of dissolved oxygen (DO) in the river follows strong diel cycles during the summer months. Other studies (Clough et al 2007, Harrison et al 2005) have shown that nitrogen cycling processes and N_2O production can be influenced by the diel oxygen cycle. It was therefore expected that N_2O production in the Grand River would also be affected by the diel DO cycle. By monitoring the concentrations of DO, N_2O, NO_3^-, NH_4^+ and N_2, it was possible to examine how nitrification and denitrification respond to the DO concentration in the river. The N_2O stable isotope model developed earlier was then used to determine in-situ enrichment factors for N_2O production through nitrification and denitrification.

The fourth objective was to fully characterize the isotopic composition of N_2O emitted from the Grand River to the atmosphere. Since many other studies have observed a wide range in the $\delta^{15}N$ and $\delta^{18}O$ values of N_2O produced in field environments (Figure 1.3), it was expected that the isotopic composition of the N_2O flux would be variable,

both spatially and temporally. Currently there is very little known about the isotopic composition of N_2O produced in riverine systems. Current estimates indicate that the N_2O emissions from rivers, estuaries and costal zones total 1.7 Tg N/year globally, and may be as high as 2.9 Tg N/year (Denman et al. 2007). This compares to the global anthropogenic N_2O source of 6.7 Tg N/year, and the total global N_2O emission rate of 17.7 Tg N/year (Denman et al. 2007). In spite of the relative importance of this N_2O source, only one published study has measured the isotopic composition of dissolved N_2O in a river (Boontanon et al 2000). Isotopic models can be used to determine the relative importance of various sources of N_2O to the atmosphere (Rahn & Wahlen 2000). Since rivers are an important source of N_2O to the atmosphere, it is necessary to characterize the isotopic composition of this source in order to refine the global N_2O budget, and determine the true contribution of riverine N_2O to the total global emissions.

Chapter 2:

Site Description and Methodology

2.1 Grand River Watershed

The Grand River is the largest river in southern Ontario. It is approximately 300 km long, and drains an area of 7000 km^2 into Lake Erie (Figure 2.1). As of 2001, approximately 720 000 people were living in the basin; this figure is projected to increase to 1 220 000 by 2031 (Table 2.1). The cities of Waterloo, Kitchener, Cambridge and Guelph form the urban centre of the watershed, accounting for approximately 72% of the total basin population. Projected growth in the Region of Waterloo is expected to be particularly extensive, with the population expanding by approximately 60% by 2031 (Table 2.1). The Grand River is an important source of drinking water, supplying approximately 500 000 people in the watershed.

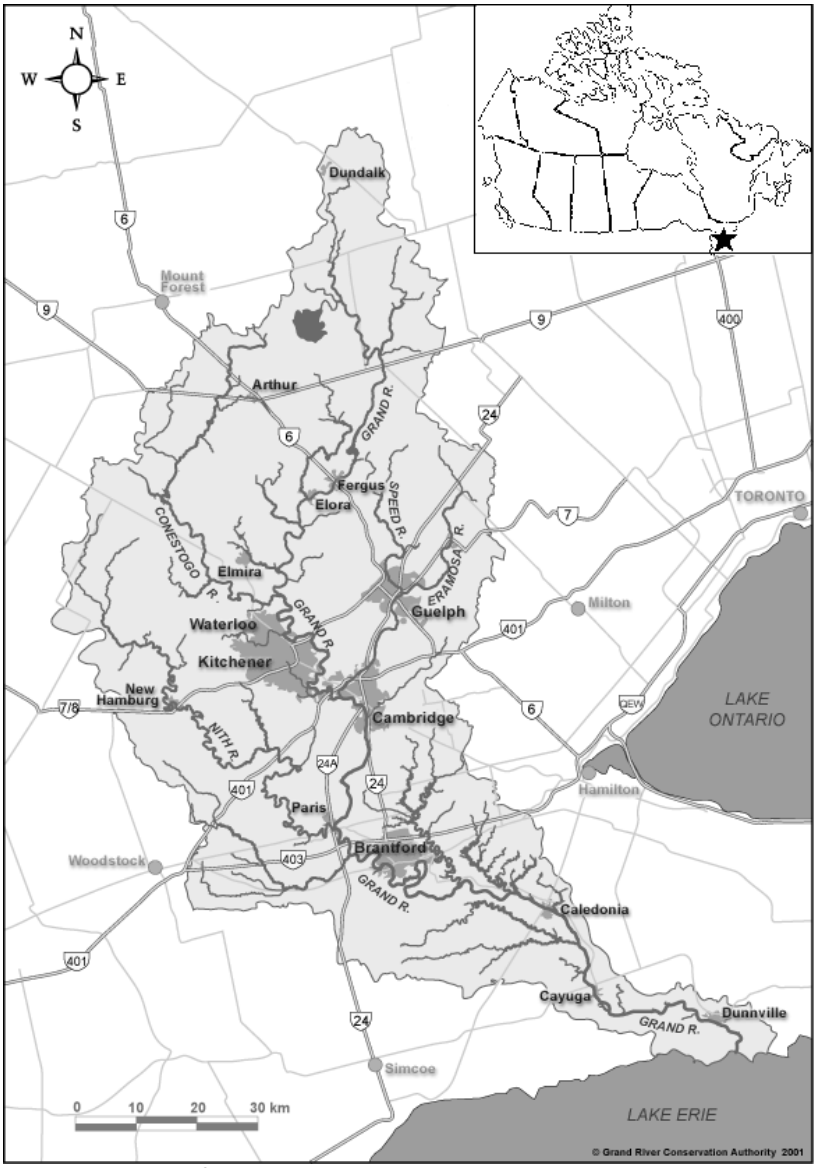

Figure 2.1: Map of the Grand River Watershed.

	Projected Population (000's)			
	2001	**2011**	**2021**	**2031**
Wellington County	85	91	269	321
City of Guelph	110	132		
Region of Waterloo	456	526	623	729
Brant County	35	39	157	173
City of Brantford	94	102		
Total	**780**	**890**	**1,049**	**1,223**

Table 2.1: Projected population growth in the Grand River Watershed (Ministry of Public Infrastructure Renewal, 2006)

The Grand River is heavily impacted by both diffuse and point-source inputs of nitrogen. Agriculture is the primary land use in the watershed, and 26 wastewater treatment plants (WWTPs) currently discharge effluent to the Grand River or its tributaries. Six of these WWTPs are required to report discharge data to the Federal National Pollutant Release Inventory (Table 2.2, NPRI 2007). Of these six, the Kitchener and Waterloo WWTPs contribute approximately 30% of the total WWTP nitrogen load to the river. Of all the WWTPs, the Kitchener plant releases the most NH_4^+ to the river, 74% of the total.

WWTP	Mass Discharged through Effluent			
	NH_4^+ tonnes/yr	NO_3^- tonnes/yr	PO_4^{3-} tonnes/yr	Total N tonnes/yr
Waterloo	77.8	196.4	-	274.2
Kitchener	633.8	35.3	-	669.1
Galt	2.2	242	-	244.2
Preston	3.5	42.3	-	45.8
Guelph	6.3	1831	4.3	1837.3
Brantford	134.9	55.4	5.2	190.3
Total	**858.5**	**2402.4**	**9.5**	**3260.9**

Table 2.2: Mass of nitrogen and phosphorous pollutants released by WWTP effluent in the Grand River Watershed. Data provided by NPRI (2007).

Downstream of the urban centre, the river is overwhelmed by the input of nutrients, and there is heavy macrophyte growth in the channel. The heavy macrophyte growth contributes to very large diel swings in dissolved oxygen (DO) concentration, especially during the hot summer months. During the summer months, night-time DO concentrations at this location often fall below the water quality target of 4 mg/L set by the Grand River Conservation Authority. This DO problem is further compounded by the fact that the effluent from the Kitchener and Waterloo WWTPs contain high

concentrations of ammonium (NH_4^+). These two major WWTPs are not designed to nitrify the effluent within the plant, and instead rely on the river to oxidize the NH_4^+ to nitrate (NO_3^-). Nitrification of WWTP derived NH_4^+ further consumes the limited DO in the river and contributes to poor river health.

2.1.1 Climate

The Grand River Watershed is located within the Warm Summer Continental (Dfb) Köppen climatic region (Ackerman 1941). Typical monthly mean temperatures and precipitation amounts for the Grand River Basin are summarized in Figure 2.2. These values are based on 30 year historical weather data collected at the Waterloo Wellington Airport (43°27'20.09"N, 80°23'08.29"W). The data was supplied by Environment Canada (2004).

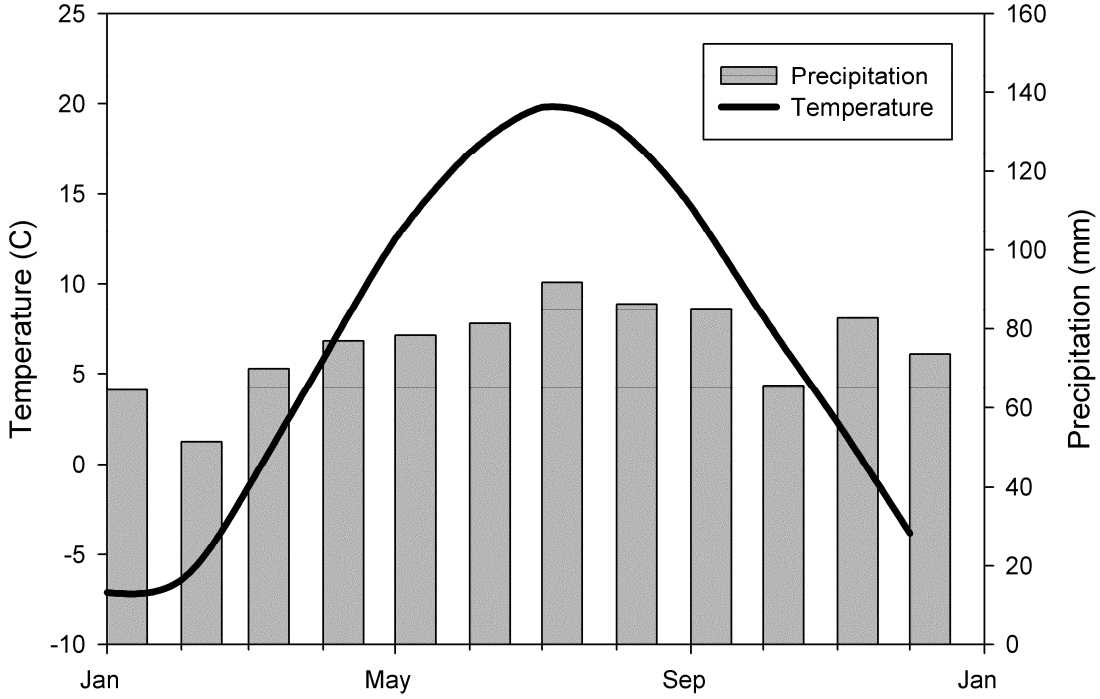

Figure 2.2: 30 Year Climate history as recorded at Waterloo – Wellington Airport

During the study period (May 2006 to May 2008), there were several periods where the weather in the basin deviated significantly from the 30 year climate average. Figure 2.3 illustrates the recorded monthly mean daily temperature as compared to the 30 year average over the course of this study. The temperature data was recorded at the University of Waterloo weather station (43°28'24.58"N, 80°33'25.95"W). Data from the University of Waterloo weather station was used because recent data is easily accessible, though the station lacks a long-term historical record. There were several periods where the mean monthly temperature was significantly higher than normal, especially the summer and early winter in 2006 (Figure 2.3). February 2007 was significantly colder than normal. Temperatures otherwise closely followed the 30-year monthly mean.

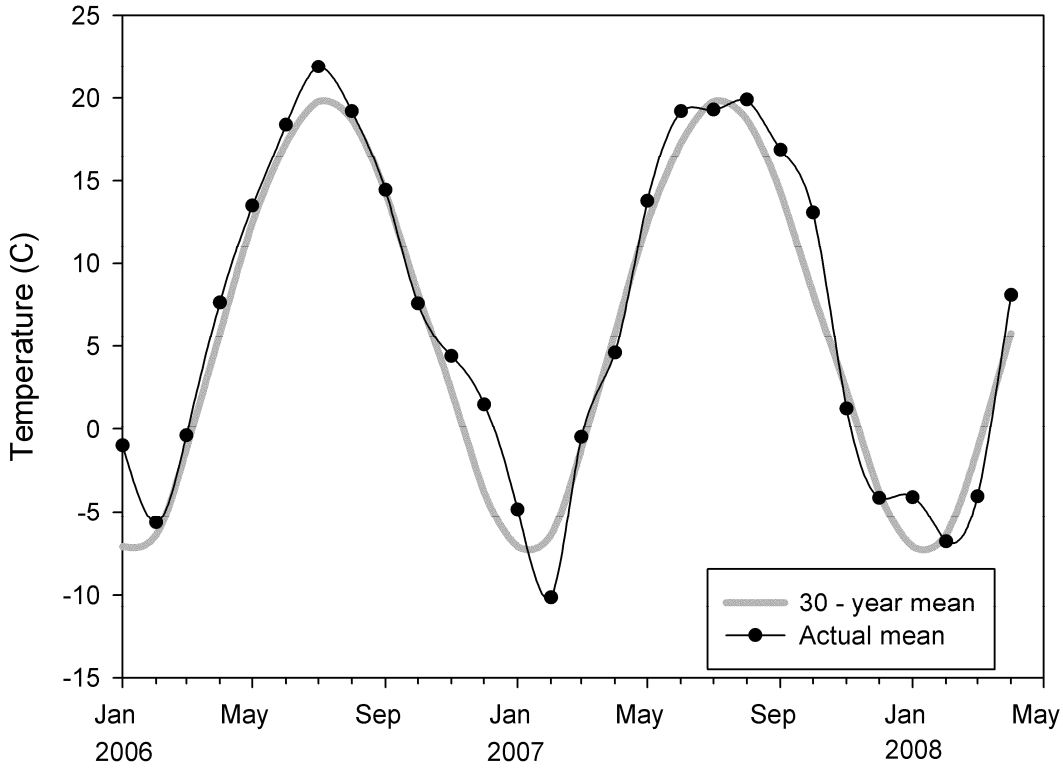

Figure 2.3: Monthly mean daily temperature data, as recorded at the University of Waterloo weather station. The 30 – year monthly mean data was collected at the Waterloo-Wellington airport.

Figure 2.4 is a plot of the total monthly precipitation measured at the University of Waterloo weather station over the course of this study (May 2006 to May 2008). As indicated, precipitation patterns were quite variable during this time period. Several months during 2006 recorded significantly higher amounts of precipitation compared to the 30 year monthly mean (Figure 2.4). Also, the summer and fall of 2007 were significantly drier than normal. The below normal precipitation led to very low flow conditions during this time period. Above normal amounts of precipitation fell during the winter of 2007-2008. The bulk of this precipitation fell as snow, and led to large snowmelt events during two major thaw periods in January and April 2008.

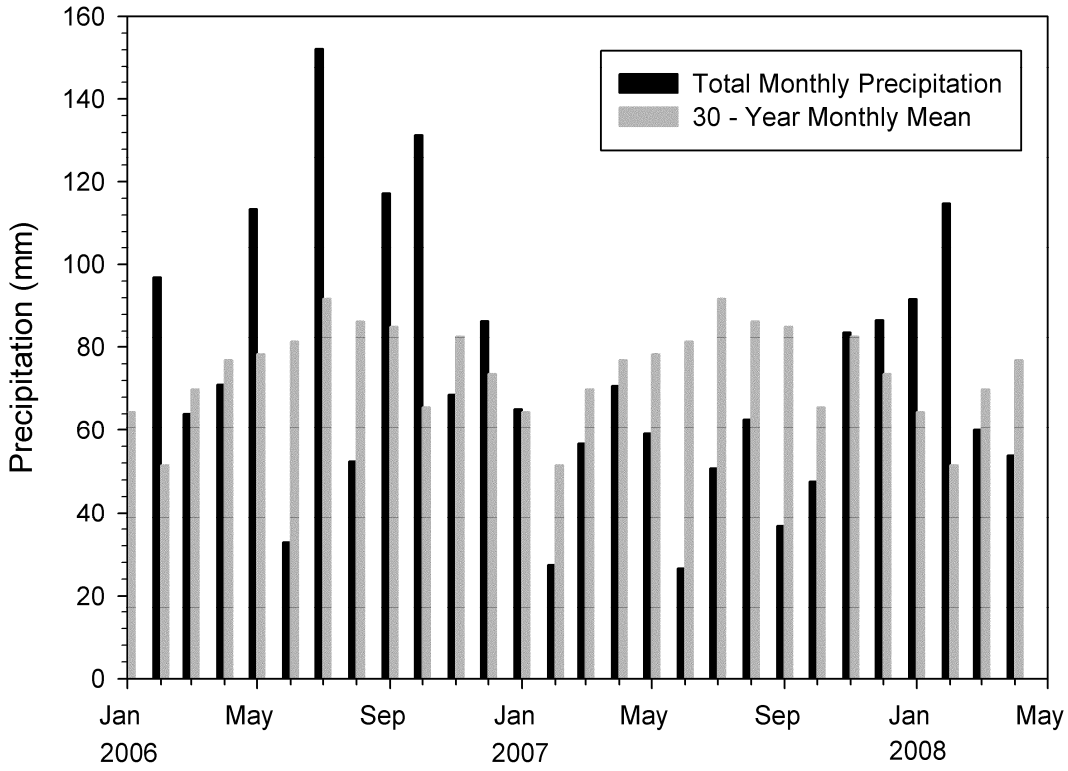

Figure 2.4: Monthly total precipitation data, as recorded at the University of Waterloo weather station. The 30 – year monthly mean data was collected at the Waterloo-Wellington airport.

2.1.2 Hydrology

Flow conditions in the Grand River are carefully controlled throughout the year by a series of 8 major dams and reservoirs. The Shand dam is the largest control structure on the Grand River. The Shand Dam was constructed in 1942, and was one of the first hydrologic control structures built on the Grand River. Generally, the various dams and reservoirs are operated to buffer the high river flows during snowmelt and heavy precipitation events, and to also supplement the low river flows during the summer months. Therefore, the reservoirs typically follow an annual operation cycle of filling during the early spring snowmelt, and slowly draining throughout the summer.

Since the flow in the river is highly regulated, it follows a predictable pattern throughout the year (Figure 2.5). River flows are lowest during the summer months, typically ranging between 10 – 20 m^3/sec at Galt, Ontario (HYDAT 2005). River flow is usually highest during the annual spring snowmelt event, which typically occurs during the months of March or April (Figure 2.5). Since the spring snowmelt event typically occurs in a sharp peak, it is not well represented in Figure 2.5. The typically peak snowmelt flow ranges between 170 to 680 m^3/sec (taken as the range between the 10^{th} and 90^{th} percentiles of the peak flow value during the period from March 1 to April 30, flow data collected from 1943 to 2004 inclusive - HYDAT 2005).

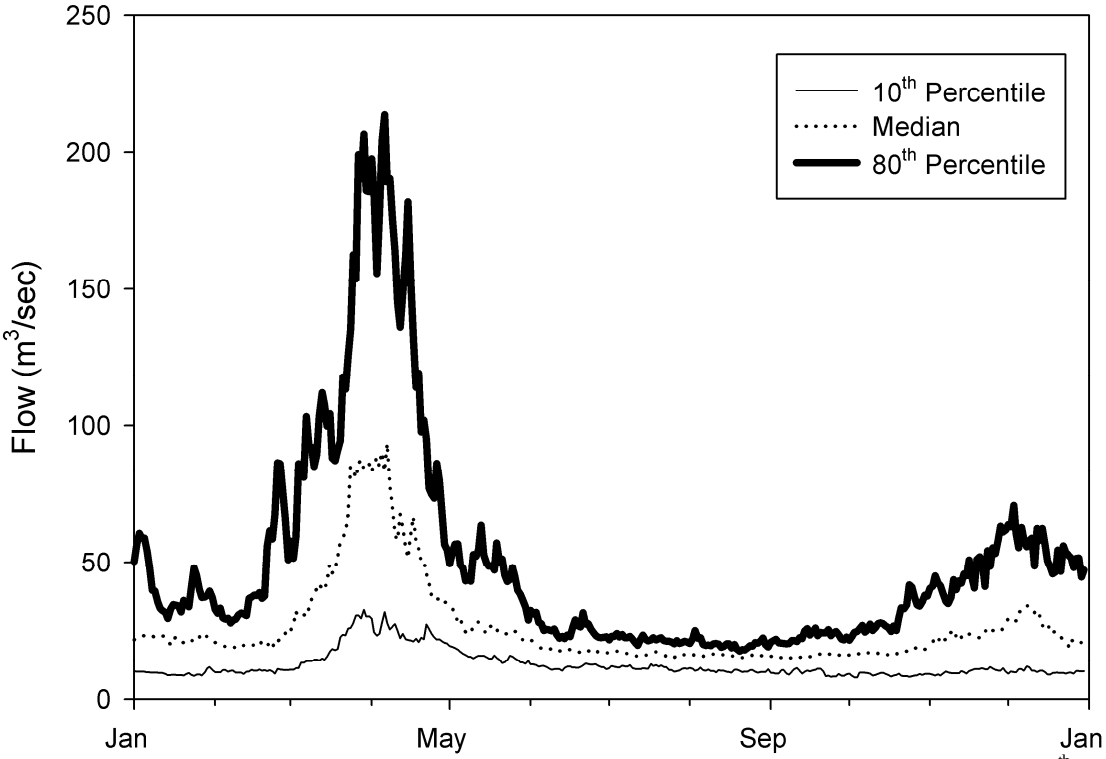

Figure 2.5: Typically annual flow for the Grand River at Galt, Ontario. Lines represent the median, 10th and 80th percentiles of daily river flow calculated for years 1943 through 2004 inclusive. Data provided by HYDAT (2005).

2.2 Methodology

2.2.1 Water Chemistry

Samples for general water chemistry analyses were collected in 120 mL plastic bottles. Samples were kept cold until brought back to the lab, usually less then 6 hours after they were collected. Water samples were then filtered with 0.45 μm membrane syringe filters and separated into two 40 mL amber vials. One of the vials was acidified to approximately pH 5 with 10% H_2SO_4. Both vials were then placed into cold storage (4°C) until analysis (usually within 1-2 weeks).

2.2.2 Nitrate Concentration

Sample water was taken from the non-acidified amber vials for analysis of anion concentrations. These samples were analyzed using a Dionex ICS-90 ion chromatography machine, equipped with an IonPac AS14A column and AS40 automated sampler. Samples were corrected to a calibration curve created from standards run at the same time as the samples. Precision for this analysis was +/- 0.05 mg N/L.

2.2.3 DOC Concentration

Samples were analyzed for dissolved organic carbon (DOC) using a Rosemount-Dohrmann high temperature total carbon analyzer equipped with an autosampler system. DOC is determined by a measurement of total carbon, after inorganic carbon is removed from the sample by sparging with phosphoric acid. Samples were corrected to a calibration curve created from standards analyzed during the same run as the samples. The precision associated with this analysis is typically +/- 0.2 mg C/L.

2.2.4 Ammonium Concentration

Ammonium concentration was analyzed using an automated colourometric method. Briefly, reagent solutions (containing sodium salicylate, sodium nitro-prusside, sodium hydroxide, potassium sodium tartrate tetrahydrate, di-sodium hydrogen phosphate, and sodium salt) are added to the samples. These reagents react with ammonium present in the sample to form a colour, the intensity of which depends on the concentration of ammonium. The concentration of NH_4^+ in the original sample is then

determined by measuring the absorption of 660 nm light through the samples. The amount of absorption at this wavelength is proportional to the amount of ammonium present in the sample. The data was then corrected against a calibration curve created from standards analyzed at the same time as the samples. The detection limit for this method is 0.01 mg $N\text{-}NH_4^+$ /L and the precision associated with this analysis is +/- 0.005 mg $N\text{-}NH_4^+$ /L.

2.2.5 Dissolved Nitrous Oxide Concentration

Samples for determination of dissolved N_2O concentration were collected in 60 mL glass serum bottles with red Vaccutainer™ (Benton-Dickson) stoppers. The bottles were filled underwater, with as little disturbance as possible, in order to prevent degassing of the sample. The bottles were then capped with no headspace, using a hypodermic needle to pierce the stopper and release excess pressure and air bubbles during capping. The samples were injected with 0.2 mL of saturated $HgCl_2$ solution to inhibit biological activity in the samples during transport and storage. The samples were kept cold until they were brought back to the lab, usually in less than 6 hours. The samples were then put into cold storage (4°C) until they were analyzed (usually within 2-3 weeks).

N_2O concentrations were determined using a headspace equilibrium technique and a Varian CP-3800 gas chromatograph. The gas chromatograph was equipped with a Combi-Pal autosampler, 2m x 1/8" SS column packed with Hayesep D 80/100 mesh, and an ECD. P-5 mix (95% Ar, 5% CH_4) was used as the carrier gas.

Samples were first prepared by injecting 10mL of He into the bottle while removing 5mL of sample water, creating a headspace. The positive pressure thus created

inside the bottle, allowed headspace gas to be removed without creating a vacuum. Bottles were then gently agitated on an orbital shaker for 90 minutes to allow the dissolved gasses to come into equilibrium with the headspace. Finally, N_2O concentration analyzed by injection of 2.5 mL headspace samples into the Varian CP-3800. Headspace concentrations were calculated using a calibration curve created by analyzing certified gas standards run in conjunction with the samples. The concentration of dissolved N_2O in the original sample is then calculated using Henry's Law, taking into account changes in temperature and pressure between sample collection and analysis (Sander 1999; Lide & Fredrikse 1995). The detection limit for this method is approximately 6.5 nmol – N_2O / L and the error associated with this analysis is approximately +/- 5% at 8.5 nmol – N_2O / L.

2.2.6 Isotopic Analysis of Nitrate

Samples for isotopic analysis of nitrate were collected in 1L plastic bottles. These samples were kept cold until they were brought back to the lab, usually less then 6 hours after they had been collected. Once the samples had been returned to the lab, they were promptly frozen until analysis.

These samples were analyzed for the isotopic signature of nitrate using the method described in Environmental Geochemistry Lab Technical Procedure 30.1. In brief, anion exchange columns are used to strip out the nitrate from a large volume of water. The nitrate is then removed from the columns by eluting them with 10% HCl. The solution is neutralized by the addition of silver oxide (AgO). This forms soluble silver nitrate ($AgNO_3$) and a solid precipitate of silver chloride ($AgCl_2$). The solution is decanted and filtered to remove any fine particles of $AgCl_2$ and subsequently frozen.

Following freeze-drying, the solid $AgNO_3$ is stored in amber vials until analysis by EA-IRMS to determine the $\delta^{15}N$ and $\delta^{18}O$ values of the nitrate in the original sample.

2.2.7 Isotopic Analysis of Ammonium

Samples for the isotopic analysis of NH_4^+ were collected in 250mL plastic bottles. The pH of these samples was adjusted to 5 – 6 in the field using a 10% sulphuric acid solution. The samples were kept on ice until they were returned to the laboratory (typically within 6 hours). Once returned to the laboratory, samples were promptly frozen until analysis.

$\delta^{15}N - NH_4^+$ analysis was conducted using a diffusion technique (Murray 2008, modified from Spoelstra et al. 2006). Briefly, an acidified quartz filter disk contained in a polytetrafluoroethylene (PTFE) packet was placed in a 60 mL serum bottle containing approximately 20 mL of sample water. The pH of the sample was adjusted with a buffer solution to convert the NH_4^+ in the sample to NH_3 gas. The serum bottle was capped and placed on a stir plate for approximately 10 days, after which the quartz filter disks were removed, freeze dried, and analyzed for $\delta^{15}N - NH_4^+$ at the University of Waterloo Environmental Isotope Laboratory (UW-EIL).

2.2.8 Dissolved Oxygen Concentration

Dissolved oxygen concentration was measured using the Winkler Titration technique (Azide modification, APHA 1995). Samples were collected in duplicate using glass BOD bottles with ground glass stoppers. The samples were fixed in the field using solutions containing manganese chloride, sodium hydroxide, sodium iodide and sodium azide. The bottles were kept cold and sealed with Parafilm to ensure they would not be

disturbed until they were returned to the lab, usually in less then 6 hours after sampling. At the lab, the samples were titrated following the standard Winkler titration technique, using sodium thiosulphate. The sodium thiosulphate solution was calibrated by titrating against a standard solution containing potassium iodide, potassium bi-iodate and sulphuric acid. The detection limit for this method is 0.2 mg – O_2 /L and the precision associated with this analysis is +/- 0.2 mg – O_2 /L.

Chapter 3:

A "Purge & Trap" Method to Extract Dissolved Nitrous Oxide for Stable Isotope Analysis

3.1 Introduction

Nitrous oxide (N_2O) is a powerful greenhouse gas with a global warming potential 310 times that of CO_2. Atmospheric concentrations have been increasing steadily during the last ~150 years by approximately 0.25%/year (Denman et al 2007). Therefore understanding N_2O production in the environment is the focus of widespread research effort. N_2O is largely produced through microbially- mediated processes of nitrification and denitrification (Zafiriou 1990). Since isotopic fractionation factors are different for these two processes, isotopic analysis of N_2O can be used to determine the dominant N_2O production pathways (Wada & Ueda 1996, Perez et al 2001). Furthermore, stable isotope ratios of different N_2O sources may be useful when quantifying the relative importance of various atmospheric sources (Stein & Yung 2003).

Many researchers have measured the isotopic composition of gaseous N_2O produced by cultured microorganisms (e.g. Sutka *et al.* 2006). Also, several studies have measured gaseous N_2O emitted from natural soils in field environments (e.g. Perez et al 2001, Kim & Craig 1993, Mandernack et al 2000). N_2O is highly soluble (K_H = 0.025 $M \cdot atm^{-1}$ at 20°C) and is also produced and transported in aquatic environments. Current estimates indicate approximately 25% of the total anthropogenic N_2O flux is produced in aquatic environments such as rivers, estuaries, and costal zones (Denman et al 2007). Other researchers have measured stable isotope ratios of dissolved N_2O in aquatic systems, mostly in marine environments (e.g. Kim & Craig 1990, Yoshinari et al.1997,

Popp et al. 2002). Only a very small number of studies have measured isotopic ratios of dissolved N_2O in freshwater environments (Wahlen & Yoshinari 1985, Boontanon et al. 2000).

Several techniques for dissolved N_2O analysis are described in the literature. Ostrom et al. (2000) and Westley et al. (2006) used a modified apparatus (Dore et al. 1998) designed for the online analysis of dissolved methane (Sansone et al 1997). Tsunogai et al (2008) also used a modified apparatus originally designed for the analysis of dissolved methane (Tsunogai et al 2000). In brief, this technique involves transferring a water sample to an extraction chamber where it is sparged with helium to remove the dissolved N_2O, which is then cryogenically trapped by liquid nitrogen. The sample is then transferred through a complex series of valves and traps to a GC-IRMS. Other online methods (Casciotti et al 2002, Coplen et al 2004) have been developed for the automated isotopic analysis of nitrate samples. In these methods, nitrate is converted to N_2O through bacterial denitrification and is sparged from small (~20mL) samples and transferred to a mass spectrometer for analysis.

Although the above mentioned online methods can be advantageous in certain situations, there are several disadvantages for using these methods for the routine isotopic analysis of dissolved N_2O. The methods developed for the isotopic analysis of NO_3^- by bacterial denitrification to N_2O (Casciotti et al 2002, Coplen et al 2004) are not applicable to the isotopic analysis of dissolved N_2O because they operate at N_2O concentrations much higher than found in the natural environment. The minimum sample size for the method developed by Dore et al (1998) is 1 nmol – N_2O. However, using a similar method, Tsunogai et al (2008) specifies a minimum sample size of 20 nmol - N.

This is equivalent to 1-2 L of water for dissolved N_2O samples near atmospheric equilibrium.

The analysis time required to process each sample using these online methods makes them impractical for most researchers. For example, the online extraction apparatus developed by Dore et al (1998) and used by several others requires 45 minutes per sample. Likewise, the latest method of Tsunogai et al. (2008) requires 30 minutes to process each sample.

Lastly, the current online methods are only useful to researchers that have access to a dedicated mass spectrometer for dissolved N_2O analysis. Many laboratories would benefit from a simple offline method that would allow them to process a large number of dissolved samples quickly. The extracted N_2O could then be stored for later isotopic analysis, or if the laboratory does not have access to a mass spectrometer, shipped elsewhere for analysis.

Presented here is a simple offline method for extracting dissolved N_2O from freshwater samples for stable isotope analysis ($^{15}N/^{14}N$ and $^{18}O/^{16}O$) from samples containing as little as 3 nmol N_2O. This limit is much lower than that obtained by Tsunogai et al (2008), Casciotti et al (2002) and Coplen et al (2004). The sensitivity of this method is almost equal to that of Dore et al (1998), but the sample processing time is much faster with our method. Samples can be processed in as little as 10 minutes, and the simplicity of our method makes it feasible to construct multiple purge and trap stations, allowing several samples to be processed simultaneously. Additionally, processing samples offline allows for the stable storage of extracted N_2O, which can then be shipped to external laboratories for isotopic analysis.

3.2 Sampling Method

Water samples for dissolved N_2O isotopic analysis are collected in either 160mL serum (Wheaton # 223748) or 500mL media (Corning # 1395-500) bottles, depending on the expected concentration. Sample bottles are filled and capped underwater to prevent the entrapment of air. Groundwater samples may be collected by pumping and filling the bottles to overflowing; however, care must be taken to prevent degassing or introduction of air into the sample. A red rubber stopper (Vaccutainer ™) is used for serum bottles and a black rubber lyophilization stopper (Wheaton # 224100-503) is used for media bottles. Once capped, samples are preserved by injection of a saturated $HgCl_2$ solution (2 mL $HgCl_2$ solution per litre of sample). Samples are stored at 4°C until they are extracted (typically within 72 hours).

3.3 Extraction Apparatus

A "purge and trap" system (Figure 3.1) is used for isolating dissolved N_2O. Dissolved N_2O gas is extracted directly from the original sample bottle by bubbling with ultra-pure helium (He), at a flow rate of 300mL/min for 10 – 20 minutes (depending on sample size). A stainless steel frit (3 micron pore size – Aimark Travers Ltd # 459500) is used to increase the extraction efficiency of the helium stream. The frit is attached to 1/16" ID stainless steel tubing threaded through a butyl-blue rubber stopper (Belco Glass Inc # 2048-11800). The sample bottle is attached to the system by uncapping the sample and inserting the stopper with the frit. Due to the high solubility of N_2O and the low equilibrium fractionation factors for ^{15}N and ^{18}O (Inoue & Mook 1994), there is

insignificant and inconsequential loss of N_2O during attachment of the sample bottle to the purge and trap system.

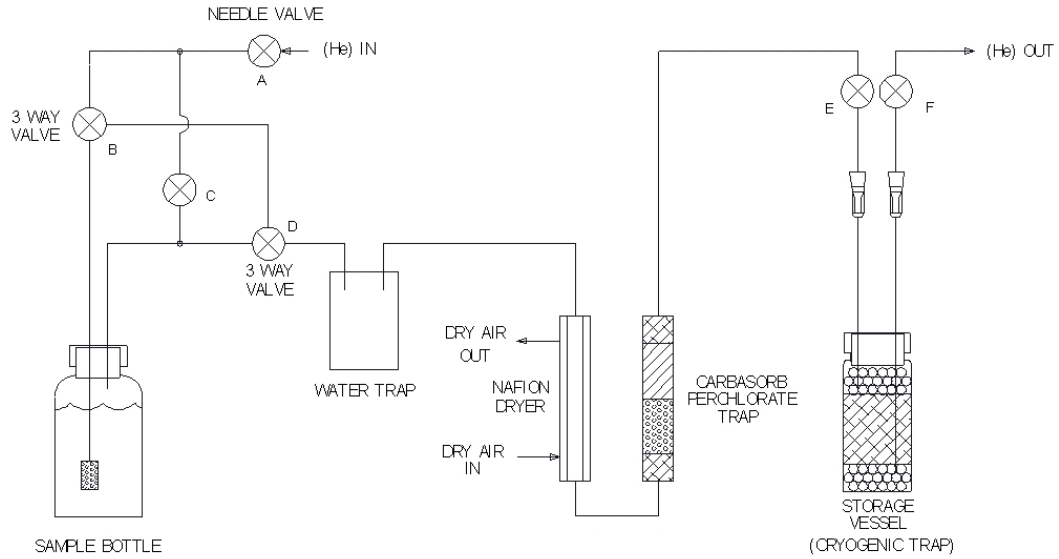

Figure 3.1: Schematic flow diagram of purge and trap system.
Valve A: Needle Valve to control He flow rate (Swagelok #SS-SS1)
Valve B: 3-way plastic stopcock with luer fittings (Kontes Part # KT420163-4503)
Valve C: 2-way valve (Swagelok #SS-41GS1)
Valve D: 3-way valve (Swagelok #SS-41XS1)
Valve E: Mininert valve with luer fittings (Vici #654051)
Valve F: Mininert valve with luer fittings (Vici #654051)
Nafion Dryer (Permapure #MD-110-24P-4)

The extracted gas passes through several stages of purification before N_2O is trapped cryogenically. A water trap is used to prevent liquid water from reaching the downstream nafion dryer and chemical traps. The water trap consists of a small glass vial fitted with a rubber stopper. The nafion membrane is permeable with respect to water, but impermeable to other gases. The gas stream is "dried" by a counter-current flow of dry air across the nafion membrane. The chemical trap contains Carbosorb to remove CO_2 and magnesium perchlorate to remove any residual water vapour. N_2O is trapped cryogenically in a storage vessel cooled with liquid nitrogen. The storage vessel consists

of a 20mL round bottom vial (Restek #21162), containing a 3 cm layer of pyrex wool in between two layers of glass beads, and capped with a butyl-blue rubber stopper and crimp seal. Preliminary method development indicated that, under high rates of He flow (>100mL/min), cryogenic trapping of N_2O is generally inefficient using a simple coiled loop of tubing. For other cryogenic trapping methods, glass fibre thimbles have been used to improve trapping efficiency (Brenninkmeijer 1991, Brenninkmeijer & Röckmann 1996). With our method, the pyrex wool and glass beads greatly increase the surface area, and allow for extremely efficient cryogenic trapping of N_2O, even under high rates of flow (> 300 mL/min). Before use, storage vessels are evacuated to ~0.1 mBar to remove any N_2O. A vessel can be re-used several times provided it is re-evacuated between uses. N_2O samples are stored in these vessels in darkness at room temperature. Repeat analysis of extracted samples yields the same isotope values after 5 months of storage indicating no sample degradation occurs under these conditions.

3.4 Extraction Method

Valves B, C and D are first positioned to allow He to flow through all lines and purge any air from the system (Figure 3.2a). After 30 seconds, valve C is closed, with valves B and D remaining in position to allow the He flow to bypass the metal frit and flow directly through the traps (Figure 3.2b). A storage vessel is attached to the system using a 1 inch, 23 gauge needle attached to valve E. The needle is positioned so its tip is protruding about 3mm through the stopper, close to the vial wall; this positioning helps prevent the needle from freezing up and becoming plugged. A 4 inch, 22 gauge needle (Air-Tite Products Co. #N224) attached to valve F is inserted through the storage vessel

stopper, and pushed to the bottom of the vial. First valve E, then valve F is opened, and the storage vessel is immersed in liquid nitrogen to the top of the pyrex wool layer. The stopper is removed from the sample bottle, and the stopper with the attached metal frit is inserted into the bottle. The line connecting valve B to the metal frit is disconnected at valve B, and a 20mL syringe is attached to the line using a luer lock fitting. A 15mL He headspace is created in the sample bottle by momentarily opening valve C, and removing the excess water through the syringe. The syringe is removed, and the line reattached. Valves B and D are positioned to allow He to flow through the metal frit in the sample bottle and through the various traps (Figure 3.2c). The sample is purged at a flow rate of 300mL/min for 10 minutes for 160mL bottles or 20 minutes for 500mL bottles. He flow rate is monitored at the outlet and is adjusted using the needle valve (valve A). Occasionally, heat may need to be applied to the top of the storage vessel to prevent freezing and plugging of the inlet needle. After the sample has been purged, valves B and D are positioned to allow the He flow to bypass the sample bottle, and to flush any remaining N_2O from the lines and traps (Figure 3.2b). After 30 seconds, valve E is closed, and any non-condensable gases are removed using a hand vacuum pump attached at valve F. Once a vacuum of approximately 0.3 Bar is achieved, valve F is closed and the storage vessel is removed from the liquid nitrogen bath. After the storage vessel has reached room temperature, the needles are removed, and 20mL of He is injected into the vial to create a positive pressure.

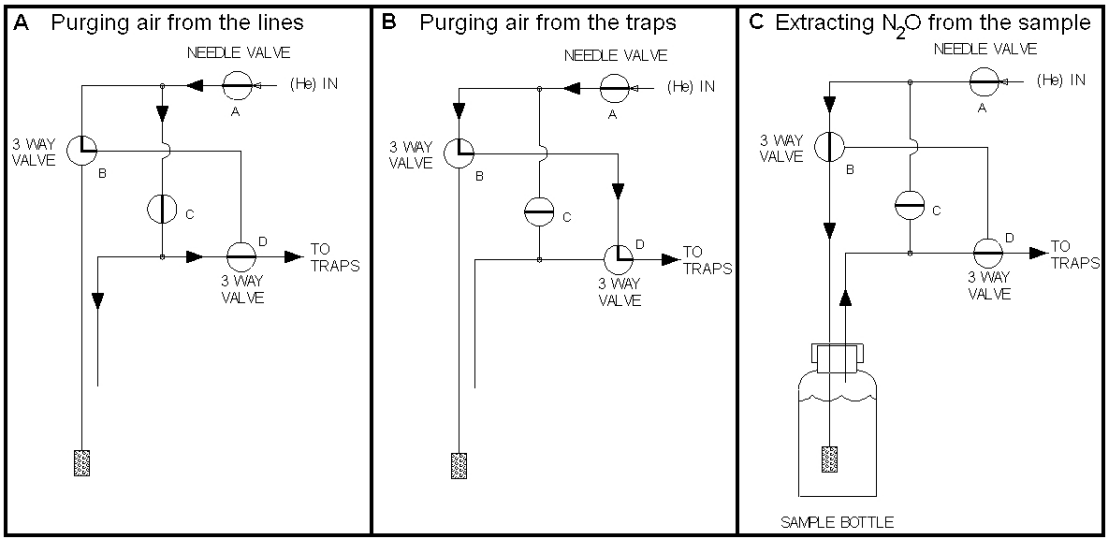

Figure 3.2: Detailed flow path diagram of purge and trap system.

3.5 Concentration and Isotopic Analysis of N_2O

Water samples were analyzed for dissolved N_2O concentration with a headspace equilibrium technique using a Varian CP-3800 gas chromatograph. The gas chromatograph is equipped with an ECD and P-5 mix (95% Ar, 5% CH_4) is used as the carrier gas. Samples are bracketed by N_2O standards with known concentration (0.1, 0.5, 1.0 and 10 ppm N_2O).

Extracted N_2O samples in storage vessels are analyzed for $\delta^{15}N$ and $\delta^{18}O$ by injection of 3 – 15 nmol of N_2O into a GV Trace Gas preconcentrator system, attached to a GV Isoprime mass spectrometer at the EIL-UW. Injection volumes are dependant on initial dissolved N_2O concentration. The Trace Gas system further purifies the sample and chromatographically separates N_2O from any remaining trace CO_2. Raw molecular ratios (mass 44, 45 and 46) from the mass spectrometer are converted to isotopic ratios ($^{15}N/^{14}N$ and $^{18}O/^{16}O$) using the data correction method described by Kaiser *et al.* (2003). Due to the lack of available internationally recognized N_2O isotope standards, N_2O

isotopic data is corrected using internal standards bracketing the isotopic ratios of nearly all natural samples (EGL-5: 10ppm N_2O, $\delta^{15}N$ = 2.76‰, $\delta^{18}O$ = 40.38; HAN2O-2: ~1700 ppm N_2O, $\delta^{15}N$ = -92.64‰, $\delta^{18}O$ = 20.52‰). $\delta^{15}N$ is reported relative to atmospheric N_2, and $\delta^{18}O$ is reported relative to VSMOW.

3.5.1 Calibration of Internal Isotope Standards

Internal N_2O standards are calibrated against tropospheric N_2O, which has been thoroughly characterized as having an isotopic composition of $\delta^{15}N = (6.72 \pm 0.12)$ ‰ and $\delta^{18}O = (44.62 \pm 0.21)$ ‰ (Kaiser *et al.* 2003). Tropospheric N_2O samples were collected in 500mL sample bottles by filling with air from the CEIT building rooftop at the University of Waterloo. Kaiser *et al.* (2003) did not observe local source contamination of tropospheric N_2O in samples taken from the rooftop of the Max Planck Institute of Chemistry in Mainz, Germany. Since there are no known point sources of N_2O nearby, air samples obtained at the University of Waterloo are assumed to be representative of tropospheric N_2O. N_2O was extracted from sample bottles using the same method for dissolved N_2O samples. The only difference in procedure was the attachment of sample bottles to the system using a pair of needles in place of the metal frit assembly, thereby allowing sample bottles to remain sealed during N_2O extraction. Once the tropospheric N_2O was trapped in storage vessels, care was taken to ensure that any non-condensable gases were purged from the vessels while they were still submerged in liquid nitrogen. Due to the low vapour pressure of oxygen (O_2) at the temperature of liquid nitrogen (-196 °C), a vacuum of less than 0.2 Bar is needed to ensure complete removal of any liquid O_2 formed (Lide 2008). A mechanical vacuum pump was used to

achieve a vacuum greater than 0.001 Bar. Internal N_2O standards were analyzed on the Trace Gas system during the same run as the tropospheric N_2O samples. Calibration used a simple calculation adapted from Werner and Brand (2001), and the $\delta^{15}N$ and $\delta^{18}O$ values of tropospheric N_2O determined by Kaiser *et al.* (2003).

Tropospheric N_2O collected and analyzed on different dates (over a period of 5 months with varying wind directions) produced the same results (n=15, standard deviation: $\delta^{15}N$=0.2‰, $\delta^{18}O$=0.5‰). This reproducibility further supports the assumption that air samples collected at the University of Waterloo are not affected by local sources of N_2O, and are thus representative of tropospheric N_2O composition.

3.6 Method Testing

Method accuracy was tested by extracting N_2O from degassed ultra-pure de-ionized water (Nanopure™) spiked with internal N_2O gas standards of known isotopic compositions (EGL-6: 1000 ppm N_2O, $\delta^{15}N$ = 1.04‰, $\delta^{18}O$=40.30‰; EGL-5: 10 ppm N_2O, $\delta^{15}N$ = 2.76‰, $\delta^{18}O$=40.38‰). Prior to spiking with N_2O isotope standards, Nanopure™ water was degassed by sparging with He for 20min, followed by application of a vacuum (0.2 Bar) while being stirred for 2 hours. A 60mL sample of degassed water was subsequently analyzed for N_2O concentration and was found to be less than the detection limit (<1.5 nmol/L). A 160mL serum bottle was filled with degassed water, and a 10mL helium headspace was created. EGL-6 standard gas (5.5mL) was injected into the headspace and the bottle placed on an orbital shaker for 2 hours to dissolve the N_2O. The resulting dissolved N_2O solution was diluted with degassed Nanopure™ water to produce a solution with a N_2O concentration representative of natural samples (approximately 30 -

40 nmol/L). Five 500mL sample bottles were filled with the mixture, and the N_2O subsequently extracted using the described method. To determine extraction efficiency, samples were extracted using increasing purging times. The concentration of dissolved N_2O remaining in the bottle, and the isotopic composition of the extracted N_2O was measured for each purging duration.

The isotopic composition of the extracted N_2O was within error of that of the standard gas (Figure 3.3a). Because of the slight equilibrium enrichment factors and the high solubility of N_2O, the dissolved N_2O was expected to be enriched by 0.07‰ and 0.11‰ for $\delta^{15}N$ and $\delta^{18}O$ with respect to the standard gas (Inoue & Mook 1994). The $\delta^{15}N$ of the extracted N_2O was consistently slightly higher than expected, however the maximum observed difference between the extracted N_2O and the standard gas (0.6‰) was similar to the precision for $\delta^{15}N$ of this analysis. The isotopic composition of extracted N_2O was not affected by incomplete sample recovery. For example, even with a sample extraction efficiency of only 70%, the isotopic composition of the extracted N_2O was not different from the N_2O standard.

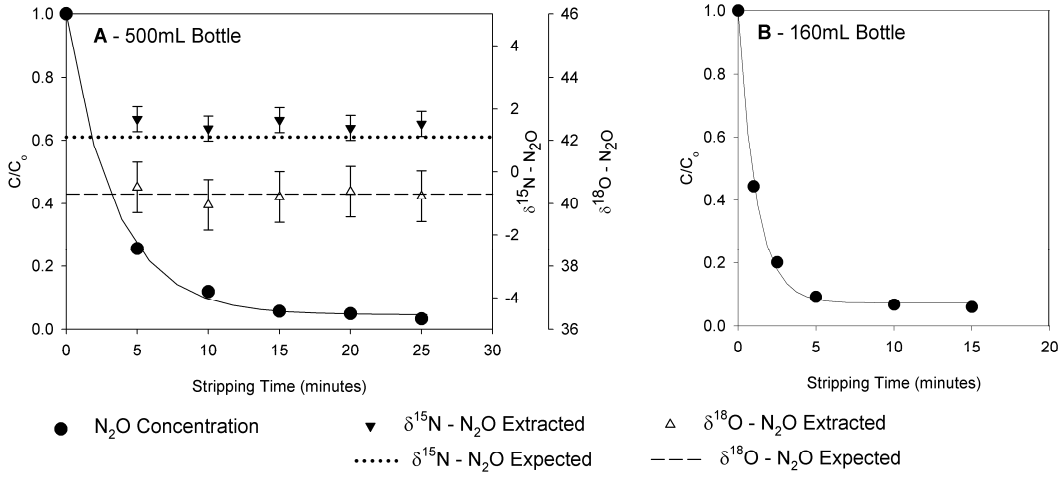

Figure 3.3: N_2O extractions of degassed water spiked with EGL-6 N_2O isotope standard

To determine the optimal purging time for 160mL bottles a similar procedure was followed and only N_2O concentrations were measured (Figure 3.3b). Isotopic composition of N_2O extracted from 160mL serum bottles for the optimal time of 10 minutes was again the same as the source gas (EGL-5 standard gas - Table 3.1). Based on these results, purge times of 10 and 20 minutes are used for extracting dissolved N_2O from 160mL and 500mL samples, respectively.

A second experiment was conducted to test the stability of dissolved N_2O samples in long-term storage. Bottles were filled with samples of Nanopure™ or water from the Grand River downstream of Kitchener, Ontario. Nanopure™ water samples contained naturally high levels of N_2O, due to high dissolved N_2O concentrations in municipal tap water in Waterloo, Ontario. Samples without a headspace were stored in 160mL serum bottles capped with red rubber (Vaccutainer™) stoppers. Samples were preserved with varying amounts of $HgCl_2$ saturated solution, at concentrations greater than and less than the concentration typically used for sample preservation (0 to 3.125 mL solution / L sample). Duplicate and triplicate samples were extracted and analyzed at intervals ranging from 2 weeks to 2 months (Table 3.2). There was no observable change in $\delta^{15}N$ and $\delta^{18}O$ of N_2O over the storage period for any treatments.

The results of the method testing also provide a measure of the precision of this method, not only within a single run, but also between runs. The average standard deviation for both sample sets indicates the average precision for the isotopic analysis of N_2O is 0.4‰ and 0.8‰ for $\delta^{15}N$ and $\delta^{18}O$ respectively.

Table 3.1: Results of the test extractions using degassed Nanopure™ water spiked with EGL-5 in 160mL serum bottles. Recovery is calculated by measuring the sample peak height on the mass spectrometer, calibrated against reference standards of known concentration.

Sample Name	Purging Time (minutes)	N_2O Concentration (nmol/L)	$\delta^{15}N$-N_2O (‰)	$\delta^{18}O$-N_2O (‰)	Recovery (%)
EGL-5 Spiked Water	10	38.6	2.8	40.4	103.6
EGL-5 Spiked Water	10	38.6	2.4	40.2	71.9
EGL-5 Spiked Water	10	42	2.7	40.7	101.8
EGL-5 Spiked Water	10	42	3.0	40.5	81.7
	Average	**40.30**	**2.7**	**40.5**	**89.7**
	Expected Value		**2.8**	**40.3**	
	Standard Deviation	**1.96**	**0.3**	**0.2**	

Table 3.2: Results of the sample storage experiment. Recovery is calculated by measuring the sample peak height on the mass spectrometer, calibrated against reference standards of known concentration. Recovery could not be accurately calculated for the Nanopure samples because only a partial sample was injected into the mass spectrometer.

Sample Name	Storage Time (Days)	Preservative (mL of $HgCl_2$ soln/L)	N_2O Concentration (nmol/L)	$\delta^{15}N$-N_2O (‰)	$\delta^{18}O$-N_2O (‰)	Recovery (%)
Nanopure	0	0	220	-12.9	-13.9	N/A
Nanopure	0	0	220	-14.0	-12.2	N/A
Nanopure	0	0	220	-13.4	-12.5	N/A
Nanopure	14	0	218	-13.6	-13.0	N/A
Nanopure	14	0	218	-13.7	-12.5	N/A
Nanopure	14	0	218	-12.8	-13.3	N/A
Nanopure	40	0	210	-12.9	-13.0	N/A
Nanopure	40	0	210	-13.1	-13.2	N/A
Nanopure	40	0	210	-12.5	-12.8	N/A
Nanopure	14	1.25	205	-12.4	-12.0	N/A
Nanopure	14	1.25	205	-12.7	-16.1	N/A
Nanopure	14	1.25	205	-13.5	-12.8	N/A
Nanopure	40	1.25	213	-12.7	-13.6	N/A
Nanopure	40	1.25	213	-12.9	-13.6	N/A
Nanopure	40	1.25	213	-13.0	-13.1	N/A
		Average	**213**	**-13.1**	**-13.2**	
		Standard Deviation	**5.6**	**0.47**	**0.97**	
Grand River	0	1.25	24.2	-0.5	40.6	103.3
Grand River	0	1.25	24.2	-0.4	40.7	96.1
Grand River	14	1.25	25	-0.6	40.4	96.8
Grand River	14	1.25	25	-1.1	40.4	90.9
Grand River	40	1.25	26.2	-0.6	40.5	93.7
Grand River	40	1.25	26.2	-1.0	40.5	88.8
Grand River	68	1.25	22	-1.0	39.5	104.9
Grand River	68	1.25	22	-1.8	38.2	97.0
Grand River	14	3.125	24.9	-0.9	40.0	99.8
Grand River	14	3.125	24.9	-1.1	40.3	93.2
Grand River	40	3.125	25.7	-1.0	39.5	92.5
Grand River	40	3.125	25.7	-1.0	40.3	93.2
Grand River	68	3.125	22.6	-1.0	40.2	97.1
Grand River	68	3.125	22.6	-1.0	39.9	104.8
		Average	**24.4**	**-0.9**	**40.1**	**96.6**
		Standard Deviation	**1.50**	**0.34**	**0.65**	
		Precision (average standard deviation)		**0.4**	**0.8**	

3.7 Field Data

Samples of dissolved N_2O were collected at two field sites in Southern Ontario, Canada and analyzed using the method described above (Table 3.3).

The Grand River stretches over 300 km and drains a watershed of 6800 km^2. The watershed is predominantly agricultural and 26 municipal wastewater treatment plants (WWTPs) discharge effluent into the river and its tributaries before the river drains into Lake Erie. Nitrogen inputs from both agriculture and the WWTPs contribute to elevated NO_3^- concentrations and the production of riverine N_2O. Water samples were collected from one site upstream of a major urban centre on 53 different occasions between May 2006 and June 2007. NO_3^- concentrations ranged from 0.8 to 6.5 mg-N/L and dissolved N_2O concentrations from 8.6 to 44 nmol/L. CH_4 concentration was elevated in these samples (57 to 740 nmol/L), reflecting production in anoxic river sediments. $\delta^{15}N - N_2O$ of the river samples ranged from -5.7 to 6.4‰, and $\delta^{18}O - N_2O$ ranged from 38.2 to 48.8‰. Analyses of duplicate samples indicate an average precision of 0.2 and 0.3‰ for $\delta^{15}N$ and $\delta^{18}O$, respectively. These results indicate that our extraction method is reliable for the isotopic analysis of samples with low concentrations of dissolved N_2O.

Table 3.3: Stable isotope analysis of dissolved N_2O from two field sites in Southern Ontario, Canada.

Site Name	**Nitrate concentration (mg N/L)**	**N_2O Concentration (nmol/L)**	**$\delta^{15}N - N_2O$ (range)**	**$\delta^{18}O - N_2O$ (range)**
Putnam Groundwater	0.5 to 61	48 to 28,000	-31.2‰ to 23.4‰	35.7‰ to 74.3‰
Grand River	0.8 to 6.5	8.6 to 44	-5.7‰ to 6.4‰	38.2‰ to 48.8‰

Groundwater samples were obtained from piezometers (1.5 to 4m below ground surface) in a groundwater plume highly contaminated with NO_3^- that originated from a large manure composting facility near Putnam, Ontario (Robertson & Schiff 2008). Dissolved N_2O samples were collected along a transect of multilevel piezometers (n=36) within the groundwater plume in September 2006. In addition to high nitrate concentrations (ranging from 0.5 to 61 mg-N/L), concentrations of dissolved CH_4 and CO_2 were also high, ranging from 20 to 15,500 nmol/L, and 0.2 to 4.2 mmol respectively.

Dissolved N_2O concentration was very high in these samples, ranging from 48 to 27,600 nmol/L. The $\delta^{15}N - N_2O$ values of these samples ranged from -31.2 to 23.4‰, and the $\delta^{18}O - N_2O$ values ranged from 33.7 to 74.3‰. Analyses of N_2O in duplicate groundwater samples yielded an average precision of 0.6 and 0.9‰ for $\delta^{15}N$ and $\delta^{18}O$, respectively. Although the overall precision for the groundwater samples was slightly lower than for the river samples, groundwater samples are more susceptible to degassing or introduction of air. These results indicate that our extraction method is suitable for the extraction of N_2O from samples containing elevated levels of nitrate, CH_4 and CO_2.

The isotope data on N_2O from the Grand River covers a narrow range of $\delta^{15}N$ and $\delta^{18}O$ values, while the data collected at the groundwater site exhibits a wide range in both isotope ratios (Table 3.3). $\delta^{18}O - N_2O$ values from the groundwater site tends to be more enriched in ^{18}O than the Grand River $\delta^{18}O - N_2O$ values. Also, the very large range in $\delta^{15}N$ values at the Putnam site indicates that the $\delta^{15}N$ of the nitrogen source and N_2O production processes are variable within the groundwater plume.

The very narrow range in $\delta^{15}N$ and $\delta^{18}O$ values from the Grand River N_2O samples indicates the nitrogen source and processes of N_2O production at this site are

relatively constant with time. Although supersaturated with respect to atmospheric equilibrium, N_2O in the Grand River has a similar isotopic composition to tropospheric N_2O ($\delta^{15}N = 6.72$, $\delta^{18}O = 44.62$) (Kaiser et al. 2003) likely reflecting the importance of gas exchange with the atmosphere. River samples with the highest concentration of N_2O were the most distinct from the isotopic composition of tropospheric N_2O, indicating that, at higher dissolved N_2O concentrations, the isotopic exchange of tropospheric N_2O and river water becomes less noticeable.

3.8 Conclusions

There is limited data published on the isotopic composition of N_2O in aqueous systems, partially due to the difficulty in preserving and preparing samples for analysis. The purge and trap method described here allows for the simple and precise determination of the stable isotope composition of dissolved N_2O. The technique provides an inexpensive and effective method for researchers to expand their capacity for analysis of dissolved N_2O. This method is especially useful for researchers who do not have direct access to a mass spectrometer, allowing them to ship the extracted N_2O samples to an external isotopic laboratory for analysis. Furthermore, our method allows for a substantial increase to sample throughput as compared to current published methods. Although this method was tested for freshwater, there are no known reasons to prevent the method from being applied to marine samples.

While it is possible to calibrate internal standards against tropospheric N_2O, an internationally recognized N_2O isotopic standard needs to be developed. Such a standard

would ensure the compatibility and consistency of N_2O isotope analysis between laboratories, allowing for the direct comparison of field data generated worldwide.

The method was shown to be reliable for the extraction and analysis of dissolved N_2O from field samples at relatively low concentrations (as low as 8.6 nmol – N_2O/L). Elevated concentrations of dissolved NO_3^-, CH_4 and CO_2 do not interfere with the isotopic analysis of dissolved N_2O using this method.

Field data indicates the isotopic composition of dissolved N_2O varies widely within and between field sites. Systems open to the atmosphere are strongly influenced by gas exchange, indicating the isotopic exchange of tropospheric N_2O may be an important control on the isotopic composition of dissolved N_2O at low concentrations (< 15 to 30 nmol/L). Stable isotope analysis of dissolved N_2O has strong potential for identifying N_2O sources and production processes in aquatic systems.

Chapter 4:

A Dynamic Model to Determine the $\delta^{15}N$ and $\delta^{18}O$ of Dissolved Nitrous Oxide in Response to Tropospheric Gas Exchange

4.1 Introduction

Nitrous oxide (N_2O) is a powerful greenhouse gas (310 times more potent than CO_2 over a 100-year timeline) and its concentration has been increasing in the atmosphere at a rate of 0.25% $year^{-1}$ over the last 150 years (Denman et al. 2007). N_2O is produced through both nitrification and denitrification, therefore, it is a useful indicator of these processes in the environment (Stein & Yung 2003). Since the various microbial pathways of N_2O production have different isotopic enrichment factors, the isotopic analysis of N_2O can potentially distinguish N_2O produced through these various pathways (Wada & Ueda 1996). Recent studies have measured the isotopic ratios of N_2O produced in soil environments (e.g. Mandernack et al. 2000, Perez et al. 2001 and Bol et al. 2003). N_2O is also produced in aquatic environments, though most studies of the isotopic composition of N_2O in aquatic systems have been limited to the oceans (Kim & Craig 1990, Naqvi et al. 1998, Yoshanari et al. 1997, Westley et al. 2006, Dore et al. 1998). Although N_2O production in rivers and estuaries is a significant portion of the global N_2O budget (approximately 1.5 Tg – N/year, Kroeze et al. 2005), only one study has reported $\delta^{15}N$ and $\delta^{18}O$ of dissolved N_2O in a river (Boontanon et al. 2000).

The isotopic composition ($^{15}N/^{`14}N$ and $^{18}O/^{16}O$) of dissolved N_2O is affected by gas exchange, and therefore is not equal to the isotopic composition of N_2O produced in that environment. Also, the isotopic composition of dissolved N_2O is not indicative of the

N_2O flux emitted to the atmosphere, due to the kinetic fractionation factors associated with N_2O evasion (Inoue and Mook 1994). Previous work to study the isotopic composition of N_2O produced in aqueous systems has not considered the isotopic effects of gas exchange (e.g. Boontanon et al. 2000).

The isotopic ratios of N_2O emitted through diffusive gas exchange with the atmosphere are controlled by the isotopic ratios of dissolved N_2O and kinetic gas exchange fractionation factors, while the dissolved N_2O isotopic composition is controlled by the composition of the source N_2O, the equilibration with N_2O from the atmosphere, and the evasion of dissolved N_2O to the atmosphere. This paper will elucidate the relationship between the isotopic ratios of source, dissolved, and emitted N_2O, to allow for proper interpretation of dissolved N_2O isotope data.

4.4.1 Stable Isotopes of N_2O

The most abundant isotopologues of N_2O are $^{14}N^{14}N^{16}O$, $^{15}N^{14}N^{16}O$, $^{14}N^{15}N^{16}O$ and $^{14}N^{14}N^{18}O$. The isotopic ratios, $^{15}N/^{14}N$ and $^{18}O/^{16}O$, are as follows:

$$^{15}R = \frac{[^{15}N^{14}N^{16}O] + [^{14}N^{15}N^{16}O]}{2[^{14}N^{14}N^{16}O]} = \frac{[^{15}N_2O]}{[^{14}N_2O]} \quad (4.1)$$

$$^{18}R = \frac{[^{14}N^{14}N^{18}O]}{[^{14}N^{14}N^{16}O]} = \frac{[N_2{}^{18}O]}{[N_2{}^{16}O]} \quad (4.2)$$

Where $[^{14}N^{14}N^{16}O]$, $[^{15}N^{14}N^{16}O]$, $[^{14}N^{15}N^{16}O]$ and $[^{14}N^{14}N^{18}O]$ represent the concentrations of the various N_2O isotopologues. Note that ^{15}R is the bulk $^{15}N/^{14}N$ ratio and represents an average ratio for the two ^{15}N isotopomers. Although it is possible to measure the isotopic ratio of the two ^{15}N isotopomers independently (Toyoda & Yoshida 1999, Brenninkmeijer & Rockmann 1999), the gas exchange fractionation factors are not affected by the intramolecular distribution of ^{15}N (Inoue and Mook 1994). Using the bulk

^{15}R greatly simplifies the gas exchange fractionation calculations. Also, many laboratories do not have the capability to measure the intramolecular distribution of ^{15}N, while analysis of the bulk ^{15}N/^{14}N of N_2O is much more accessible.

Isotopic ratios are reported as δ values in permil (‰) units, relative to air – N_2 and Vienna Standard Mean Ocean Water (VSMOW).

$$\delta^{15}\mathrm{N} = \left(\frac{R^{15}_{sample}}{R^{15}_{AIR-N_2}} - 1 \right) \tag{4.3}$$

$$\delta^{18}\mathrm{O} = \left(\frac{R^{18}_{sample}}{R^{18}_{VSMOW}} - 1 \right) \tag{4.4}$$

4.2 Dynamic Isotope Model for Dissolved N_2O

A simple three box model (SIDNO, **S**table **I**sotopes of **D**issolved **N**itrous **O**xide) was created using Stella modeling software (version 9.0.1, http://www.iseesystems.com) in order to study the relationships between the isotopic ratios of source, dissolved and emitted N_2O. This model is an adaptation of the isotopic gas exchange portion of the PoRGy model (Venkiteswaran et al. 2007), which successfully simulated the stable isotope dynamics of dissolved oxygen in response to photosynthesis, respiration and gas exchange in aquatic ecosystems. One box in SIDNO is used for the total mass of dissolved N_2O and two additional boxes in the model for the dissolved masses of the heavy isotopologues ($^{15}N_2O$, and $N_2{}^{18}O$ – Figure 4.1). The depth and surface area of the boxes in the model are set by the user. This allows a dissolved concentration to be calculated from the mass contained in each box and its volume.

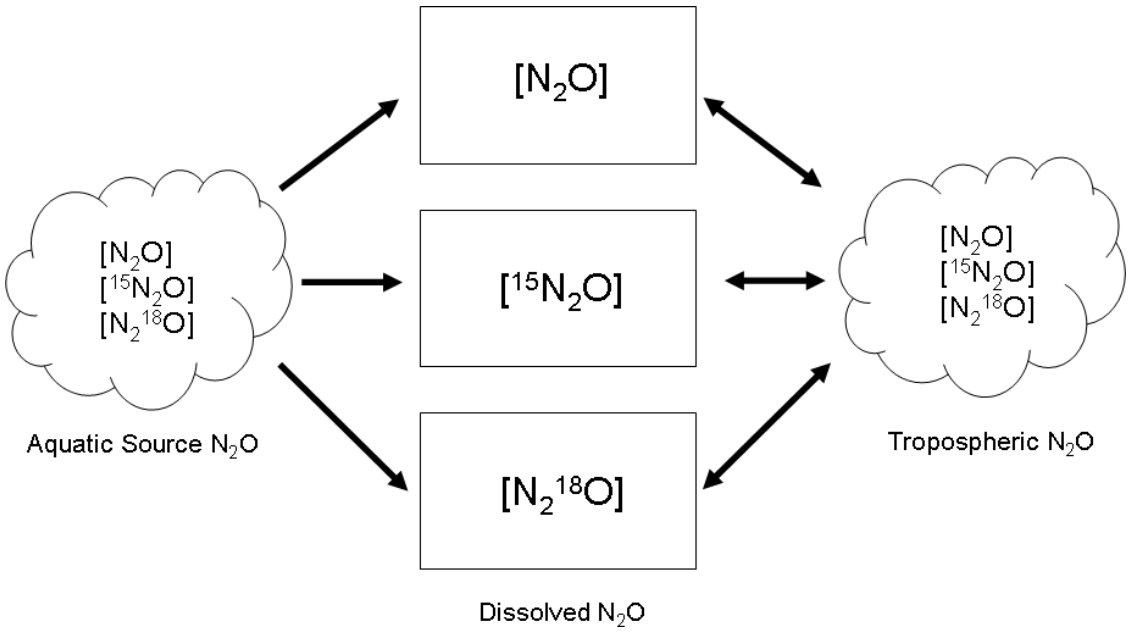

Figure 4.1: A simplified representation of the SIDNO model. The three boxes represent dissolved masses of bulk N_2O and heavy isotopologues ($^{15}N_2O$, $N_2{}^{18}O$). The flows from the left represent N_2O production from the aquatic source, and the two-way flows on the right represent gas exchange. The ratios between the masses in the boxes are used to calculate the isotopic ratios of dissolved N_2O. The flow rates for bulk N_2O, $^{15}N_2O$, and $N_2{}^{18}O$ in and out of the respective boxes are not equal, and the ratios between the flows are the various isotopic ratios of source and emitted N_2O.

4.2.1 Stable Isotope Dynamics of N_2O Production

In SIDNO, the masses and magnitude of the flows of $^{15}N_2O$ and $N_2{}^{18}O$ relative to bulk N_2O are used to calculate the isotopic composition of source, dissolved and emitted N_2O. For example, the isotopic ratios of dissolved N_2O in the model are as

$$^{15}R_{dissolved} = \frac{[^{15}N_2O]_{dissolved}}{[^{14}N_2O]_{dissolved}} = \frac{[^{15}N_2O]_{dissolved}}{[N_2O]_{dissolved} - [^{15}N_2O]_{dissolved}} \quad (4.5)$$

$$^{18}R_{dissolved} = \frac{[N_2{}^{18}O]_{dissolved}}{[N_2{}^{16}O]_{dissolved}} = \frac{[N_2{}^{18}O]_{dissolved}}{[N_2O]_{dissolved} - [N_2{}^{18}O]_{dissolved}} \quad (4.6)$$

Where $[N_2O_{dissolved}]$, $[^{15}N_2O_{dissolved}]$, and $[N_2{}^{18}O_{dissolved}]$ are the concentrations of these species in their respective boxes in the model (Figure 4.1). Since the model is mass

based, the concentration is calculated by dividing the mass in each box by a user defined volume.

In SIDNO, N_2O production is represented by three separate inflows, one for bulk N_2O production, and two for the less abundant isotopologues (Figure 4.1). Bulk N_2O inflow rate and its isotopic composition is set by the user, and the inflows to the dissolved $^{15}N_2O$ and $N_2{}^{18}O$ boxes are

$$\text{Production Rate } {}^{15}\text{N}_2\text{O} = \text{Production Rate N}_2\text{O} \times \left(\frac{{}^{15}R_{source}}{1+{}^{15}R_{source}} \right) \tag{4.7}$$

$$\text{Production Rate N}_2{}^{18}\text{O} = \text{Production Rate N}_2\text{O} \times \left(\frac{{}^{18}R_{source}}{1+{}^{18}R_{source}} \right) \tag{4.8}$$

Where Production Rate N_2O, Production Rate $^{15}N_2O$, and Production Rate $N_2{}^{18}O$ are the inflow rates to the bulk N_2O, $^{15}N_2O$ and $N_2{}^{18}O$ boxes, respectively.

4.2.2 Stable Isotope Dynamics of Gas Exchange

The isotopic composition of the gas exchange flux is controlled by the kinetic fractionation factors for evasion ($\alpha_{ev} = R_{evaded}/R_{dissolved}$) and invasion ($\alpha_{in} = R_{invaded}/R_{gas}$) of N_2O (Inoue & Mook 1994, Table 4.1). These two factors are related to the equilibrium fractionation factor by the following relationship $\alpha_{eq} = (R_{gas}/R_{aq.\ solution}) = (\alpha_{ev}/\alpha_{in})$.

Table 4.1: Kinetic and equilibrium fractionation factors for gas exchange of N_2O (Inoue & Mook 1994). Equilibrium fractionation factors defined as: $\alpha_{eq} = R_{dissolved}/R_{gas} = \alpha_{ev}/\alpha_{in}$

Invasion	
$\alpha_{in}{}^{15}$	1.0000
$\alpha_{in}{}^{18}$	0.9992
Evasion	
$\alpha_{ev}{}^{15}$	0.9993
$\alpha_{ev}{}^{18}$	0.9981
Equilibrium	
$\alpha_{eq}{}^{15}$	0.99925
$\alpha_{eq}{}^{18}$	0.99894

These fractionation factors are not temperature dependant over the range of 0 to 44.5°C (Inoue and Mook 1994). The equilibrium fractionation factors (α_{eq}^{15} and α_{eq}^{18}) can be used to predict the isotopic ratios of dissolved N_2O for a solution in equilibrium with the atmosphere. The $\delta^{15}N$ and $\delta^{18}O$ of tropospheric N_2O is 6.72‰ +/- 0.12 and 44.62‰ +/- 0.21, respectively (Kaiser et al. 2003). An equilibrium saturated solution will be slightly enriched in ^{15}N and ^{18}O relative to tropospheric N_2O, with a $\delta^{15}N$ and $\delta^{18}O$ of 7.48‰ and 45.73‰, respectively.

The net N_2O flux from the atmosphere into the dissolved phase can be calculated (equation 4.9).

$$N_2O\ \text{Flux} = K\left(P_{N_2O} K_h - [N_2O]_{dissolved}\right) \tag{4.9}$$

Where the N_2O flux is calculated in $mol \cdot m^{-2} \cdot h^{-1}$, K is the gas exchange coefficient ($m \cdot h^{-1}$), P_{N2O} is the partial pressure of tropospheric N_2O (atm), K_h is the Henry's constant for N_2O ($mol \cdot atm^{-1} \cdot m^{-3}$), and $[N_2O]_{dissolved}$ is the dissolved concentration of N_2O ($mol \cdot m^{-3}$). In SIDNO, P_{N2O} is constant, while the value of K is set by the user, and the value for K_h is calculated as a function of water temperature, which is also set by the user (adapted from Gevantman 2008):

$$K_h = 55394 \times e^{\left(-60.7467 + \frac{8882.8}{T} + 21.2531 \ln \frac{T}{100}\right)} \tag{4.10}$$

where T is water temperature (K) and K_h is expressed in $mol \cdot atm^{-1} \cdot m^{-3}$.

Gas exchange is a two-way process, and the net N_2O flux is the difference between the invasion rate of gaseous N_2O into solution, and the evasion rate of dissolved N_2O into the gas phase. Since the concentration of tropospheric N_2O (P_{N2O}) is relatively

constant with time, the absolute invasion rate of gaseous N_2O into solution is also constant with time (assuming K and K_h are constant) and is not influenced by the concentration of dissolved N_2O. However, the net flux rate (the difference between the invasion and evasion rates) does depend on the concentration of dissolved N_2O. The evasion rate of N_2O out of solution is a first order function of dissolved N_2O concentration. When a solution is at equilibrium with the atmosphere, the invasion and evasion rates will be equal, and the net flux will be zero.

As with the bulk N_2O flux, the flux of the heavy isotopologues ($^{15}N_2O$ and $N_2{}^{18}O$) can be calculated by including the kinetic fractionation factors for N_2O (adapted from Venkiteswaran et al. 2007)

$$\text{Flux } {}^{15}\text{N}_2\text{O} = K\left(\alpha_{in}^{15}\text{P}_{{}^{15}\text{N}_2\text{O}}\text{K}_\text{h} - \alpha_{ev}^{15}[{}^{15}\text{N}_2\text{O}]_{dissolved}\right) \quad (4.12)$$

$$\text{Flux } \text{N}_2{}^{18}\text{O} = K\left(\alpha_{in}^{18}\text{P}_{\text{N}_2{}^{18}\text{O}}\text{K}_\text{h} - \alpha_{ev}^{18}[\text{N}_2{}^{18}\text{O}]_{dissolved}\right) \quad (4.13)$$

Where, P_{15N2O} and P_{N218O} are calculated by multiplying the partial pressure of tropospheric N_2O (atm) by $^{15}N/^{14}N$ and $^{18}O/^{16}O$ ratios of tropospheric N_2O. The ^{15}N and ^{18}O isotopic ratios of the N_2O flux can then be calculated:

$$R_{flux}^{15} = \frac{\text{Flux } {}^{15}\text{N}_2\text{O}}{\text{Flux } {}^{14}\text{N}_2\text{O}} = \frac{\text{Flux } {}^{15}\text{N}_2\text{O}}{\left(\text{Flux } \text{N}_2\text{O} - \text{Flux } {}^{15}\text{N}_2\text{O}\right)} \quad (4.14)$$

$$R_{flux}^{18} = \frac{\text{Flux } \text{N}_2{}^{18}\text{O}}{\text{Flux } \text{N}_2{}^{16}\text{O}} = \frac{\text{Flux } \text{N}_2{}^{18}\text{O}}{\left(\text{Flux } \text{N}_2\text{O} - \text{Flux } \text{N}_2{}^{18}\text{O}\right)} \quad (4.15)$$

4.2.3 Model Testing

To test the ability of SIDNO to reproduce observed data, input parameters were set to replicate a series of experiments that were conducted by Inoue & Mook (1994) to

derive empirical kinetic enrichment factors for N_2O gas exchange. In these experiments, degassed water was exposed to N_2O gas in a sealed container for varying lengths of time. At the end of each experiment, the N_2O concentration and isotopic composition in the gaseous and dissolved phases were measured.

The initial dissolved N_2O concentration and production rate were both set to zero. The model was then run and the model output was allowed to come into steady state. The results were then superimposed on the Inoue & Mook experimental results (Figure 4.2).

As expected, the modeled dissolved N_2O concentration and isotopic ratios increased in response to gas exchange. The model output closely matched the experimental results. The model fit to the experimental data is not accurately reflected by the r^2 values (r^2= 0.76 for $\delta^{15}N$ and 0.78 for $\delta^{18}O$), since there is a large amount of scatter in the experimental data. When the dissolved N_2O concentration was close to zero, the isotopic composition of the invading N_2O was a function solely of the kinetic fractionation factors for invasion of N_2O (α_{in}^{15} =1.000 and α_{in}^{18} =0.9992). As a result, the initial isotopic composition of dissolved N_2O was identical to the $\delta^{15}N$ of tropospheric N_2O, but was slightly depleted with respect to $\delta^{18}O$. As the dissolved N_2O approached the equilibrium saturation, the isotopic composition became slightly enriched in both $\delta^{15}N$ and $\delta^{18}O$ with respect to tropospheric N_2O. At chemical and isotopic equilibrium, the rates of N_2O invasion and evasion are equal for each isotopologue. Therefore, the isotopic composition of dissolved N_2O at equilibrium is determined by the equilibrium fractionation factors, defined by the ratios of the evasion and invasion fractionation factors. ($\alpha_{eq}^{15} = \alpha_{ev}^{15}/\alpha_{in}^{15}$ =0.99925 and $\alpha_{eq}^{18} = \alpha_{ev}^{18}/\alpha_{in}^{18}$ =0.99894). The model successfully simulates the kinetic and equilibrium stable isotope fractionation

during both equilibrium and non equilibrium gas exchange under the experimental conditions of Inoue & Mook (1994).

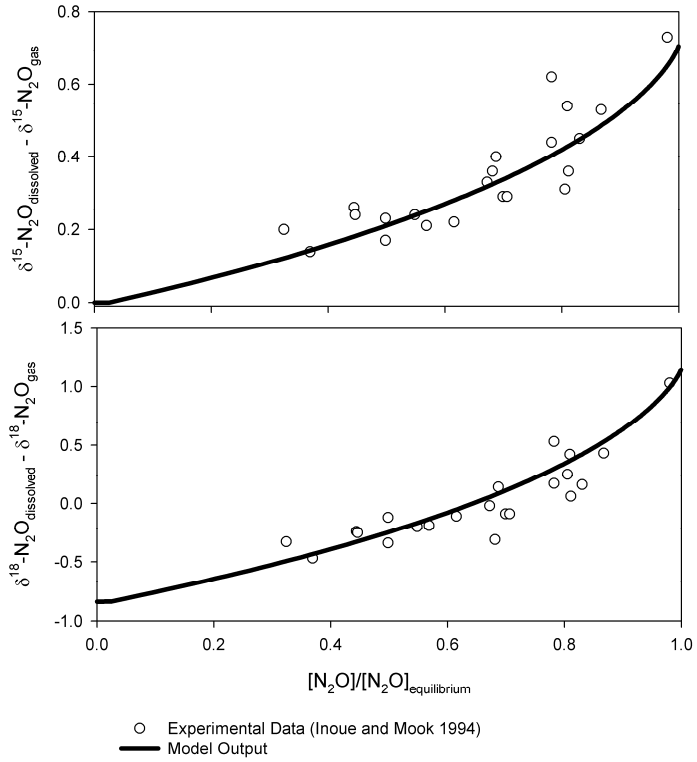

Figure 4.2: Comparing the model output to the experimental data of Inoue and Mook (1994). $R^2 = 0.76$ for $\delta^{15}N$ and 0.78 for $\delta^{18}O$. Precision of measurements for the experimental data is ± 0.05‰ for $\delta^{15}N$ and ± 0.1‰ for $\delta^{18}O$.

4.3 Model Predictions

The SIDNO model was used to make predictions about the stable isotope dynamics of N_2O in a variety of situations that may be encountered in aquatic environments. These predictions will help to elucidate the relationship between source, dissolved, and emitted N_2O in these environments.

4.3.1 Gas Exchange Trajectories

SIDNO was used to investigate the relationship between the stable isotope composition of dissolved and emitted N_2O in the absence of N_2O production. This was

done to provide insight into how the $\delta^{15}N$ and $\delta^{18}O$ of dissolved N_2O and the emitted N_2O flux change with time as a supersaturated N_2O solution is allowed to come to equilibrium with the atmosphere. The output from two model runs with the same initial N_2O concentration but different initial isotopic compositions of dissolved N_2O is shown in Figure 4.3.

As the initially supersaturated solution comes to equilibrium with the atmosphere, the dissolved N_2O concentration decreases, and the $\delta^{15}N$ and $\delta^{18}O$ approach the equilibrium saturated values. The instantaneous values of $\delta^{15}N$ and $\delta^{18}O$ of the emitted N_2O remains relatively constant with time when the solution remains very supersaturated (>300% saturation), but increases rapidly as the concentration approaches 100% saturation. Because the light isotopologue diffuses out of solution faster than the heavy isotopologue, the instantaneous values of $\delta^{15}N$ and $\delta^{18}O$ of the emitted N_2O are more negative than the instantaneous dissolved composition. The cumulative composition of the emitted N_2O does not necessarily have the same $\delta^{15}N$ and $\delta^{18}O$ of the initial dissolved N_2O. The total mass of N_2O emitted is not equal to the mass originally in solution, because the concentration is not zero at equilibrium. The various isotopologues of N_2O will reach equilibrium independently of each other, and therefore the total mass emitted for each isotopologue will depend on the initial concentration and isotopic ratios relative to the equilibrium values. However, if the initial concentration of dissolved N_2O is high (>1000% saturation), these effects will be minor, and the cumulative isotopic composition of emitted N_2O will be similar to the initial composition of dissolved N_2O.

The gas exchange coefficient K does not affect the isotopic gas exchange trajectories, only the speed at which the solution reaches equilibrium.

The curvature of the trajectories on the $\delta^{15}N$ vs $\delta^{18}O$ plot (Figure 4.3C) is influenced by the initial N_2O concentration. Qualitatively, a higher initial concentration will result in more curvature. This curvature is related to the difference in slope of the dissolved $\delta^{15}N$-N_2O vs concentration curve (Figure 4.3A) relative to the $\delta^{18}O$-N_2O vs concentration curve (Figure 4.3B).

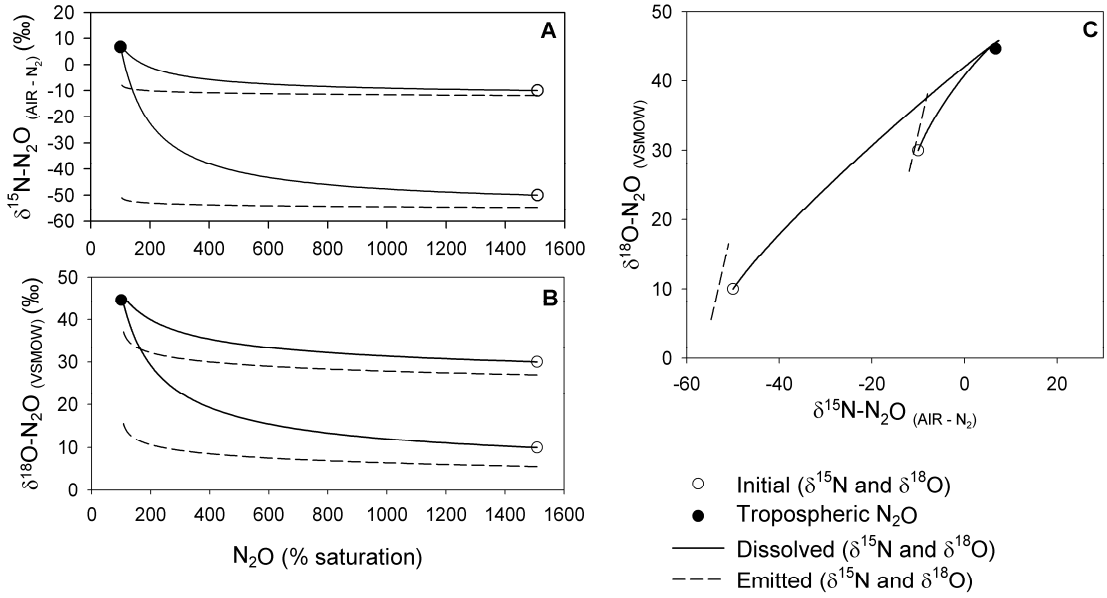

Figure 4.3: $\delta^{15}N$ and $\delta^{18}O$ trajectories for dissolved and emitted N_2O in two supersaturated solutions with zero N_2O production. Initial dissolved isotopic values for the two dissolved N_2O solutions were $\delta^{15}N$ = -50‰, $\delta^{18}O$ = 10‰, and $\delta^{15}N$ = -10‰, $\delta^{18}O$ = 30‰. Both runs used an initial dissolved N_2O concentration of 1500% saturation. Note that in the $\delta^{15}N$ vs. $\delta^{18}O$ plot, the dissolved N_2O curves do not pass through the tropospheric N_2O value due to the small equilibrium isotope effect.

4.3.2 Steady State Production

During the steady state production of N_2O (i.e. at a constant rate and with a constant isotopic composition), the isotopic composition of the emitted N_2O is equal to the isotopic composition of the N_2O source once steady state is achieved. However, the

isotopic composition of dissolved N_2O is not equal to that of the source (or emitted) N_2O, because it is altered by equilibration with tropospheric N_2O. The isotopic contribution of tropospheric N_2O becomes more important as the dissolved concentration approaches the equilibrium saturated value.

SIDNO was used to simulate the $\delta^{15}N$ and $\delta^{18}O$ of dissolved N_2O in a system open to gas exchange with the atmosphere with production of N_2O at a constant rate and isotopic composition. The model output for concentration, $\delta^{15}N$ and $\delta^{18}O$ was allowed to come to steady state and this procedure was repeated several times, altering the production rate but keeping the isotopic composition of the source constant.

The equilibration with tropospheric N_2O had a dramatic effect on the $\delta^{15}N$ and $\delta^{18}O$ of dissolved N_2O, especially at low concentrations (Figure 4.4). As production rate and concentration increases, the dissolved $\delta^{15}N$ and $\delta^{18}O$ in the model approach a value (represented by a "*") that is not equal to that of the source. At very high production rates, the contribution of tropospheric N_2O is insignificant relative to the production rate of N_2O, however the $\delta^{15}N$ and $\delta^{18}O$ of dissolved N_2O are still slightly enriched relative to the source because the heavy isotopologues are preferentially retained in solution. This effect is controlled by α^{15}_{ev} and α^{18}_{ev}, as a result, the $\delta^{15}N$ and $\delta^{18}O$ values for dissolved N_2O will always be offset by at least 0.7‰ and 1.9‰ respectively from that of the source.

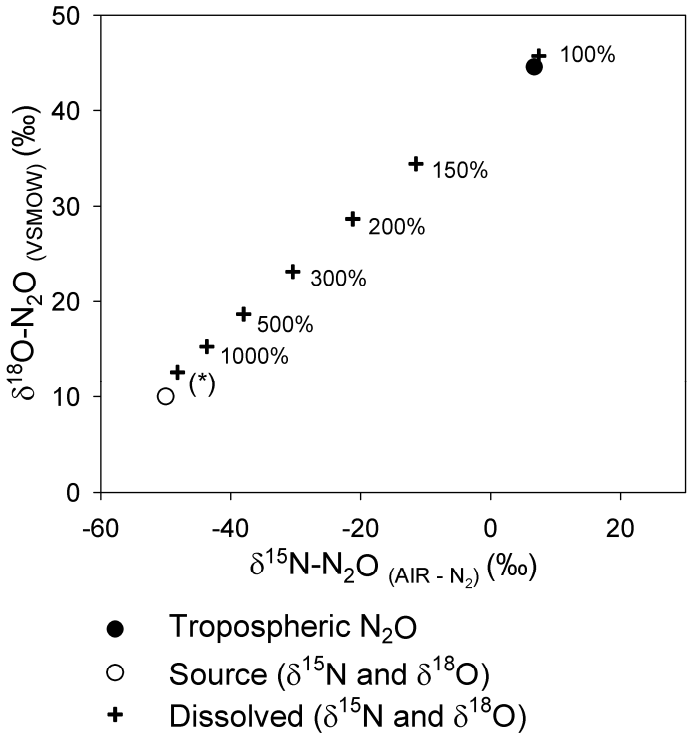

Figure 4.4: The relationship between $\delta^{15}N$, $\delta^{18}O$ and N_2O concentration in a system at steady state with constant N_2O production and open to gas exchange with the atmosphere. The point marked with a (*) represents the minimum difference between the isotopic composition of dissolved and source N_2O. The point at 100% saturation is the equilibrium value, the $\delta^{15}N$ and $\delta^{18}O$ of this point is controlled by the isotopic composition of tropospheric N_2O and the equilibrium enrichment factors.

4.3.3 Variable Production of N_2O

Compared to steady state production, the relationship between $\delta^{15}N$ and $\delta^{18}O$ of source, dissolved and emitted N_2O are much more complicated when N_2O production is variable. N_2O production can be variable with respect to either production rate or isotopic composition, or both. In many environments, N_2O production is not constant. The N_2O production processes nitrification and denitrification are sensitive to redox conditions. In many aquatic systems, the redox conditions are highly variable, due to diel changes in dissolved oxygen concentration driven by photosynthesis during the day and respiration at night. For example, Laursen & Seitzinger (2004) observed diel changes in the

denitrification rate in the Iroquois River and Sugar Creek (Midwestern USA), and found that the denitrification rates were consistently higher during the day compared to the night. Also, since the processes of nitrification and denitrification are sensitive to redox conditions, the dominant N_2O production process can change in response to the diel oxygen cycle. For example, Harrison et al. (2005) observed a diel change from nitrification during the day to denitrification during the night in a subtropical eutrophic stream. Since the fractionation factors and substrates are different for these two processes, the isotopic composition of N_2O produced in such systems is not constant. In many situations, it is likely that both the N_2O production rate and the isotopic composition of the source would vary with time in response to the diel oxygen cycle.

To simulate the variable production of N_2O driven by diel changes in dissolved oxygen concentration, various scenarios were run while changing either production rate or isotopic composition or both over diel time periods. These input parameters with diel variation were driven by a sine function with a 24 hour period, so as to mimic the diel DO cycle. The range used for production rate in the model was based on a review of relevant literature data (Table 4.2). The published data on N_2O flux rates was used as a proxy indicator of N_2O production rates in theses environments. In the following scenarios, the N_2O production rates ranged from 1 to 5 $\mu mol/m^2/hour$ (Table 4.3), which is intermediate in range between the diel variation in N_2O flux observed by Clough et al. (2007) and Harrison et al (2005).

The value of K was varied between 0.1 and 0.3 m/day (Table 4.3). These values were within the range that have been observed in other studies (Table 4.2). The combination of production rates and K values were chosen to produce N_2O

concentrations ranging between 150 to 500 % saturation (Table 4.3). This concentration range was selected because it falls within the range of published data (Table 4.2) and the isotope effects of gas exchange on dissolved N_2O are the greatest in this range (Figure 4.4).

The range in $\delta^{15}N$ and $\delta^{18}O$ used as the input values for the N_2O source (Table 4.3) falls well within the range of published values for N_2O collected in various field studies (Rock et al 2007). For scenarios where the isotopic composition of the source N_2O was variable, the sine function for $\delta^{15}N$ and $\delta^{18}O$ was synchronized, with maximum and minimum values coinciding. This was done for simplicity, and since $\delta^{15}N$ and $\delta^{18}O$ are independent values, any combination of source values would give the same result. The following parameters were held constant across comparisons, unless otherwise stated: temperature of 20°C, depth of 1m, and surface area subject to gas exchange of $1m^2$. Model scenarios were run until the output parameters reached dynamic steady state (i.e., model parameters were not constant over the 24 hour period, but repeated in successive diel cycles). Model results are summarized in Table 4.4.

Table 4.2: Summary of relevant published data on N_2O production in aquatic environments.

Location	N_2O Concentration (range) % saturation	N_2O Flux (range) μmol/m^2/hour	K (range) m/h	Reference
LII River, New Zealand	201 to 404	1.35 to 17.9	0.13 to 0.82	Clough et al. 2006
LII River, New Zealand	402 to 644	0.46 to 0.89	14.76	Clough et al. 2007
Agricultrual Stream, UK	100 to 630	0 to 37.5	-	Reay et al. 2003
Bang Nara River, Thailand	170 to 2000	-	-	Boontanon et al. 2000
Seine River, France	-	2.2 to 5.2	0.04 to 0.06	Garnier et al. 2006
Canal Two, Yaqui Valley, Mexico	100 to 6000	0 to 34.9	0.3 to 0.6	Harrison et al. 2005
Grand River, Ontario, Canada	100 to 8540	0 to 69.8	0.06 to 0.35	Rosamond et al (Unpublished Data)

Table 4.3: Summary of input parameters SIDNO model scenarios for non-steady state production of N_2O. If an input parameter was variable with time, the maximum and minimum values are given. *Maximum production rate coincides with the most depleted $\delta^{15}N$ and $\delta^{18}O$ values of the source. **Maximum production rate coincides with the most enriched $\delta^{15}N$ and $\delta^{18}O$ values of the source.

		N_2O Source	
Scenario #	**K**	**Production Rate**	**($\delta^{15}N$, $\delta^{18}O$)**
	(m/h)	μmol/m^2/h	permil
Variable Production Rate, Constant Isotopic Composition of Source			
1	0.3	1 to 5	(-50, 10)
2	0.1	1 to 5	(-50, 10)
Constant Production Rate, Variable Isotopic Composition of Source			
3	0.3	3	(-50, 10) to (-10, 30)
4	0.1	3	(-50, 10) to (-10, 30)
Variable Production Rate, Variable Isotopic Composition of Source			
5*	0.3	1 to 5	(-50, 10) to (-10, 30)
6**	0.3	1 to 5	(-50, 10) to (-10, 30)
7*	0.1	1 to 5	(-50, 10) to (-10, 30)

Table 4.4: Summary of SIDNO output for model scenarios simulating non-steady state production of N_2O. If an output parameter was variable with time, the maximum and minimum values are given. *Maximum production rate coincides with the most depleted $\delta^{15}N$ and $\delta^{18}O$ values of the source. **Maximum production rate coincides with the most enriched $\delta^{15}N$ and $\delta^{18}O$ values of the source. $\Delta\ \delta^{15}N$ and $\Delta\ \delta^{18}O$ are the maximum difference between the range of source N_2O and the range for the model output parameter.

	Dissolved N_2O				**Emitted N_2O**		
Scenario #	**Concentration**	**($\delta^{15}N$, $\delta^{18}O$)**	**$\Delta\ \delta^{15}N$**	**$\Delta\ \delta^{18}O$**	**($\delta^{15}N$, $\delta^{18}O$)**	**$\Delta\ \delta^{15}N$**	**$\Delta\ \delta^{18}O$**
	% SAT	‰	‰	‰	‰	‰	‰
Variable Production Rate, Constant Isotopic Composition of Source							
1	153 to 263	(-27.8, 24.6) to (-12.1,34.4)	37.9	24.4	(-49.6, 9.5) to (-50.2, 11.1)	0.2	0.5
2	345 to 501	(-38.1, 18.4) to (-32.8, 22.1)	17.2	12.1	(-50.1, 9.6) to (-49.8, 10.6)	0.1	0.6
Constant Production Rate, Variable Isotopic Composition of Source							
3	208	(-19.6, 29.4) to (-3.7 to 37.4)	30.4	19.4	(-45.3, 12.3) to (-14.7, 27.7)	4.7	2.3
4	423	(-26.1, 24.8) to (-15.1, 30.3)	23.9	14.8	(-37.2, 16.4) to (-22.8, 23.6)	12.8	6.4
Variable Production Rate, Variable Isotopic Composition of Source							
5*	153 to 263	(-25.8, 25.6) to (-1.2, 39.8)	24.2	15.6	(-46.9, 11.3) to (-18.0, 26.5)	8	3.5
6**	153 to 263	(-11.2, 33.8) to (-5.0, 36.1)	38.8	23.8	(-41.6, 14.6) to (-13.4, 28.1)	8.4	4.6
7*	345 to 501	(-31.6, 21.6) to (-18.4, 29.3)	18.4	11.6	(-42.1, 13.7) to (-29.4, 20.6)	19.4	9.4

In scenario #1 (Table 4.3), the isotopic composition of source N_2O was held constant and production rate was variable. An example of such a system may be N_2O production through denitrification in sediments in a river with abundant NO_3^-. Denitrification rates in rivers have been observed to fluctuate in response to the diel dissolved oxygen cycle (Laursen & Seitzinger 2004). If the fractionation factors for denitrification are constant and not dependent on rate, the resulting N_2O production rate would be variable, but the isotopic composition of the produced N_2O would be constant.

In model scenario #1, the maximum concentration lagged approximately 2.75 hours behind the maximum N_2O production rate. The values for the emitted N_2O were relatively constant and always nearly equal to that of the source within (within 0.4‰ for $\delta^{15}N$ and 1.1‰ for $\delta^{18}O$, Figure 4.5, Table 4.4). However, the $\delta^{15}N$ and $\delta^{18}O$ values for dissolved N_2O were more variable, varying by approximately 16‰ and 10‰ for $\delta^{15}N$ and $\delta^{18}O$ respectively. These results indicate that a change in the isotopic composition of dissolved N_2O can be driven simply by a change in production rate (and therefore concentration) rather than by a change in the isotopic signature of the source.

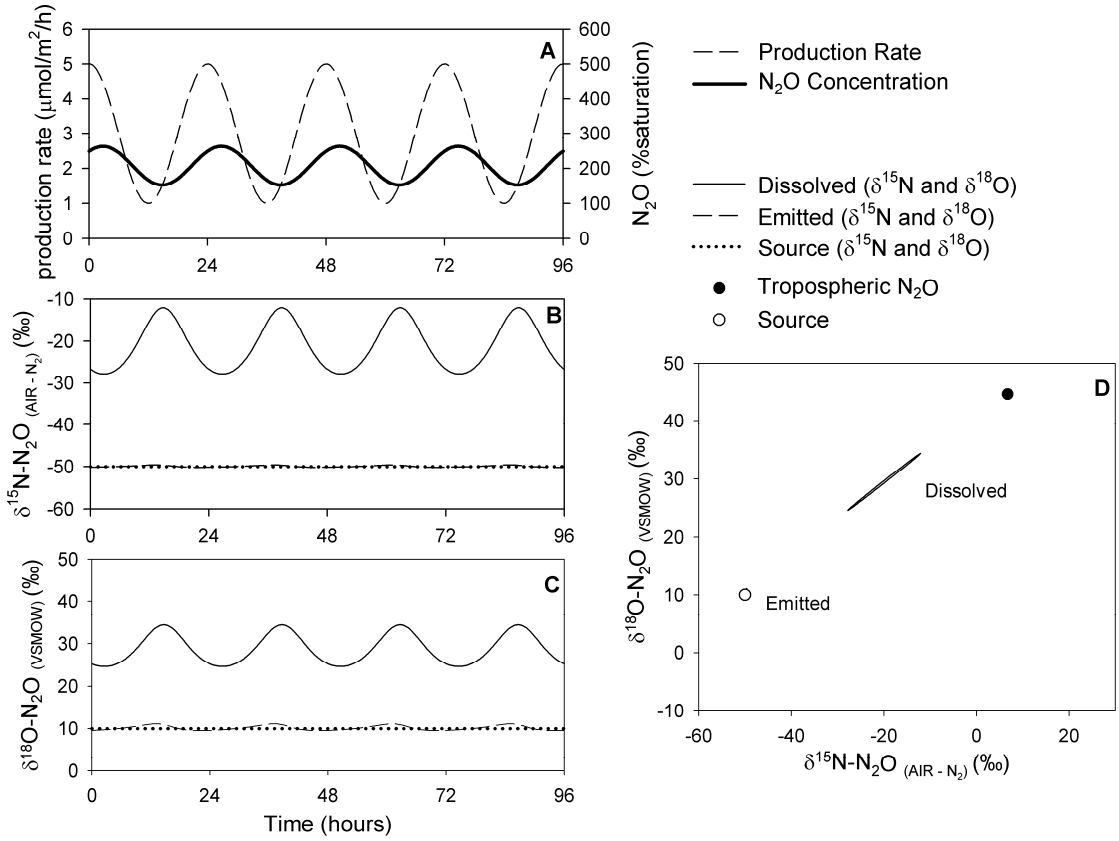

Figure 4.5: Model scenario #1, the isotopic composition of dissolved and emitted N_2O with a variable production rate and constant isotopic composition of the source. Note, figure 4.5 D, the data points for emitted N_2O are masked by the data point for source N_2O.

In scenario #2, the effect of altering K was investigated. When K was altered in this scenario, the isotopic composition of emitted N_2O remained relatively constant and

nearly equal to that of the source (Table 4.4). However, as K was decreased, the lag time between the maximum N_2O production rate and the maximum N_2O concentration increased. Also, since the dissolved N_2O concentration is a function of the ratio of production rate to K, the system was able to sustain a higher N_2O concentration for the same production rate. Therefore, the isotopic composition of dissolved N_2O was closer to that of the source, since the contribution of tropospheric N_2O was not as significant relative to the total mass of dissolved N_2O present. Also, the total range for $\delta^{15}N$ and $\delta^{18}O$ in dissolved N_2O was reduced when compared to scenario #1.

SIDNO was used to investigate the stable isotope dynamics of dissolved N_2O in the case where the production rate is constant, but the isotopic composition of the source is changing with time. In rivers or lakes that do not have a strong diel DO cycle, denitrification in the sediments would be expected to produce N_2O at a generally constant rate. However, the isotopic composition of the source N_2O may change if that of the nitrate substrate is not constant with time. For example, many studies have shown that the isotopic composition of residual nitrate becomes more enriched in both $\delta^{15}N$ and $\delta^{18}O$ as it is consumed during denitrification (e.g. Mengis et al. 1999). The following model runs were used to simulate this situation.

In model scenario #3, when the N_2O production rate was held constant, and the isotopic signature of the source was variable with time, the isotopic composition of the emitted N_2O was again much closer to the composition of the source compared that of the dissolved N_2O (Figure 4.6, Table 4.4). The difference between the maximum and minimum $\delta^{15}N$ and $\delta^{18}O$ values for the emitted and source N_2O was 4.7‰ and 2.3 ‰

respectively. However, since the N_2O flux is driven by the dissolved composition, the emitted $\delta^{15}N$ and $\delta^{18}O$ also lagged 2.75 hours behind that of the source. Since the system is at dynamic steady state, the average $\delta^{15}N$ and $\delta^{18}O$ of the emitted N_2O is identical to the average isotopic composition of the source. This must be true in all cases to conserve mass of N_2O produced.

To examine the effects of varying K it was reduced from 0.3 to 0.1 m/hour in model scenario #4 (Figure 4.7, Table 4.4). All other parameters were the same as model scenario #3.

The isotopic values for the emitted N_2O are centred between those of the source N_2O, but the values for the dissolved N_2O are offset by some amount towards the $\delta^{15}N$ and $\delta^{18}O$ values for tropospheric N_2O (Figure 4.7 D). This offset is the same as seen in steady state N_2O production (Figure 4.4). In scenario #4, the average $\delta^{15}N$ and $\delta^{18}O$ values for the source and the dissolved N_2O, follow a similar pattern as seen in Figure 4.4. The relationship between these average values for source and dissolved N_2O depend on the concentration of dissolved N_2O, and therefore the relative importance of equilibration with tropospheric N_2O compared to the production of N_2O. The slope of the line connecting the dissolved N_2O isotope data points is always the same as the slope of the line connecting the source data points. Therefore, if the slope of the line connecting the dissolved N_2O isotope data points does not trend through the value for tropospheric N_2O, there must be a variation in the isotopic composition of the source N_2O.

Again, in scenario #4, since concentration is a function of the ratio of production rate to K, the effect of reducing K was to support a higher concentration with the same production rate, and to cause the $\delta^{15}N$ and $\delta^{18}O$ of the dissolved N_2O to be closer to that

of the source as compared to the previous example. Increasing the production rate while keeping K fixed would have produced the same effect. Reducing K also tends to dampen the response of the instantaneous $\delta^{15}N$ and $\delta^{18}O$ of the emitted N_2O to changes in the isotopic composition of the source. The lag time between the isotopic composition of the source and emitted N_2O increased as K decreased. Also the difference between the maxima and minima of the source and emitted $\delta^{15}N$ and $\delta^{18}O$ increased. In scenario #4, lag time increased to 4.75 hours, and the maximum difference between the source and emitted $\delta^{15}N$ and $\delta^{18}O$ maxima and minima increased to 12.8 and 6.4 respectively.

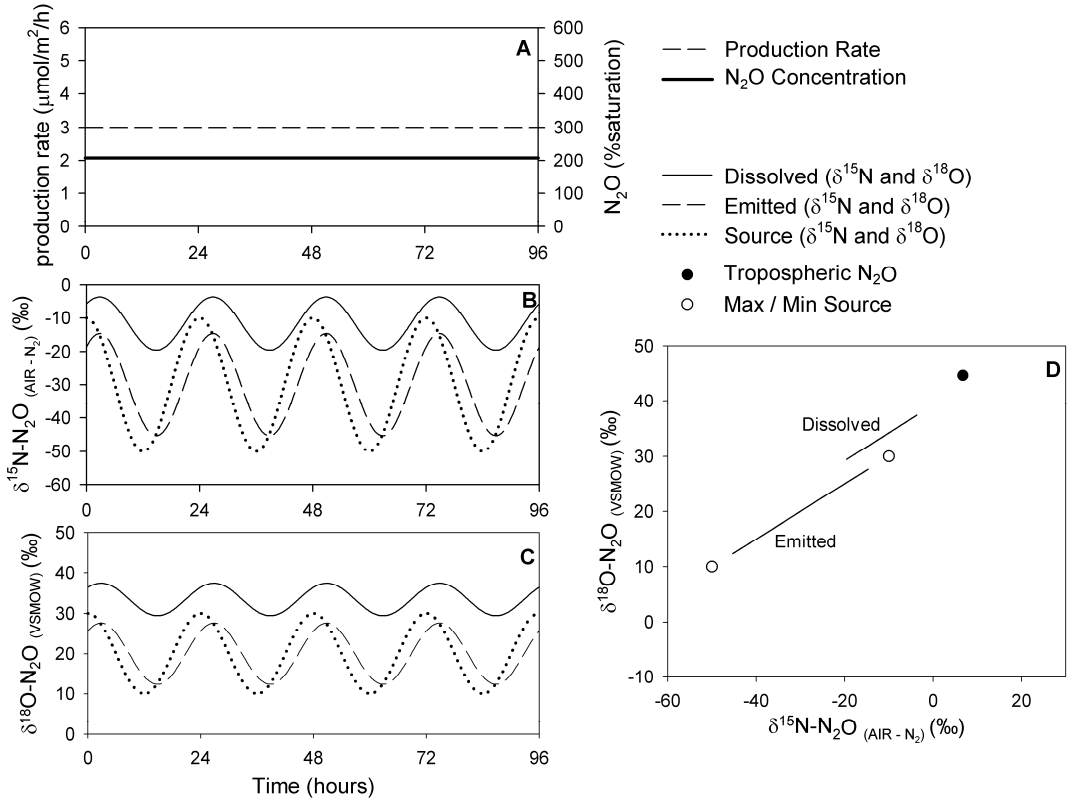

Figure 4.6: Model scenario #3 -Isotopic composition of dissolved and emitted with a constant production rate and variable isotopic composition of the source.

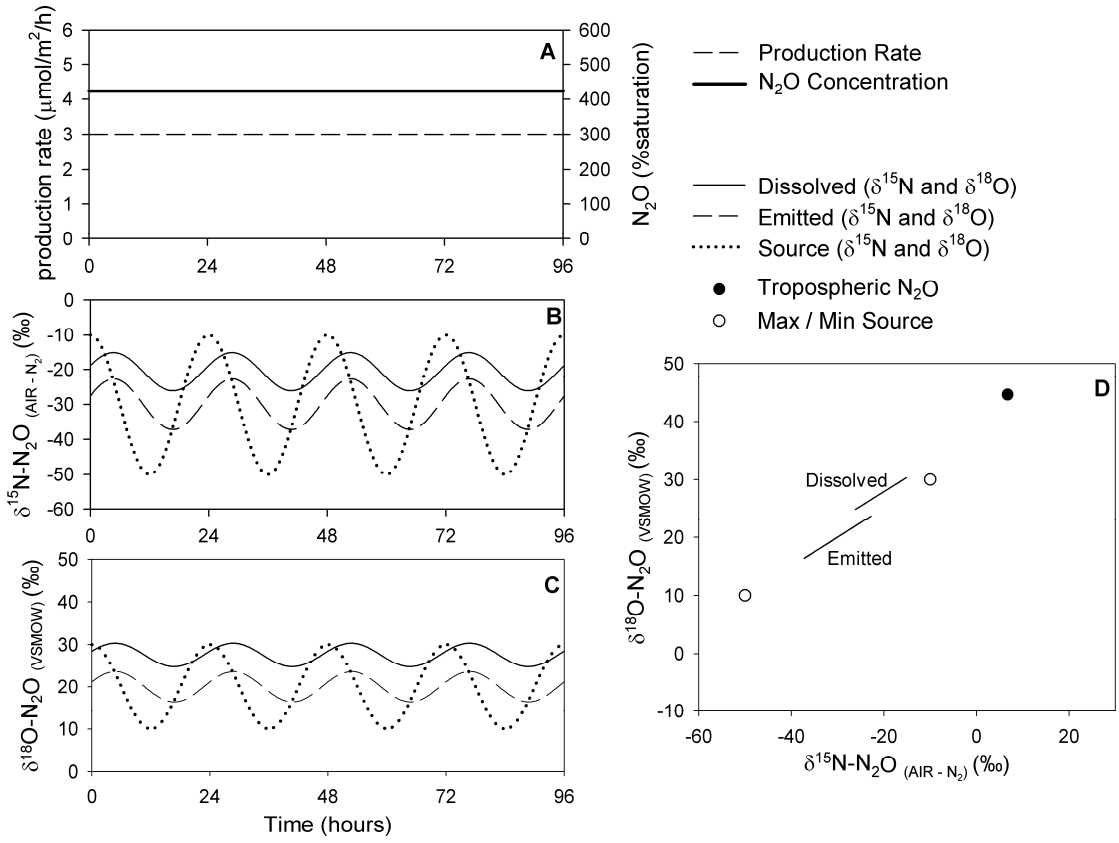

Figure 4.7: Model scenario #4 - Isotopic composition of dissolved and emitted N_2O with a constant production rate and variable isotopic composition of the source. K is reduced from 0.3 m/h to 0.1 m/h.

To simulate a system alternating between two N_2O production processes (such as nitrification and denitrification) that have different rates of N_2O production and different isotopic compositions, the model was run with both the production rate and the isotopic composition variable with time (model scenario #5). The production rate was timed so that the maximum production rate coincided with the most depleted $\delta^{15}N$ and $\delta^{18}O$ values for the source N_2O.

The resulting N_2O concentrations were identical to those in model scenario #1, with the maximum concentration lagging approximately 2.75 hours behind the maximum production rate (Figure 4.8, Table 4.4). The relationship between the $\delta^{15}N$ and $\delta^{18}O$ of the

dissolved and emitted N_2O were more complex than in the other model scenarios. The shape of the dissolved and emitted N_2O $\delta^{15}N$ and $\delta^{18}O$ curves were altered from a true sine curve. The lag time between the maximum $\delta^{15}N$ and $\delta^{18}O$ of the source and that of the dissolved and emitted N_2O (when the production rate was at a minimum) was 3.75 hours. The lag time between the minimum $\delta^{15}N$ and $\delta^{18}O$ of the source and that of the dissolved and emitted N_2O (when the production rate was at a maximum) was only 2.25 hours. The difference between the source and most positive emitted $\delta^{15}N$ was 8.0‰, while the difference between the minimum values was only 3.1‰. Similarly, the difference between the source and the maximum $\delta^{18}O$ for the emitted was 3.4‰, and for the minimums it was 1.3‰. In short, the isotopic composition of the emitted N_2O was closer to that of the source during periods coinciding with high production rates and thus higher concentrations, compared to periods of low production rates. However, the flux-weighted average $\delta^{15}N$ and $\delta^{18}O$ of emitted N_2O is equal to the average source composition weighted by production rate, because the system was at dynamic steady state.

To determine the effects of a high production rate with an isotopically enriched N_2O source, the timing of the maximum production rate was altered to coincide with the most enriched $\delta^{15}N$ and $\delta^{18}O$ values of the source in model scenario #6. All other parameters remained the same as in model scenario #5 (Table 4.4). The resulting pattern for the $\delta^{15}N$ and $\delta^{18}O$ of dissolved was very different than in model scenario #5 (Figure 4.9, Table 4.4). The dissolved N_2O concentrations were identical to the model scenario #5, but the $\delta^{15}N$ and $\delta^{18}O$ of dissolved N_2O was nearly constant. The relationship between the isotopic composition of emitted and source N_2O was the same as in the

previous example (scenario #5). The isotopic composition of the emitted N_2O was close to the source values, though it lagged behind by several hours.

In scenario #6, the $\delta^{15}N$ and $\delta^{18}O$ curves of the dissolved N_2O are greatly dampened by the equilibration with tropospheric N_2O. In the previous example (Figure 4.8), the equilibration with tropospheric N_2O and the isotopic composition of the source had an additive effect, and increased the amplitude of the oscillations of $\delta^{15}N$ and $\delta^{18}O$ in the dissolved N_2O. However, in scenario #6 (Figure 4.9), the two effects move the $\delta^{15}N$ and $\delta^{18}O$ of dissolved N_2O in opposite directions, and the result is a nearly constant $\delta^{15}N$ and $\delta^{18}O$ of dissolved N_2O.

To determine the effects of a lower K on model scenario #5, K was reduced from 0.3 from 0.1 m/hour in scenario #7. This had the effect of increasing the dissolved N_2O concentration compared to model scenario #5, and damping the oscillations in the $\delta^{15}N$ and $\delta^{18}O$ of the dissolved and emitted N_2O (Table 4.4, Figure 4.10).

In scenario #7, the lower K also dampened the oscillation in the $\delta^{15}N$ and $\delta^{18}O$ of the N_2O, and the lag time between the isotopic composition of emitted and source N_2O increased. As a result, there is a greater difference between the isotopic composition of the emitted and source N_2O than in model scenario #5 (Figure 4.10). As in scenario #5, the flux-weighted average $\delta^{15}N$ and $\delta^{18}O$ of emitted N_2O is equal to the average source composition weighted by production rate.

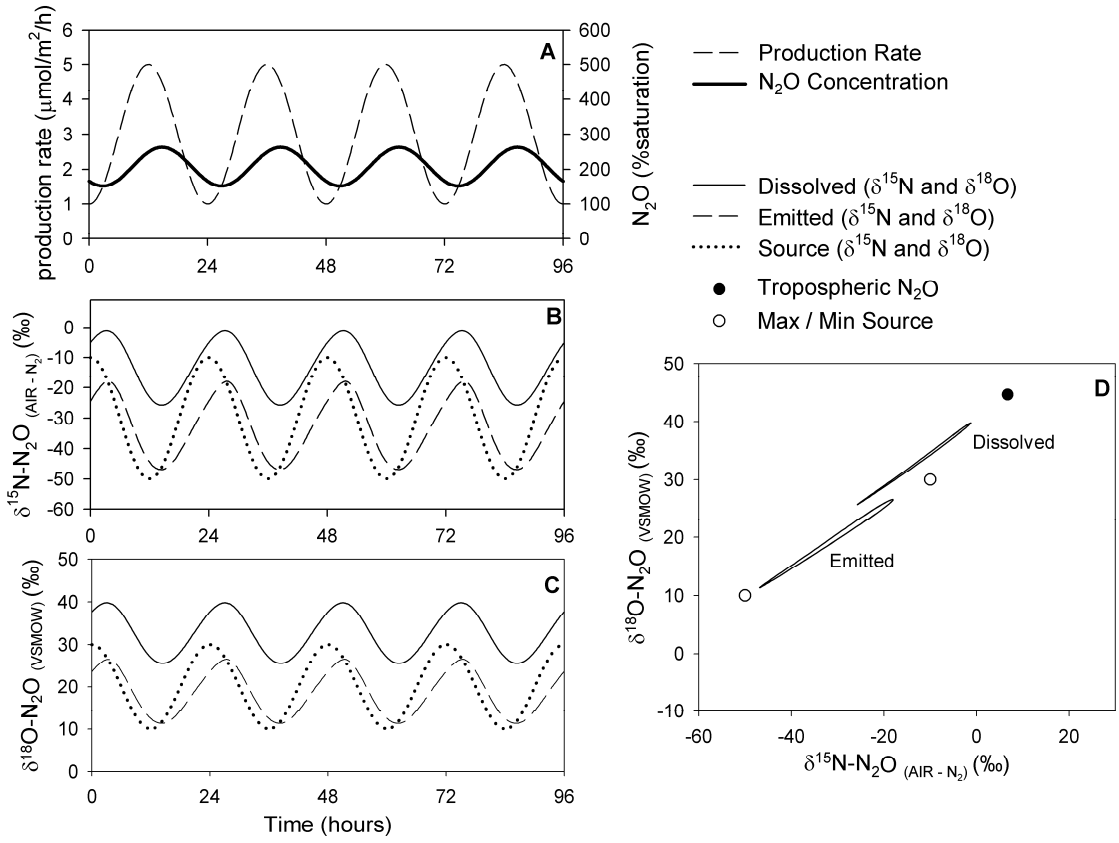

Figure 4.8: Model scenario #5 - Isotopic composition of dissolved and emitted N_2O with a variable production rate and variable isotopic composition of the source. Maximum production rate is in sync with the most depleted $\delta^{15}N$ and $\delta^{18}O$ of the source.

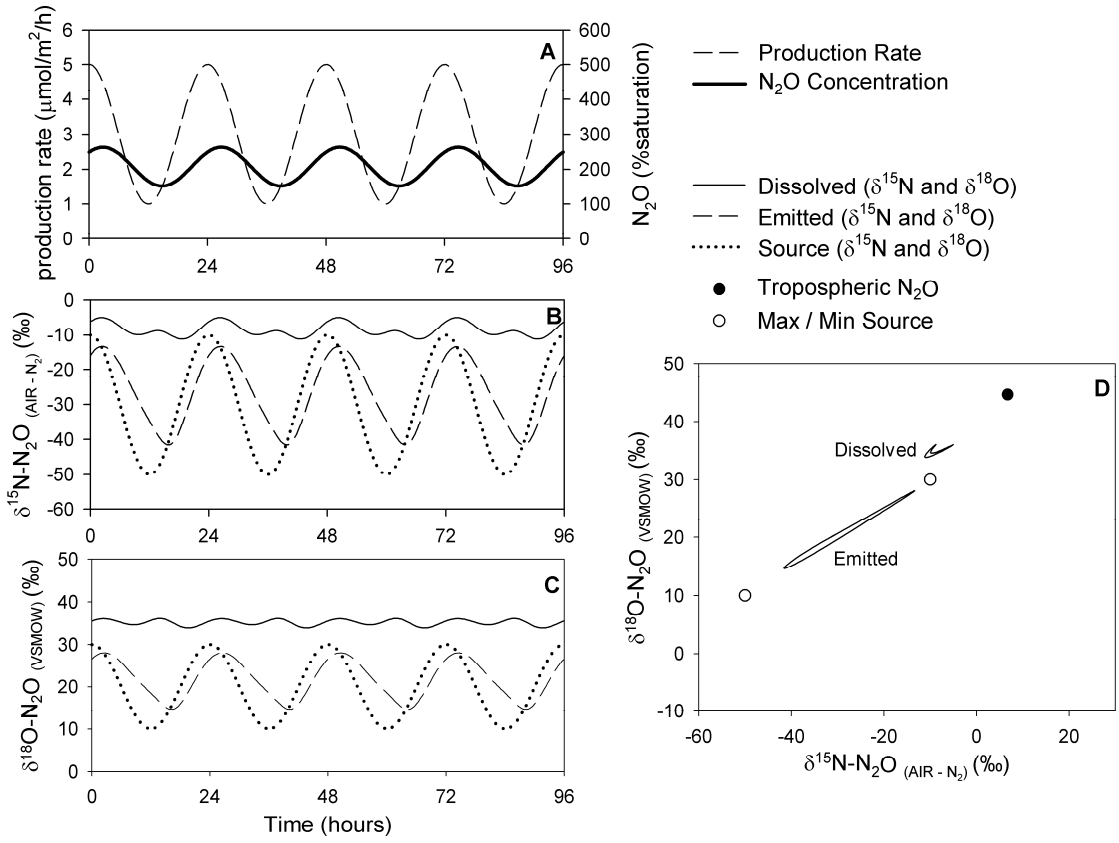

Figure 4.9: Model scenario #6 - Isotopic composition of dissolved and emitted N_2O with a variable production rate and variable isotopic composition of the source. Maximum production rate is in sync with the least depleted $\delta^{15}N$ and $\delta^{18}O$ of the source.

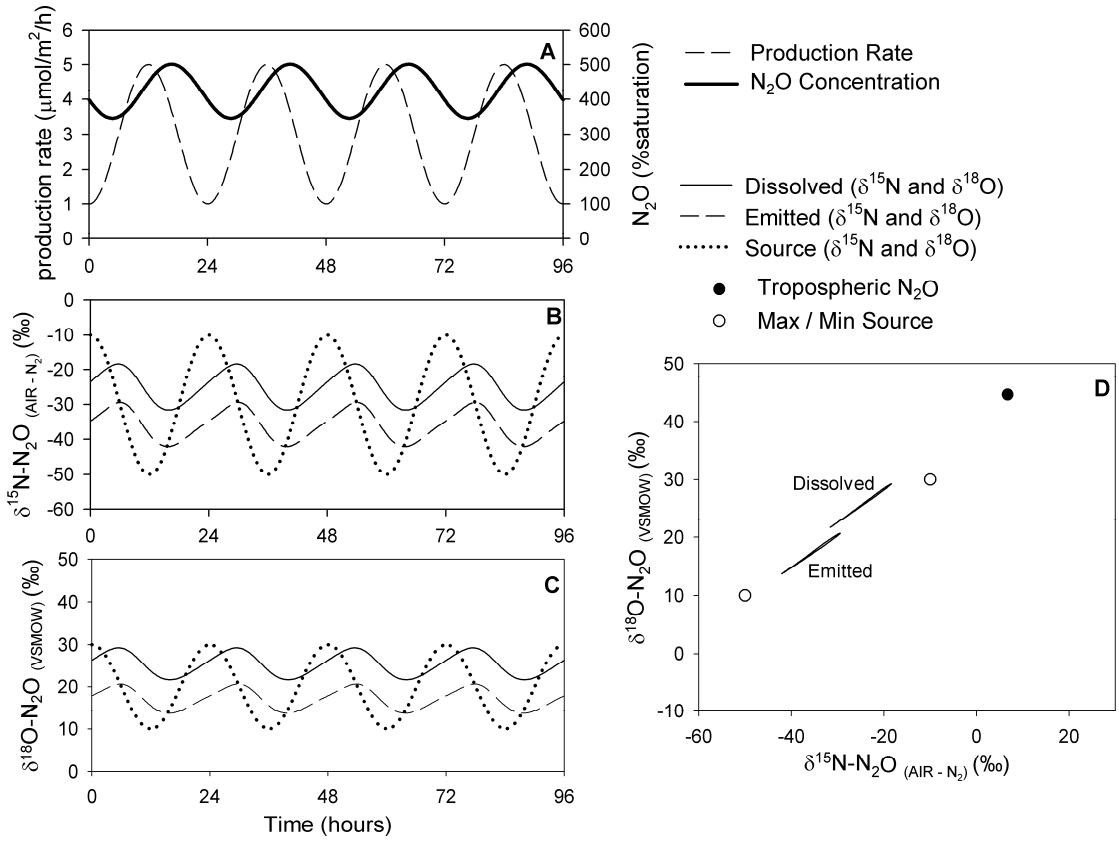

Figure 4.10: Model scenario #7 - Isotopic composition of dissolved N_2O and emitted N_2O with a variable production rate and variable isotopic composition of the source. Maximum production rate is in sync with the most depleted $\delta^{15}N$ and $\delta^{18}O$ of the source. K is reduced from 0.3 m/h to 0.1 m/h.

4.4 Discussion & Conclusions

The relationship between the isotopic composition of dissolved, source and emitted N_2O is complex for aquatic systems that are open to gas exchange with the atmosphere. The SIDNO model was able simulate this relationship, and provided additional insight into the stable isotope dynamics of dissolved N_2O.

For a solution with no N_2O production at equilibrium with tropospheric N_2O, the isotopic composition of dissolved N_2O will be slightly enriched with respect to tropospheric N_2O. At equilibrium, the rates of N_2O invasion into solution and evasion out of solution are equal. Therefore, the offset between the dissolved N_2O isotopic

composition and that of tropospheric N_2O is dictated by the ratios between the kinetic enrichment factors for evasion and invasion.

In a system at steady state with respect to rate of N_2O production and its isotopic composition, the $\delta^{15}N$ and $\delta^{18}O$ of dissolved N_2O are not directly indicative of the isotopic composition of the source N_2O. The difference between the isotopic composition of dissolved and source N_2O increases as the N_2O concentration decreases. This is because the equilibration with tropospheric N_2O becomes more important relative to the input of source N_2O from N_2O production. However, even at concentrations higher than 1000% saturation (resulting from either high production rates, low K, or both), the $\delta^{15}N$ and $\delta^{18}O$ of the dissolved N_2O will not be equal to that of the source, and will approach a value that is offset from the source composition by 0.7‰ and 1.9‰ for $\delta^{15}N$ and $\delta^{18}O$ respectively. This offset is a function of the $\alpha_{ev}{}^{15}$ and $\alpha_{ev}{}^{18}$ values, as determined by Inoue & Mook (1994). However, for a system at steady state with respect to N_2O production rate and the isotopic composition of the source, isotopic composition of the emitted N_2O is identical to that of the source, and is easily calculated from the concentration, $\delta^{15}N$ and $\delta^{18}O$ of dissolved N_2O (equations 4.11 to 4.14).

Calculating the isotopic composition of emitted N_2O also provides information about the composition of the source N_2O in systems that are not at steady state. If the concentration changes with time, the N_2O production rate must also changes with time (provided K and temperature are constant). However, a change in $\delta^{15}N$ or $\delta^{18}O$ of dissolved N_2O did not necessarily indicate a change in the isotopic composition of the source (Figure 4.5). If the change in $\delta^{15}N$ and $\delta^{18}O$ of dissolved N_2O is only a result of a change in N_2O concentration, the data points for dissolved N_2O on a $\delta^{15}N$ vs. $\delta^{18}O$ plot

will trend towards the equilibrium saturated value as the concentration falls. Additionally, a constant $\delta^{15}N$ and $\delta^{18}O$ of dissolved N_2O does not indicate a constant isotopic composition of the source (Figure 4.9).

When the $\delta^{15}N$ and $\delta^{18}O$ of the source N_2O is variable, the relationship of the emitted N_2O to the composition of the source becomes complicated. The composition of the emitted N_2O will lag behind that of the source, and the amplitude of the $\delta^{15}N$ and $\delta^{18}O$ fluctuations will be dampened relative to the source. The amount of lag and dampening is a function of concentration and flux. Qualitatively; the isotopic composition of emitted N_2O will be nearly equal to that of the source if the residence time of dissolved N_2O is small relative to the period of source variability. The residence time is the average length of time that a dissolved N_2O molecule will remain in solution from the time it is produced to the time it is emitted to the atmosphere, and is defined as the areal N_2O concentration / N_2O flux. The residence time can be approximated by the ratio between mean depth and K if the N_2O concentration is substantially greater than atmospheric saturation. If the mean depth is low and the K is high, the residence time will be short, and the isotopic composition of the emitted N_2O will be close to that of the source. As the residence time increases, the isotopic composition of the emitted N_2O will increasingly lag behind and be dampened relative to the isotopic composition of the variable source. In the most extreme case, the variability in the $\delta^{15}N$ and $\delta^{18}O$ of the emitted N_2O will be dampened to the point that they are nearly constant, and the system will appear to be at steady state. At this point, the isotopic composition of the emitted N_2O is equal to the average isotopic composition of the source.

In aquatic environments, the instantaneous isotopic composition of N_2O emitted to the atmosphere is easily calculated if the water temperature, concentration, $\delta^{15}N$ and $\delta^{18}O$ of dissolved N_2O are measured. The $\delta^{15}N$ and $\delta^{18}O$ of dissolved N_2O is not directly representative of either the isotopic composition of N_2O produced or emitted to the atmosphere. Thus, the calculated $\delta^{15}N$ and $\delta^{18}O$ of the emitted N_2O should be used to draw important conclusions regarding N_2O production in aquatic systems (Table 4.5). The flux weighted $\delta^{15}N$ and $\delta^{18}O$ of emitted N_2O provides the average production rate weighted isotopic composition of the N_2O source in aquatic environments. If the $\delta^{15}N$ and $\delta^{18}O$ of emitted N_2O are constant with time, either the isotopic composition of the source must also be constant, or the residence time of N_2O in the aquatic system is very long. However, if the calculated $\delta^{15}N$ and $\delta^{18}O$ of emitted N_2O is variable with time, the isotopic composition of the source must also be variable with time. Depending on the N_2O production rate and the value of K, range of values for $\delta^{15}N$ and $\delta^{18}O$ of the emitted N_2O will be smaller than that of the source. Also, N_2O residence time (again dependant on production rate and K) will determine the lag time between the isotopic composition of the emitted N_2O and the source. However, the timing of the maximum and minimum values for $\delta^{15}N$ and $\delta^{18}O$ of emitted N_2O relative to maximum and minimum dissolved N_2O concentrations indicates how the isotopic composition of the source changes with production rate. For example, if the emitted N_2O is most depleted when the concentration is the highest, this indicates that the source is most depleted when the production rate is relatively high.

Table 4.5: Implications of the SIDNO results.

Parameter	Observation	Implications	Examples
Concentration of Dissolved N_2O	Constant with time	The N_2O production rate is constant with time (if K and temperature are also constant). The N_2O flux to the atmosphere is equal to the production rate. This may not be true if the concentration is close to atmospheric equilibruim.	Scenarios 3 and 4
	Variable with time	The N_2O production rate is variable with time (if concentration change cannot be explained by change in K or temperature). The average N_2O flux to the atmosphere is equal to the average production rate.	Scenarios 1 and 2
$\delta^{15}N$ and $\delta^{18}O$ of Dissolved N_2O	Constant with time	The observation is inconclusive. At concentrations near atmospheric equilibrium, isotopic composition of dissolved N_2O will approximate tropospheric N_2O, regardless of source values. A constant isotopic signature of dissolved N_2O that is different from tropospheric N_2O can indicate either a constant source (if production rate is constant), or a variable source.	Scenario 6
	Variable with time, slope of data points trends through value for tropospheric N_2O	The change in $\delta^{15}N$ and $\delta^{18}O$ of dissolved N_2O is likely a result of a change in concentration, but it is possible that the source is variable with time, if the $\delta^{15}N$ and $\delta^{18}O$ values of the source also trend through the value for tropospheric N_2O.	Scenario 1
	Variable with time, slope of data points does not trend through value for tropospheric N_2O	The change in $\delta^{15}N$ and $\delta^{18}O$ of dissolved N_2O is likely the result of a change in the isotopic composition of the source.	Not Shown
Calculated $\delta^{15}N$ and $\delta^{18}O$ of Emitted N_2O	Constant with Time	The isotopic composition of the source is constant with time, and equal to the calculated value for emitted N_2O	Scenarios 1 and 2
	Variable with Time	The isotopic composition of the source is variable with time. The range in $\delta^{15}N$ and $\delta^{18}O$ of emitted N_2O is the minimum for the range in that of the source. The flux weighted average $\delta^{15}N$ and $\delta^{18}O$ of emitted N_2O is equal to the production weighted average source values.	Scenarios 3 to 7
Residence Time Relative to Variability of Source (Need to independently determine K)	Long	The changes in N_2O concentration and $\delta^{15}N$ and $\delta^{18}O$ of emitted N_2O will be dampened relative to, and lag behind, that of the source	Scenarios 2, 4, and 7
	Short	The changes in N_2O concentration and $\delta^{15}N$ and $\delta^{18}O$ of emitted N_2O will be indicative of changes in the source	Scenarios 1, 3, 4 and 5

SIDNO can potentially be used to back calculate the K value, N_2O production rate and isotopic composition of the N_2O source in aquatic environments. If physical properties, such as depth and temperature, are entered into the model, SIDNO can be used to fit the measured field data (concentration, $\delta^{15}N$ and $\delta^{18}O$ of dissolved N_2O) by adjusting the N_2O source parameters. In this way, SIDNO could be used to estimate K, the N_2O production rate, and the source $\delta^{15}N$ and $\delta^{18}O$. SIDNO could easily be adapted to simulate the stable isotope dynamics of other dissolved gases, such as CH_4.

Chapter 5:

Diel Changes in Nitrous Oxide Production in the Grand River, Ontario, Canada

5.1 Introduction

The amount of biologically available nitrogen in the environment is increasing; anthropogenic sources release more than 160 Tg of reactive nitrogen each year, compared to 250 Tg/year of natural nitrogen fixation (Gruber & Galloway 2008). Much of this nitrogen is released to rivers through diffusive sources (e.g. agriculture) or point sources (e.g. municipal wastewater treatment). This excess nitrogen leads to eutrophication in freshwater and coastal zones (Dumont et al 2005, Thornber et al 2008).

To understand the fate of natural and anthropogenic nitrogen in river systems, it is necessary to study the biological nitrogen processing occurring in these environments. Methods have been developed to measure the *in-situ* rates of riverine denitrification (Laursen & Seitzinger 2002). Nitrification also takes place in oxic river waters and sediments, and the production of nitrate (NO_3^-) can further stimulate denitrification in the anoxic river sediments (Laursen & Seitzinger 2004). Since nitrous oxide (N_2O) is produced through both of these processes, rivers are an important source of this powerful greenhouse gas (Clough et al 2006, Cole & Caraco 2001, McMahon & Dennehy 1999).

The relative importance of nitrification and denitrification in a riverine system has been shown to vary spatially in an agriculturally influenced stream (Kemp & Dodds 2002). Recent studies on the Seine River in France have shown that nitrification and

denitrification rates can vary spatially as well as seasonally (Garnier et al 2006, Garnier et al 2007).

The concentration of dissolved oxygen (DO) in rivers can vary widely over diel cycles, driven by changing rates of photosynthesis and respiration (Venkiteswaran et al. 2007 and references within). Since nitrogen cycling processes depend on redox conditions in the system, it would be expected that nitrogen cycling in many rivers is linked to the diel oxygen cycle. Laursen & Seitzinger (2004) measured rates of denitrification in the Iroquois River and Sugar Creek (Midwestern USA) and found that these rates were consistently higher during the day than at night. The authors attributed this finding to increased nitrification during the day in response to elevated DO and temperature, providing NO_3^- for denitrification in the river sediments. Harrison et al (2005) also studied diel changes in nitrogen cycling in a eutrophic subtropical stream. The authors observed a complete change in redox conditions in the stream from day to night, with high DO concentrations in the day due to photosynthesis, and hypoxic conditions at night due to excessive respiration. The large diel changes in redox conditions resulted in a reduction in N_2O emitted during the night-time period and a change in the form of nitrogen transported downstream. Most recently, Clough et al (2007) studied the diel changes in nitrogen cycling in the LII river in New Zealand. These authors did not observe the dramatic changes in nitrogen cycling observed by Harrison et al (2005). This is likely due to the fact that the DO cycle was not as extreme at this location, and thus the redox conditions in the river did not vary enough to produce a large change in the nitrogen speciation observed. However, these authors did observe a peak in N_2O saturation (though absolute concentration remained relatively constant) during the

late afternoon, which subsequently declined at night. The small diel changes in N_2O saturation did not translate into a significant diel change in N_2O flux to the atmosphere.

Stable isotope analysis is a useful tool to study nitrogen cycling, and numerous studies have used $\delta^{15}N$ and $\delta^{18}O$ analysis of NO_3^- and $\delta^{15}N$ analysis of ammonium (NH_4^+) to study nitrogen cycling in the environment, including river systems (e.g. Sebilo et al 2006). Recently, more studies have employed $\delta^{15}N$ and $\delta^{18}O$ analysis of N_2O as an indicator of nitrogen cycling in soils, (e.g. Perez et al 2001, Bol et al 2003); however, to our knowledge, only one study (Boontanon et al 2005) has measured the stable isotope ratios of N_2O in a river. If N_2O produced through nitrification and denitrification has a different isotopic composition, the isotopic analysis of dissolved N_2O is useful to study diel changes in the riverine nitrogen cycle; however, currently no published studies have done so.

Researchers often make use of isotopic enrichment factors for N_2O produced through denitrification and nitrification that have been obtained in laboratory culture studies (e.g. Sutka et al. 2006, Toyoda et al. 2005, Casciotti et al. 2002). However, the in-situ microbial community in a natural environment may be very different from the microbial species used in these laboratory culture studies (Iribar et al 2008, Amann et al 1995). As a result, the enrichment factors for nitrification and denitrification in the natural environment may be significantly different than those obtained during laboratory studies.

The purpose of this chapter is to investigate the nitrogen cycling processes and N_2O production in the Grand River. The first objective was to determine the dominant processes responsible for riverine N_2O production, and how these processes are

influenced by diel changes in dissolved oxygen concentration. Previous work conducted at the University of Waterloo (Terra Jamesion, Gao Chen, and Tim Kuntz – unpublished data) and continuous DO monitoring by the Grand River Conservation Authority has shown that the magnitude of DO fluctuations at certain locations in the river is much greater than those measured by Clough et al (2007) in the LII River, and thus it was expected that a greater change in nitrogen cycling processes and N_2O production would be observed in the Grand River.

The second objective of this study was to determine if stable isotope analysis of NO_3^-, NH_4^+ and N_2O can provide greater insight into N_2O production in the Grand River. Very little data is available in the published literature regarding the isotopic composition of N_2O produced in riverine environments, and this study will help to characterize this important source of N_2O to the atmosphere.

The final objective was to use the SIDNO model to simulate N_2O production in the Grand River. The SIDNO model will determine the apparent $\delta^{15}N$ and $\delta^{18}O$ of N_2O produced through separate processes in the river. In this study, the SIDNO model output was used to provide a measure of the apparent enrichment factors for N_2O produced through riverine denitrification that have not previously been measured in-situ.

5.2 Study Site

The Grand River is the largest river in southern Ontario. It is approximately 300 km long, and drains an area of approximately 7000 km^2 into Lake Erie (Figure 5.1). As of 2001, approximately 720 000 people were living in the watershed, this figure is projected to increase to 1 220 000 by 2031 (Ministry of Public Infrastructure Renewal 2006).The

Grand River is a source of drinking water for approximately 500 000 people in the watershed.

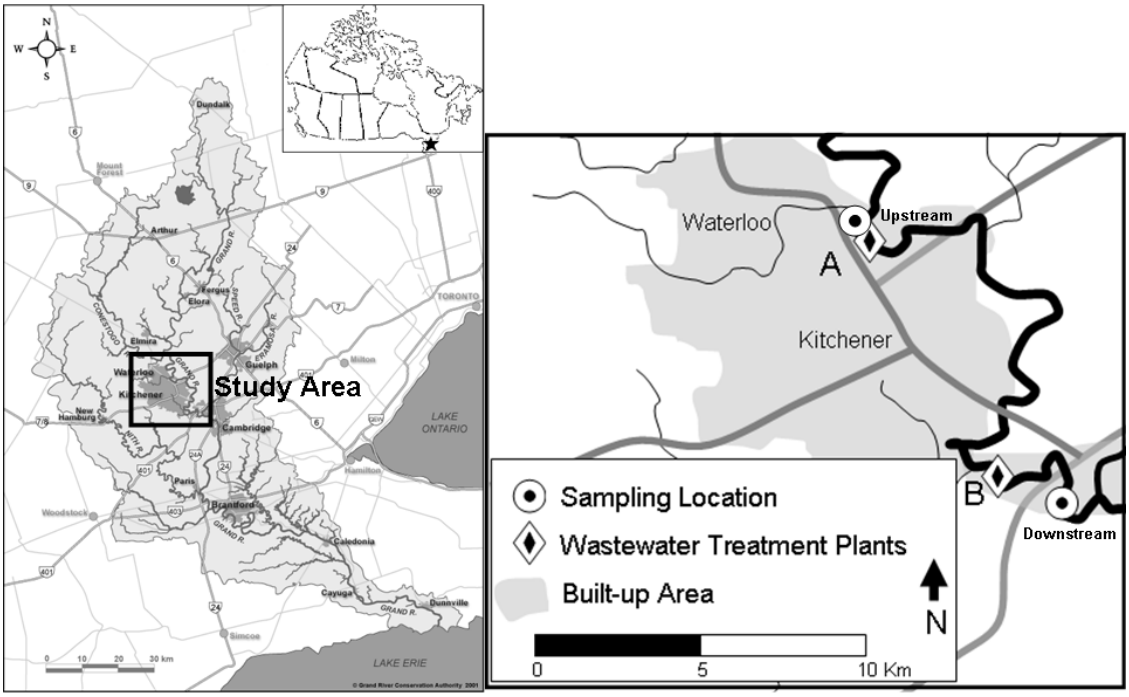

Figure 5.1: Map of the Grand River Watershed and study area. WWTPs on the map are labelled A (Waterloo WWTP) and B (Kitchener WWTP).

The Grand River is heavily impacted by both diffuse and point-source inputs of nitrogen. Agriculture is the primary land use in the watershed, and 26 wastewater treatment plants (WWTPs) currently discharge effluent to the Grand or its tributaries. The cities of Kitchener and Waterloo form the urban centre of the watershed, and the Kitchener and Waterloo WWTPs contribute 10% of the total NO_3^- load and 83% of the total NH_4^+ load of the six major WWTPs in the watershed (NPRI 2007). Sampling for this study was conducted approximately 6 km downstream of the Kitchener WWTP (Figure 5.1). To provide additional background data, samples were collected concurrently at a site approximately 0.5 km upstream of the Waterloo WWTP (Figure 5.1). Downstream of the urban centre, the river receives heavy nutrient input, resulting in

dense macrophyte growth in the channel. In the summer, macrophyte photosynthesis results in elevated DO concentrations during the day, and community respiration results in decreased DO concentrations at night (Terra Jamesion and Gao Chen– unpublished data). During the summer months, night-time DO concentrations at this location often fall below the water quality target set by the Grand River Conservation Authority. This DO problem is further compounded by the fact that the effluent from the Kitchener and Waterloo WWTPs contain high concentrations of ammonium (NH_4^+). These two major WWTPs are not operated to nitrify the effluent within the plant, and instead rely on the river to oxidize the NH_4^+ to nitrate (NO_3^-). Nitrification of NH_4^+ further consumes the limited DO in the river and contributes to poor river health.

5.3 Methods

Sampling for this study was conducted over a period of 28 hours on June 26 to June 27, 2008. Samples were collected for NH_4^+, NO_3^-, N_2, N_2O, CH_4, DO and DOC concentration approximately every 1.5 hours. At the same time these concentration samples were collected, pH measurements were taken using a YSI meter (650 MDS), fitted with a 600 QS Multi-Parameter Water Quality Monitor probe. Samples for dissolved gas concentration were collected in 60mL serum bottles (except for dissolved N_2 samples, which were collected in 160mL bottles), capped with no headspace with a baked red Vaccutainer stopper and preserved with 0.2mL of saturated $HgCl_2$ solution. All samples were kept on ice until they were transported back to the University of Waterloo. Chemistry samples were filtered to 0.45μm and the NH_4^+ samples were acidified to pH 5 using H_2SO_4. All samples were stored at 4°C until they were analyzed.

Photosynthetically active radiation (PAR) and barometric pressure were measured continuously at the downstream sampling location using a HOBO Micro Station datalogger (Onset Computer Corporation). DO, conductivity, and water temperature were measured continuously at the downstream location using a Hydrolab MiniSonde 4a.

Samples for $\delta^{15}N$ and $\delta^{18}O$ analysis of and NO_3^-, and $\delta^{15}N$ analysis of NH_4^+ were collected every 3-5 hours. NH_4^+ isotope samples were acidified on site to pH 5 using H_2SO_4. Samples for $\delta^{15}N$ and $\delta^{18}O$ of N_2O were collected every 1.5 hours along with the concentration samples. N_2O isotope samples were collected in 160mL serum bottles, capped with no headspace with red Vaccutainer stoppers and preserved with 0.4 mL of saturated $HgCl_2$ solution. All isotope samples were kept on ice until they were transported back to the University of Waterloo. N_2O samples were stored at 4°C and NH_4^+ and NO_3^-samples were frozen until further processing.

NH_4^+ concentrations were measured using a Technicon Auto Analyzer and an automated salicylate procedure, with a method precision of +/- 0.005 mg N/L (Technicon Industrial Method No. 329-74 W/B). NO_3^- concentrations were measured using a Dionex ICS 90 ion chromatograph, with a precision of +/- 0.05 mg N/L.

Dissolved gasses (with the exception of DO) were measured using a headspace equilibration technique. A 5 mL headspace was created in sample bottles by injection of ultra high purity helium. Sample bottles were then placed on an orbital shaker for 2 hours to equilibrate. Analysis was conducted with a Varian 3800 GC equipped with TCD, FID and ECD. Method precision for N_2O and CH_4 was +/- 5 %. Method precision for N_2 analysis was +/- 7 %.

DO concentration in discreet samples was measured by Winkler titration with sodium azide modification (APHA 1995). Method precision was +/- 0.2 mg O_2/L. The results of the Winkler titrations were used to calibrate the continuous DO measurements obtained by the Hydrolab datalogger.

$\delta^{15}N - NH_4^+$ analysis was conducted using a diffusion technique (Murray 2008, modified from Spoelstra et al. 2006). Briefly, an acidified quartz filter disk contained in a polytetrafluoroethylene (PTFE) packet was placed in a 60 mL serum bottle containing approximately 20 mL of sample water. The pH of the sample was adjusted with a buffer solution to convert the NH_4^+ in the sample to NH_3 gas. The serum bottle was capped and placed on a stir plate for approximately 10 days, after which the quartz filter disk was removed, dried, and analyzed for $\delta^{15}N - NH_4^+$ at the University of Waterloo Environmental Isotope Laboratory (uwEILAB). Precision for this technique was +/- 0.3‰.

$\delta^{15}N$ and $\delta^{18}O$ analysis of NO_3^- was conducted using the silver nitrate method described by Spoelstra et al. (2004). Samples were pre-concentrated by evaporation, and nitrate was stripped from the samples using an anion exchange resin. Nitrate was eluted from the resin using an HCl solution, and converted to $AgNO_3$ by addition of silver oxide. The concentrated samples were freeze dried, and the resulting $AgNO_3$ was stored in amber vials until isotopic analysis at the uwEILAB. Precision for this technique was +/- 0.5 ‰ for $\delta^{15}N$ and +/- 1 ‰ for $\delta^{18}O$.

$\delta^{15}N$ and $\delta^{18}O$ of dissolved N_2O was measured by first extracting the N_2O with helium and cryogenic trapping and subsequent analysis by IRMS as described in Chapter 3. Precision for this method was +/- 0.4‰ for $\delta^{15}N$ and +/- 0.8‰ for $\delta^{18}O$.

5.3.1 SIDNO Model

The $\delta^{15}N$ and $\delta^{18}O$ of N_2O produced in the river are not necessarily the same as the measured values for dissolved N_2O. Specifically, gas exchange with tropospheric N_2O and the mixing of sources makes it particularly difficult to interpret dissolved N_2O isotopic data. For this reason, a simple box model was developed using Stella Modeling software to determine the relationship between the stable isotope composition of source, dissolved and emitted N_2O. This model is described in detail in Chapter 4, however a few small modifications were made for this study to better represent the theoretical framework for nitrogen cycling in the Grand River.

In brief, there are three major reservoirs in the model, representing the dissolved isotopologues of N_2O (N_2O, $^{15}N_2O$, and $N_2{}^{18}O$). The $\delta^{15}N$ and $\delta^{18}O$ of dissolved N_2O are calculated from the ratios of masses in each of these boxes. The production of N_2O is modeled by adding mass to each box at a rate dictated by the N_2O production rate and isotopic ratios of the N_2O source. These parameters are set by the user. Gas exchange is modeled using the kinetic and equilibrium gas exchange fractionation factors determined by Inoue and Mook (1994). N_2O in each reservoir is allowed to exchange with a tropospheric N_2O pool, with a fixed concentration and isotopic ratios as determined by Kaiser et al (2003), Prinn et al (1990), Prinn et al (2000).

The model described in Chapter 4 was modified to better simulate conditions in the Grand River at the study site. First of all, a new function was added to the model to simulate the flow of the river. In this study, it is assumed that most of the N_2O production in the river occurs downstream of the Kitchener WWTP effluent outfall. This assumption is justified by samples collected upstream of the Waterloo and Kitchener WWTPs; these

samples had N_2O concentrations much lower than the downstream samples, with a nearly constant concentration, $\delta^{15}N$ and $\delta^{18}O$ values (average values: concentration = 220 % SAT, $\delta^{15}N$ = 5.3 ‰, $\delta^{18}O$ = 44.6 ‰). From continuous streamflow and conductivity measurements provided by the Grand River Conservation Authority, it is known that the travel time during summer baseflow from the Kitchener WWTP outfall to the sampling site is approximately 2 hours. Calculations indicate that the average residence time of a dissolved N_2O molecule in the river (areal N_2O concentration / flux rate) is also approximately 2 hours. The short residence time coupled with the low upstream concentration means that the N_2O measured at the sampling location is most representative of production downstream of the Kitchener WWTP. Therefore, for the purpose of this study, the river was modeled as a well mixed reservoir with a turnover time equal to the hydraulic travel time between the Kitchener WWTP and the sampling site. An extra inflow and outflow was added to each box in the model, such that the turnover time of each reservoir was 2 hours. The N_2O concentration and isotopic composition of the inflow was dictated by the average values observed Kitchener WWTP effluent outfall during this sampling period, assuming complete mixing of the effluent in the river.

The second modification made to the model was to allow for two separate source N_2O processes. This allows a separate characterization of the dominant N_2O source for the oxic period during the day and dominant source during the hypoxic period at night. The model was designed to allow the N_2O production rate from these two processes to vary, but the $\delta^{15}N$ and $\delta^{18}O$ of each process was fixed.

The temperature parameter in the model was set to correspond with the field measurements. The gas exchange constant (K) was determined with the PoRGy model (Venkiteswaran 2007) using DO concentration and $\delta^{18}O$ – DO measurements collected on four separate occasions at the sampling location during May to October 2006. The average K value calculated using this method was 0.2 m/hour. Determining K using the PoRGy model is advantageous compared to other methods because it integrates at the whole-reach scale, and is not influenced by small scale features in the river. The average depth of the river was known to be approximately 0.4 m at the site.

5.3.2 Calculations of N_2O Flux and Isotopic Composition of Emitted N_2O

The net N_2O flux from the dissolved phase to the atmosphere is calculated as follows,

$$N_2O\ \text{Flux} = K\left([N_2O]_{dissolved} - P_{N_2O}K_h\right) \tag{5.1}$$

Where the N_2O flux is calculated in $mol \cdot m^{-2} \cdot h^{-1}$, K is the gas exchange coefficient ($m \cdot h^{-1}$), P_{N2O} is the partial pressure of tropospheric N_2O (atm), K_h is the Henry's constant for N_2O ($mol \cdot atm^{-1} \cdot m^{-3}$), and $[N_2O]_{dissolved}$ is the dissolved concentration of N_2O ($mol \cdot m^{-3}$). The value for K_h is calculated as a function of water temperature, (adapted from Gevantman 2008):

$$K_h = 55394 \times e^{\left(-60.7467 + \frac{8882.8}{T} + 21.2531 \ln \frac{T}{100}\right)} \tag{5.2}$$

Where T is water temperature (K) and K_h is expressed in mol· atm^{-1}·m^{-3}.

As with the bulk N_2O flux, the flux of the heavy isotopologues ($^{15}N_2O$ and $N_2{}^{18}O$) can be calculated by including the kinetic fractionation factors for N_2O (adapted from Venkiteswaran et al. 2007)

$$\text{Flux } {}^{15}\text{N}_2\text{O} = K\left(\alpha_{in}^{15}\text{P}_{{}^{15}\text{N}_2\text{O}}\text{K}_\text{h} - \alpha_{ev}^{15}[{}^{15}\text{N}_2\text{O}]_{dissolved}\right) \quad (5.3)$$

$$\text{Flux N}_2{}^{18}\text{O} = K\left(\alpha_{in}^{18}\text{P}_{\text{N}_2{}^{18}\text{O}}\text{K}_\text{h} - \alpha_{ev}^{18}[\text{N}_2{}^{18}\text{O}]_{dissolved}\right) \quad (5.4)$$

Where, P_{15N2O} and P_{N218O} are calculated by multiplying the partial pressure of tropospheric N_2O (atm) by $^{15}N/^{14}N$ and $^{18}O/^{16}O$ ratios of tropospheric N_2O. $\alpha_{in}{}^{15}$, $\alpha_{ev}{}^{15}$, $\alpha_{in}{}^{18}$, and $\alpha_{ev}{}^{18}$ are the kinetic fractionation factors for N_2O invasion and evasion, as determined experimentally by Inoue and Mook (1994).

The ^{15}N and ^{18}O isotopic ratios of the N_2O flux can then be calculated as the ratio between the flux rates of the various isotopologues:

$$R_{flux}^{15} = \frac{\text{Flux } {}^{15}\text{N}_2\text{O}}{\text{Flux } {}^{14}\text{N}_2\text{O}} = \frac{\text{Flux } {}^{15}\text{N}_2\text{O}}{\left(\text{Flux N}_2\text{O} - \text{Flux } {}^{15}\text{N}_2\text{O}\right)} \quad (5.5)$$

$$R_{flux}^{18} = \frac{\text{Flux N}_2{}^{18}\text{O}}{\text{Flux N}_2{}^{16}\text{O}} = \frac{\text{Flux N}_2{}^{18}\text{O}}{\left(\text{Flux N}_2\text{O} - \text{Flux N}_2{}^{18}\text{O}\right)} \quad (5.6)$$

5.4 Results

During the sampling period and the proceeding week, the river flow was generally constant at the study location at approximately 10 m^3/sec. The air temperature during the

sampling period ranged from 16.7°C to 32.0°C, measured at the University of Waterloo weather station (17.3 km from the sampling location). The University of Waterloo weather station did not record any precipitation during the sampling period, and the most recent rainfall was 6 days prior to sampling when 7mm of rain was recorded.

The observed diel variation in DO was large, ranging from approximately 140% saturation during the late afternoon to 10% saturation just before sunrise (Figure 5.2). The DO concentration dropped off slightly in the late afternoon, likely due to a reduction in photosynthesis in response to intermittent cloud cover, which can be seen in the PAR data. The water temperature ranged from approximately 24°C to 29°C, the maximum temperature occurring in the early evening. The pH and conductivity of the river also followed a diel cycle, ranging from 7.7 to 8.7 (highest during the day) and 670 to 850 μS/cm (highest during the night) respectively. The first few pH measurements are missing due to a malfunction of the YSI probe. The diel cycles of DO, pH, temperature and conductivity measured here are typical of the diel variability observed by continuous water quality monitoring by the Grand River Conservation Authority at this location during the summer months.

Large diel changes in concentration were also observed for NO_3^-, NH_4^+, N_2, N_2O and CH_4 (Figure 5.2). NO_3^- ranged from 1.4 to 2.7 mg N/L, with the peak concentration occurring just before sunset, and the minimum occurring just after sunrise. Similarly, NH_4^+ concentrations ranged from 0.07 to 1.1 mg N/L, the peak concentration occurring just after sunrise and the minimum concentration occurring during midday. The dissolved gasses N_2, N_2O and CH_4 were always above saturation during the sampling period, indicating the river is a source of these gases to the atmosphere. The concentration of

N_2O and CH_4 peaked during the night, at 8,500 % saturation and 30,700 % saturation respectively. Day time concentrations of both N_2O and CH_4 were significantly lower, at approximately 990 % saturation and 21,200 % saturation respectively. N_2 concentration also peaked during the night at approximately 160 % saturation, though there is much more scatter in the N_2 data compared to the other gasses. This is because there is more error associated with the analysis of dissolved N_2 by the headspace equilibration technique. DOC concentration was relatively constant, ranging from 6.6 to 7.6 mg C/L, with a slight increasing trend over the sampling period.

The concentrations of NO_3^-, NH_4^+ and N_2O in effluent from the two WWTPs upstream of the site were generally constant during the sampling period, however a few samples had abnormally low concentrations of NH_4^+ and N_2O (Table 5.1). This data has been reported in more detail elsewhere (Rosamond 2008). The contribution of wastewater effluent to river flow was calculated using chloride concentrations as a conservative tracer. The average chloride concentration upstream and downstream of the WWTPs was 23 and 93 mg/L, respectively. Chloride concentrations in the WWTP effluent averaged 255 and 442 mg/L for the Waterloo and Kitchener plants, respectively. Assuming that the volume of effluent for each plant is proportional to the populations of Waterloo and Kitchener, the effluent outflow contributed 6.2% and 13.1% of the river flow at the downstream location, respectively during the sampling period. However it is possible that this calculation overestimates the WWTP contribution, due to the input of chloride to the Grand River from urban use of road salts.

Table 5.1: NO_3^-, NH_4^+, and N_2O concentrations measured in the WWTP effluent during the sampling period.

Location	Date/Time	NO_3^- mg N/L	NH_4^+ mg N/L	N_2O %SAT
Waterloo WWTP	26/06/2007 13:55	2.2	9.6	5,120
Waterloo WWTP	26/06/2007 16:06	1.7	5.2	5,370
Waterloo WWTP	26/06/2007 17:37	1.7	5.2	4,801
Waterloo WWTP	27/06/2007 7:06	0.8	8.8	3,425
Waterloo WWTP	27/06/2007 8:49	1.1	0.5	213
	Average	**1.5**	**5.9**	**3,786**
Kitchener WWTP	26/06/2007 12:44	0.0	24.2	781
Kitchener WWTP	26/06/2007 15:08	0.2	23.3	9,486
Kitchener WWTP	26/06/2007 16:49	0.2	21.9	10,257
Kitchener WWTP	27/06/2007 6:19	-	27.9	12,989
Kitchener WWTP	27/06/2007 8:03	0.2	26.7	14,103
Kitchener WWTP	27/06/2007 10:34	-	27.4	537
	Average	**0.1**	**25.2**	**8,025**

The concentration of DO, NO_3^-, NH_4^+ and N_2O measured at the upstream site did not have the strong diel variation seen in the downstream site (Table 5.2). The concentration of NH_4^+ measured in the river upstream of the WWTPs was insignificant compared to that of NO_3^-. N_2O concentrations measured upstream of the WWTPs were always much less than the concentrations measured at the downstream location. CH_4 concentrations were similar at the two locations, with night time concentrations slightly higher than during the day.

Table 5.2: The diel variation of measured parameters upstream of the WWTPs as compared to those measured at the downstream location. Day values are an average of the data collected from 12:00 to 15:00, and night values are an average of the data collected from 2:00 to 5:00.

		Upstream		Downstream	
		Day	Night	Day	Night
DO	(% saturation)	140	64	128	10
NO_3^-	(mg N/L)	1.3	1.3	2.0	1.8
NH_4^+	(mg N/L)	0.02	0.03	0.1	0.9
N_2O	(% saturation)	190	270	990	7,600
N_2	(% saturation)	130	130	125	130
CH_4	(% saturation)	22,300	26,500	21,200	29,500

The stable isotope composition of NO_3^-, NH_4^+ and N_2O also followed a diel cycle during the sampling period (Figure 5.3). The $\delta^{15}N - N_2O$ reached a peak of -6‰ during the day, and a minimum of -27‰ at night. The $\delta^{18}O - N_2O$ was also variable, ranging from 28 to 35 ‰. $\delta^{18}O - N_2O$ was generally higher during the day compared to the night-time values, however, there was a sudden decrease in $\delta^{18}O$ values at midday. This decrease also corresponded to a smaller decrease in $\delta^{15}N - N_2O$. The $\delta^{15}N$ and $\delta^{18}O$ values of dissolved N_2O were closest to the isotopic composition of tropospheric N_2O ($\delta^{15}N = 6.72$, $\delta^{18}O = 44.62$, Kaiser et al. 2003) during the day when the dissolved N_2O concentration was at a minimum. The $\delta^{15}N$ and $\delta^{18}O$ values for N_2O measured in the Grand River were more negative than the only other published values for riverine N_2O ($\delta^{15}N$ ranging from -3.8‰ to 15.6‰, $\delta^{18}O$ ranging from 36.6‰ to 63.8‰, Boontanon et al. 2000).

The $\delta^{15}N$ of NH_4^+ ranged between 22.9‰ and 35‰ during the sampling period. The $\delta^{15}N - NH_4^+$ exhibited an increasing trend during the day, while NH_4^+ concentrations were low. The $\delta^{15}N$-NH_4^+ peaked early in the night, just as the NH_4^+ concentrations began to rise.

The $\delta^{15}N - NO_3^-$ also displayed a diel variation. The $\delta^{15}N - NO_3^-$ ranged between 0.9‰ to 11.7‰. The $\delta^{15}N - NO_3^-$ followed the same trend as the NO_3^- concentration, with the highest value for $\delta^{15}N$ corresponded to the highest concentration, and lowest value for $\delta^{15}N$ corresponded to the lowest concentration. The $\delta^{18}O - NO_3^-$ was more consistent than the $\delta^{15}N$, and ranged between -5.0‰ to -1.5‰, with the most negative value occurring during the day.

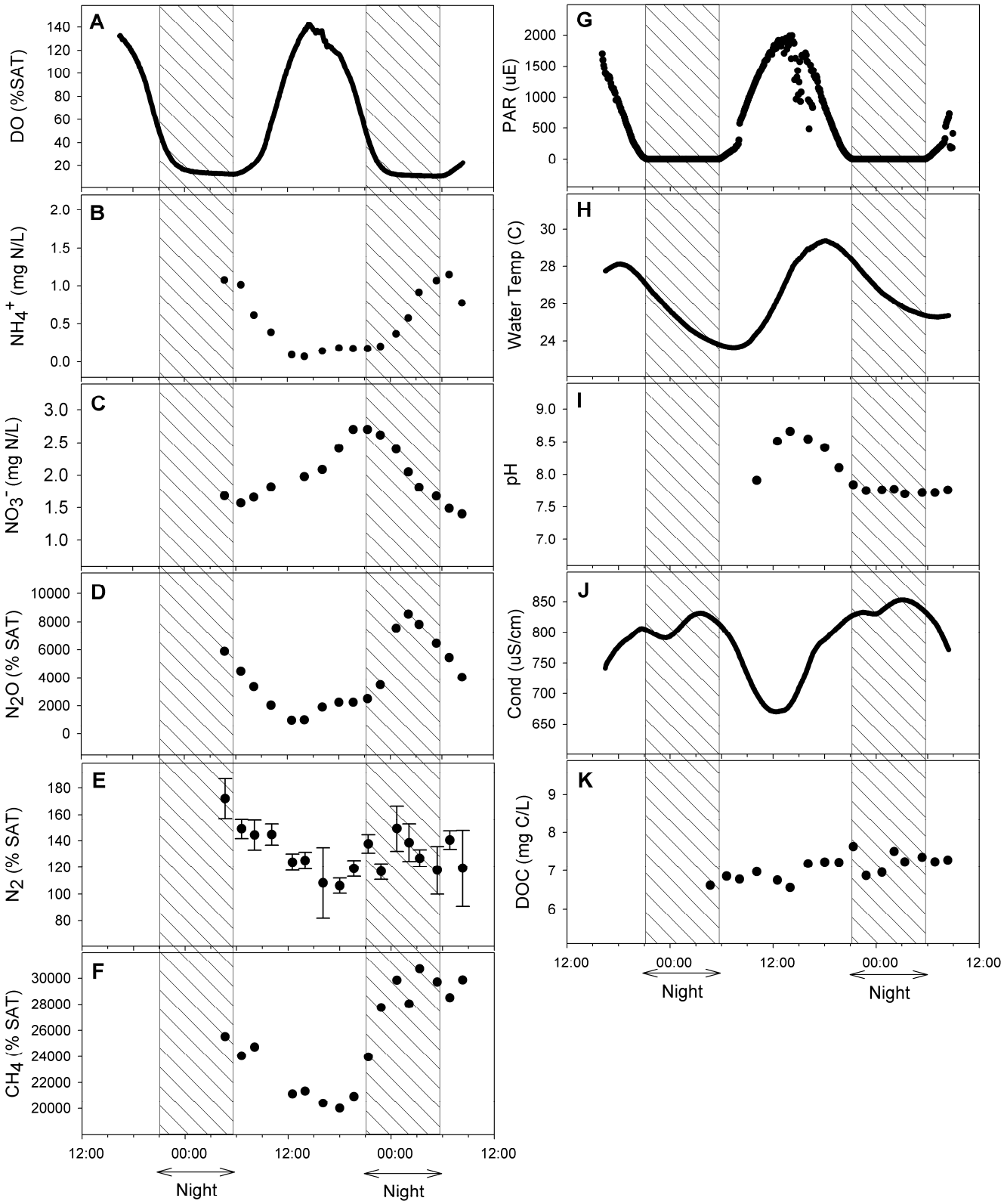

Figure 5.2: Physical and chemical parameters monitored during the sampling period. Time scale runs from noon June 25, 2007 to noon June 27, 2007. A – DO (% SAT), B – NH_4^+ (mg N/L), C – NO_3^- (mg N/L), D – N_2O (%SAT), E – N_2 (%SAT), F – CH_4 (% SAT), G – Photosynthetically active radiation (PAR - µE), H – water temperature (°C), I – pH, J – electrical conductivity (µS/cm), K – dissolved organic carbon (DOC – mg C/L).

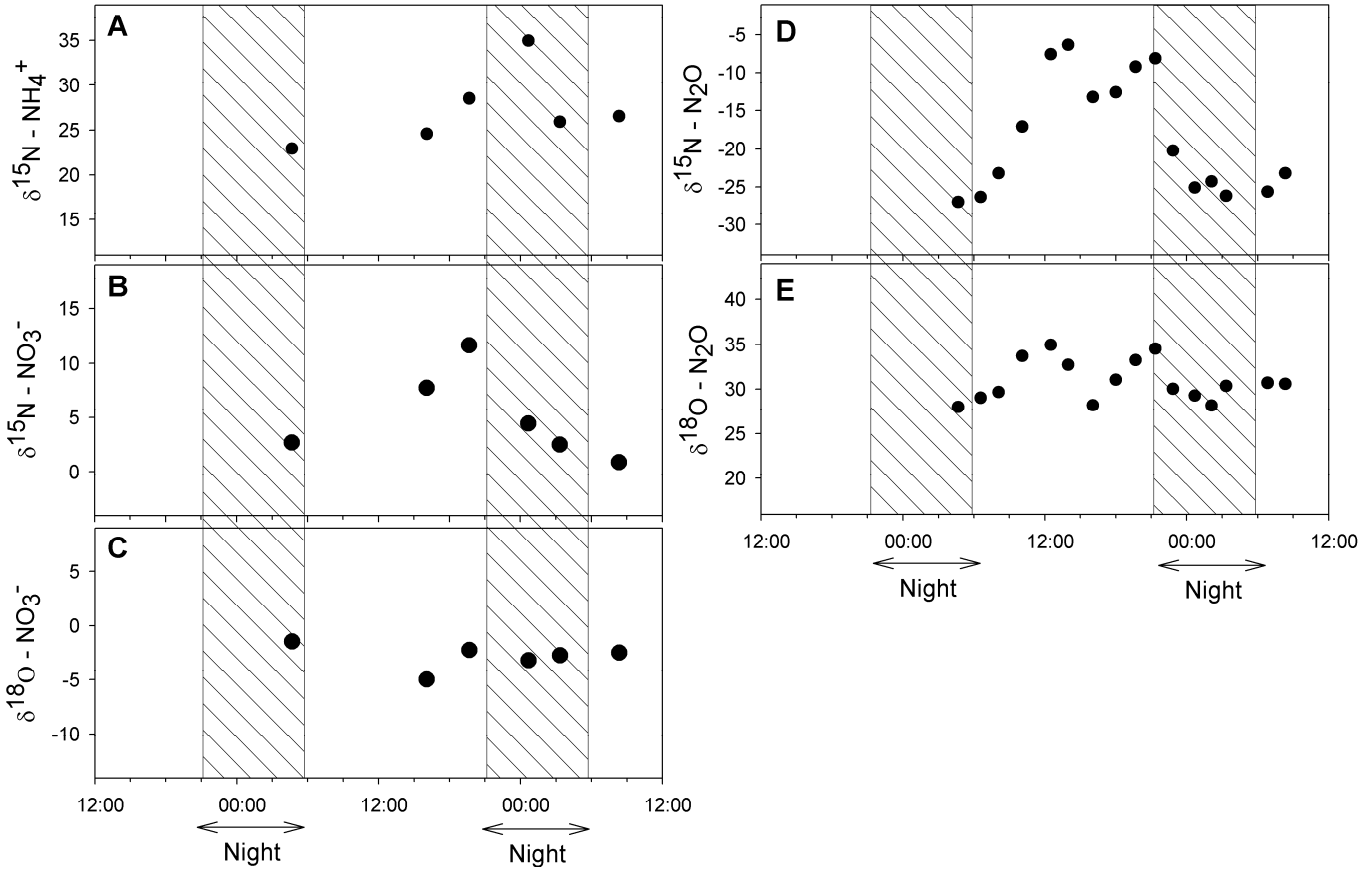

Figure 5.3: Results of isotopic analysis of water samples collected from the sampling site. Time scale runs from noon June 25, 2007 to noon June 27, 2007. A – $\delta^{15}N$ of NH_4^+, B – $\delta^{15}N$ of NO_3^-, C – $\delta^{18}O$ of NO_3^-, D – $\delta^{15}N$ of N_2O, E – $\delta^{18}O$ of N_2O.

5.5 Discussion

5.5.1 Sources of Nitrogen

The major inputs of nitrogen to the study reach of the Grand River are NH_4^+ from WWTP effluent (Table 5.1), and NO_3^- loading from upstream sources (mainly agricultural runoff, Table 5.2). As observed during concurrent sampling at the WWTPs, NO_3^- concentrations in the effluent from both plants were low, while NH_4^+ concentrations were elevated and generally constant (Table 5.1). Concurrent sampling in the Grand

River upstream of Waterloo WWTP effluent outfall indicated that the contribution of NH_4^+ from upstream sources was negligible (Table 5.2). However, upstream sources of NO_3^- were significant. The concentration of NO_3^- measured upstream of the Waterloo WWTP was nearly constant, ranging from 1.2 mg N/L to 1.4 mg N/L (Table 5.2).

Nitrification of NH_4^+ released from the WWTPs was an additional source of NO_3^- measured at the downstream location. Evidence for nitrification in the river was given by the increase in NO_3^- concentration from upstream of the WWTPs (approximately 1.3 mg N/L) to downstream of the WWTPs (ranging from 1.4 to 2.7 mg N/L), since the only significant source of nitrogen between these points was NH_4^+ in WWTP effluent (Figure 5.4). The general rise in $\delta^{15}N$ - NH_4^+ during the day is consistent with NH_4^+ consumption through nitrification. The $\delta^{15}N$ –NH_4^+ reached a maximum value just before the concentration began to rise, and quickly dropped again as the concentration recovered to previous levels.

The results of $\delta^{15}N$ and $\delta^{18}O$ analysis of NO_3^- also suggests nitrification is a significant source of NO_3^- downstream of the WWTPs. Using the expected nitrogen fractionation factors for NO_3^- production through nitrification (-29‰ to -12‰, Shearer & Kohl 1986, Kendall 1998), and the observed $\delta^{15}N$ values for NH_4^+ measured in the WWTP effluent, the $\delta^{15}N$ value of NO_3^- produced through nitrification in the Grand River should range between -24.9‰ and 4‰. Furthermore, using the 1/3 O_2, 2/3 H_2O rule for the oxygen isotopic composition of NO_3^- produced through nitrification, the expected range in $\delta^{18}O$ of NO_3^- can also be calculated (Aleem et al. 1965, Andersson & Hooper 1983, Kumar et al. 1983, Hollocher 1984). The $\delta^{18}O$ of DO was measured to range between 8.3‰ to 25.2‰ during the day, with the minimum value corresponding to

the maximum DO concentration (data not shown). Furthermore, it is known that the $\delta^{18}O$ of H_2O in the river is typically around -10‰. Therefore the expected range of $\delta^{18}O$ in NO_3^- produced through nitrification is -3.9‰ to 1.7‰, with the more negative values corresponding to NO_3^- production when the DO concentration and expected nitrification rate are at a maximum. Therefore, the $\delta^{15}N - NO_3^-$ values measured at the downstream location are greater than would be expected from nitrification of WWTP derived NH_4^+ alone. The $\delta^{18}O - NO_3^-$ values are slightly lower than expected, but are mostly consistent with NO_3^- production through nitrification.

The concentration of dissolved inorganic nitrogen (DIN, calculated as $[NO_3^-] + [NH_4^+]$) measured downstream of the WWTPs is less than would be expected considering only the upstream input of NO_3^- and the NH_4^+ from the WWTP effluent (Figure 5.4). Accounting for dilution, the DIN concentration downstream of the WWTPs would be expected to range from 4.6 to 5.6 mg N/L. However, the measured concentration ranged from 2.0 to 2.8 mg N/L, indicating that a significant amount of nitrogen is lost in the study reach of the river. It is possible that the difference between the expected and actual DIN concentration is due to an overestimation of the contribution of WWTP effluent to river flow.

DIN concentrations were generally lower during the day than at night. Although the magnitude of the variations in DIN concentration measured in the river are similar to those expected from the variation in WWTP effluent composition, the timing is incompatible and does not explain the observations (Figure 5.4). Therefore, other processes must be responsible for the change in DIN concentration.

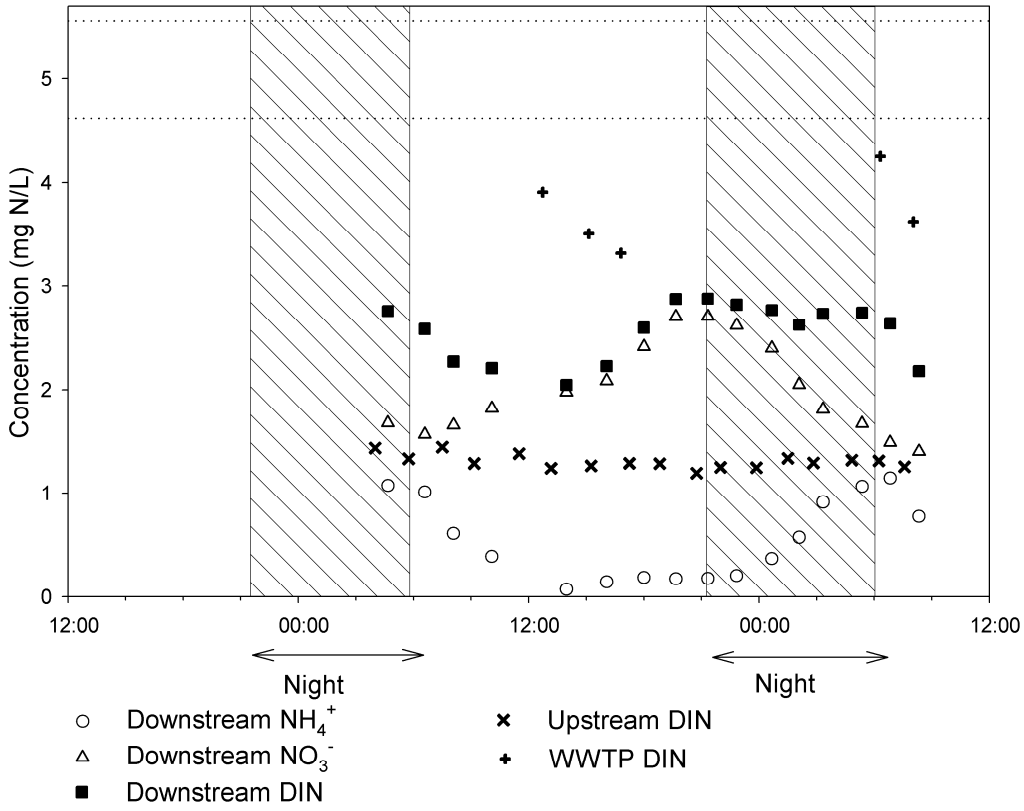

Figure 5.4: Dissolved inorganic nitrogen (DIN) measured downstream of the WWTPs compared to upstream DIN inputs. Time scale runs from noon June 25, 2007 to noon June 27, 2007. WWTP DIN is calculated from concentrations of NO_3^- and NH_4^+ measured in WWTP effluent and corrected for dilution. The dotted lines represent the range of DIN concentration expected at the downstream location considering only the upstream and WWTP DIN inputs and ignoring any losses.

During the day, the loss of DIN through the volatilization of NH_3 would have been particularly important. Near midday on July 26, 2007, the pH of the river water was at a maximum of 8.7, and the water temperature was 27.6°C. Under these conditions 25% of the total ammonia would be in the form of NH_3. The NH_3 would then be available for loss through gas exchange with the atmosphere. At night, when the pH and water temperature were lower (pH = 7.7, temperature = 25.3°C, Figure 5.2 H, I), only 3% of the total ammonia would be in the form of NH_3, reducing the rate of NH_3 loss through volatilization.

Other processes may also be important for the loss of DIN in the study reach. NH_4^+ can be lost through plant uptake or adsorption to suspended sediment. However, these processes have no effect on the $\delta^{15}N$ of NH_4^+, and the high values measured in the river at the downstream location (Figure 5.3) indicate that these processes are not the major pathway for DIN loss in the study reach. Although nitrification also consumes NH_4^+ and causes elevated $\delta^{15}N$ values, these values remain high even during the night when nitrification rates would be expected to be minimal. DIN may also be lost to the atmosphere as N_2O or N_2 during denitrification. The elevated concentrations of these two gasses (Figure 5.2) above the excess expected from diel changes in temperature at the upstream and downstream sites indicate that denitrification is a significant process for the removal of DIN from the Grand River.

Dissolved N_2O from WWTP effluent would have contributed significantly to the dissolved N_2O measured at the downstream location, especially during the day when river N_2O concentrations were low. The hydraulic transport time in the Grand River from the Waterloo and Kitchener WWTPs to the sampling location was approximately 8 and 2 hours, respectively. Using the observed range of dissolved N_2O measured in the WWTP effluent (Table 5.1), the range in expected concentrations of WWTP derived N_2O can be calculated for the sampling location by considering both dilution and gas exchange. Assuming that the effluent was uniformly mixed with the river, the average river depth was 0.4 m, the gas exchange coefficient (K) was 0.2 m/hour (calculated previously for the reach using the PoRGY model, Venkiteswaran et al. 2007), and no riverine N_2O production, the expected concentration of WWTP derived N_2O at the sampling location would range between 9.3 and 66.2 nmol N_2O/L. This corresponds to a range in the excess

N_2O concentration ($[N_2O] - [N_2O]_{saturated}$) of 1.8 to 58.7 nmol/L. This excess N_2O was almost entirely derived from the Kitchener WWTP. The contribution of N_2O from the Waterloo WWTP was insignificant, since all almost the N_2O from this source was lost to gas exchange with the atmosphere during the 8 hour travel time from the effluent outfall to the sampling location.

It is possible to calculate the expected contribution of WWTP derived N_2O to the total dissolved N_2O measured in the river, using the 2 hour hydraulic travel time from the Kitchener WWTP to the sampling site. During the day when the measured N_2O concentration in the river was low, WWTP derived N_2O accounted for approximately 4% to 28% of the excess N_2O at the downstream sampling location. Using the maximum N_2O concentration measured in the WWTP effluent, WWTP derived N_2O accounted for approximately 9% of dissolved N_2O in the river at its peak night time concentration. Therefore, the contribution of WWTP effluent derived N_2O to that measured in the river was variable, ranging from <5% to approximately 30% of the excess dissolved N_2O. These estimates represent a maximum contribution of WWTP derived N_2O, since the estimates of effluent discharge rates may have been influenced by the contribution of chloride from urban runoff.

Although the concentration of dissolved N_2O in the WWTP effluent was not measured during the night period, it is extremely unlikely that the large increase in dissolved N_2O at the downstream location during the night could be explained by an increase in WWTP N_2O. To reach the maximum dissolved N_2O concentration of 8,540% saturation (640 nmol/L) measured in the river, the concentration of N_2O in the effluent

would have to exceed 180,000% saturation (13,500 nmol N_2O/L), which is almost 14 times higher than the maximum observed effluent N_2O concentration.

5.5.2 Diel Variability in Nitrogen Cycle Processes

The observed variation in concentrations of DO, NO_3^-, NH_4^+, N_2, N_2O and CH_4 cannot be explained by changes in upstream or WWTP input. The diel variation in the DO concentration was caused by photosynthesis during the day, and respiration at night. Many redox sensitive measured parameters varied concurrently with changes in the DO concentration at the downstream sampling site (Figure 5.5). Thus redox conditions in the river were likely affected by the diel variation in DO concentration.

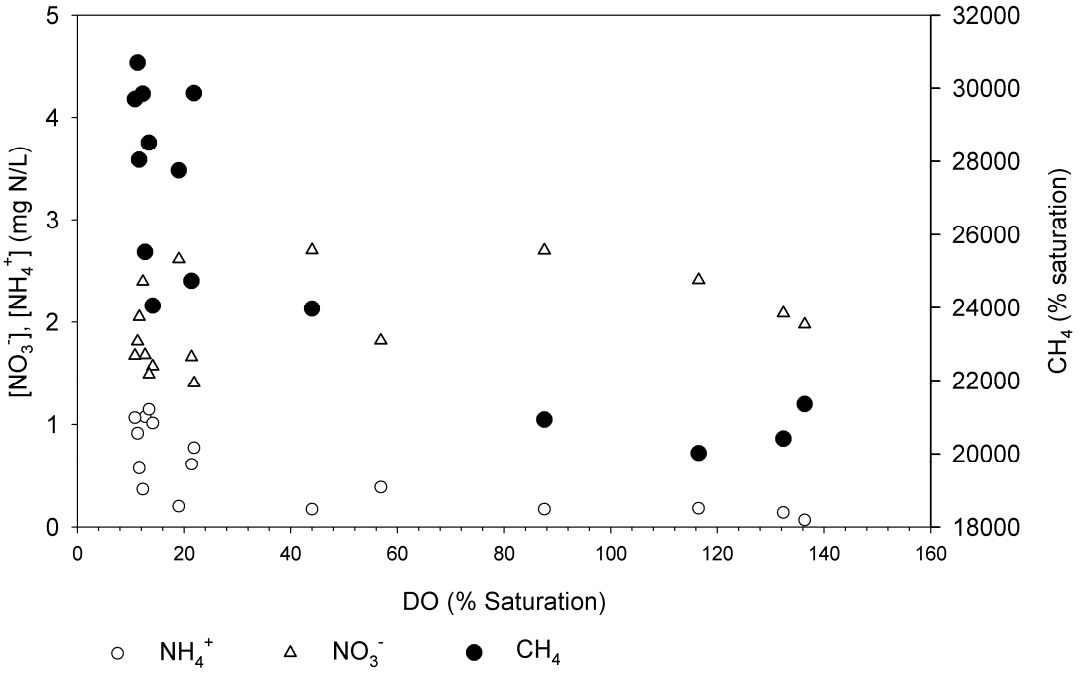

Figure 5.5: The concentration of NO_3^-, NH_4^+ and CH_4 downstream of the WWTPs plotted against the concentration of DO. This indicates that changes in redox conditions are driven by changes in DO concentration.

The dominant N_2O production pathways were likely different during the day when DO concentrations were high, than at night when DO concentrations were low. The diel change in N_2O concentration and isotopic composition (Figures 5.2 and 5.3) likely resulted from a change in the N_2O production pathway. The separate characterization of N_2O produced during the day and night can provide further insight into the diel variation of nitrogen cycling in the Grand River.

5.5.3 Stable Isotope Composition of Riverine N_2O Production

The isotopic composition of emitted N_2O is more representative of the N_2O source than the $\delta^{15}N$ and $\delta^{18}O$ measured for dissolved N_2O in aquatic environments open to gas exchange with the atmosphere. The average residence time of a N_2O molecule in solution (defined as the areal concentration / flux rate) was approximately 2 hours at the sampling location during the study period. Therefore, the residence time is short relative to the period of variability (diel, approximately 24 hours), and the isotopic composition of the N_2O flux will closely match that of the N_2O source (See Chapter 4). The isotopic composition of the N_2O flux can be calculated from the dissolved concentration, $\delta^{15}N$ and $\delta^{18}O$ of N_2O (Figure 5.6, equations 5.1 – 5.6). Downstream of the WWTPs, the isotopic composition of the emitted N_2O was very similar to that of the dissolved N_2O (Figure 5.3 D, E) because the concentration of dissolved N_2O was high. N_2O emitted at night had a $\delta^{15}N$ ranging from -28‰ to -22‰, and a $\delta^{18}O$ ranging from 26‰ to 29‰. N_2O emitted during the day had a $\delta^{15}N$ ranging from -15‰ to -9‰, and a $\delta^{18}O$ ranging from 25‰ to 32‰.

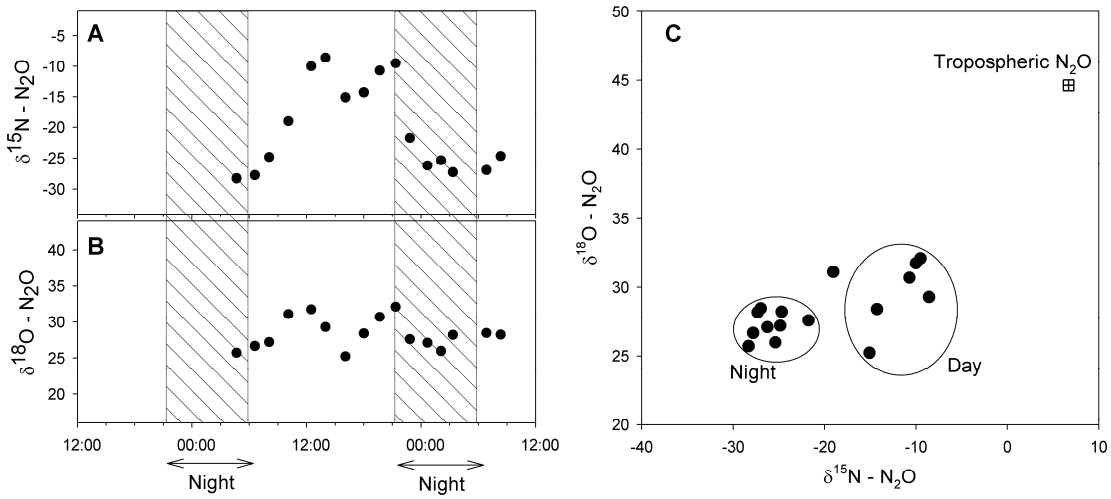

Figure 5.6: The isotopic composition of the N_2O emitted to the atmosphere from the Grand River during the sampling period. Due to the high dissolved N_2O concentration, the isotopic composition of emitted N_2O was very similar to the dissolved. Time scale runs from noon June 25, 2007 to noon June 27, 2007. A – $\delta^{15}N$ of emitted N_2O. B – $\delta^{18}O$ of emitted N_2O. C – $\delta^{15}N$ vs. $\delta^{18}O$ of emitted N_2O indicating a difference in the isotopic composition of N_2O emitted during the day compared to the night. Isotopic composition of tropospheric N_2O was determined by Kaiser et al. (2003).

The diel change in $\delta^{15}N$ and $\delta^{18}O$ of emitted N_2O indicates that the isotopic composition of the N_2O source must have varied on a diel basis. This is consistent with the diel change in redox conditions and suggests the dominant N_2O production pathways are different during the day compared to the night.

Using the modified SIDNO model (Chapter 4), it was possible to further characterize the isotopic composition of N_2O produced in the Grand River. The modified SIDNO model allowed for the isolation of N_2O production in the river, by assuming a constant WWTP effluent N_2O source. Additionally, the modified SIDNO model allowed for the separate characterization of day time and night time N_2O production. This provided additional insight into the diel variation in riverine nitrogen cycling.

Since the diel change in N_2O production appeared to be driven by the diel change in DO concentration, the timing of peak day and night N_2O production was set to match the timing of maximum and minimum DO concentration. The duration of the day time N_2O production was set to correspond to the time period that the DO concentration was greater than 20% saturation. The peak of the nighttime N_2O production was set to occur when the DO concentration was low, and the timing was adjusted to match the nighttime peak in N_2O concentration.

SIDNO produced a best fit for the field data by setting the peak daytime N_2O production rate 50 μmol N_2O/m^2/hour, and the peak night time N_2O production rate to 250 μmol N_2O/m^2/hour (Figure 5.7). N_2O produced during the day was found to have a $\delta^{15}N$ of -22‰ and a $\delta^{18}O$ of 43‰. N_2O produced at night was found to have a $\delta^{15}N$ of -30‰ and a $\delta^{18}O$ of 30‰.

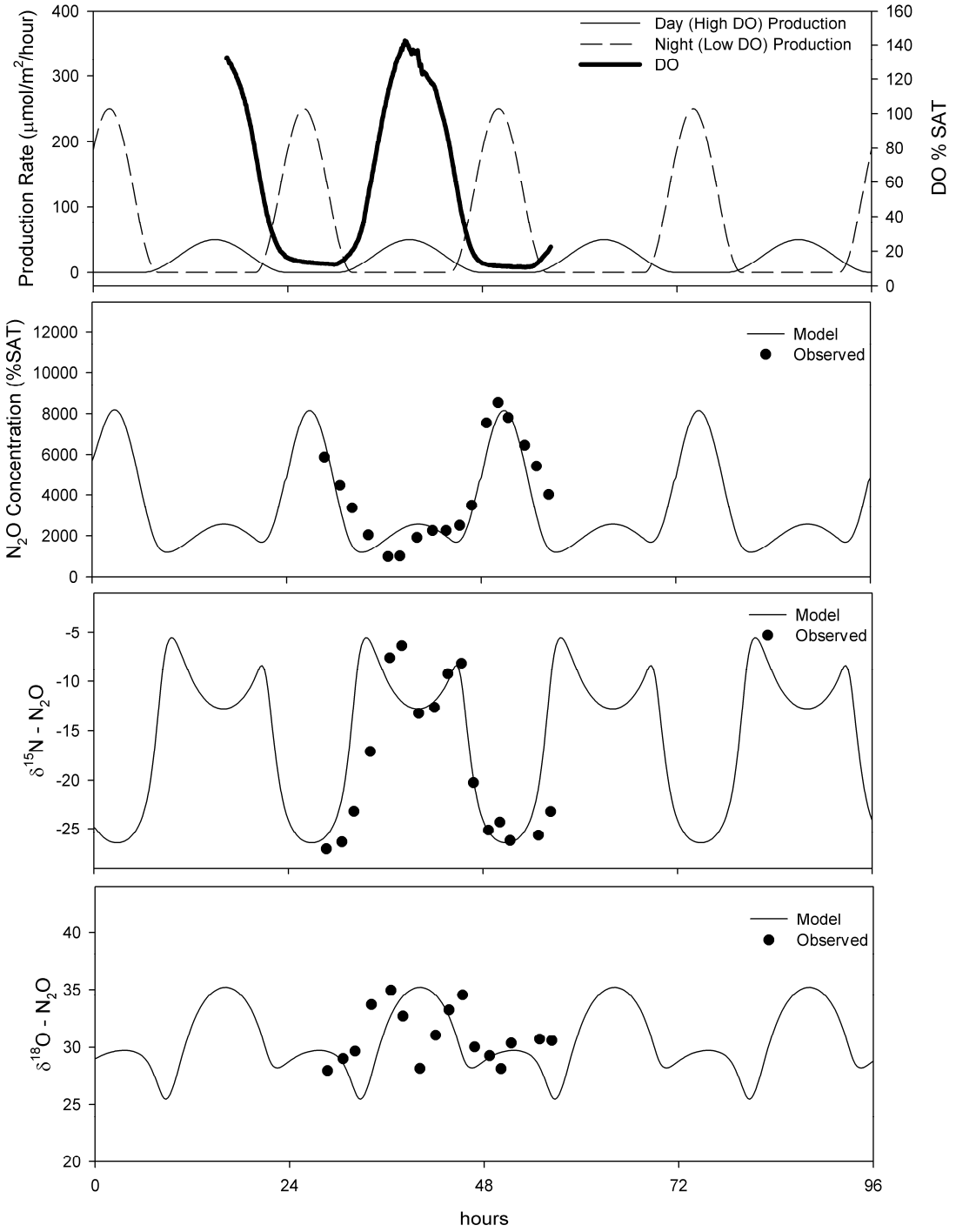

Figure 5.7: Model output compared to measured field data. Day time N_2O production parameters: Peak N_2O production rate = 50 µmol N_2O/m^2/hour, $\delta^{15}N$ = -22‰, $\delta^{18}O$ = 43‰. Night time N_2O production parameters: Peak N_2O production rate = 250 µmol N_2O/m^2/hour, $\delta^{15}N$ = -30‰, $\delta^{18}O$ = 30‰.

In general, the modeled data matches the field data quite well for dissolved N_2O concentration and $\delta^{15}N$. However, the model does not fit well to the $\delta^{18}O$ values of dissolved N_2O. The model predicted a drop in $\delta^{18}O$ of dissolved N_2O shortly after the DO concentration began to rise. However, the field data indicates that $\delta^{18}O$ actually increased at that time. This is likely explained by a change in the amount of N_2O released through the WWTP effluent. The WWTP N_2O input is assumed to be constant in the model, but it is known that the N_2O output from the Kitchener WWTP was low in the morning of June 26, 2007 (Table 5.1). Therefore, the model overestimated the WWTP contribution at that time, and since the average $\delta^{18}O$ of the WWTP derived N_2O is much less than that produced in the river (average WWTP N_2O $\delta^{18}O$ = 15.2‰), the model underestimated the value for $\delta^{18}O$ at that time. For the same reason, the model also slightly overestimated the $\delta^{15}N$ value for dissolved N_2O at the same time (average WWTP N_2O $\delta^{18}O$ = 4.4‰). The model also does not recreate the day time drop in dissolved N_2O $\delta^{18}O$ values.

Although the model was not able to recreate the $\delta^{18}O$ of N_2O produced during the day, the fit to the night time field data was much better. This indicates that the $\delta^{18}O$ of N_2O produced at night was constant, and variations in WWTP output were not significant. Therefore, it can be assumed that the night time $\delta^{15}N$ and $\delta^{18}O$ values for produced N_2O determined using SIDNO are representative of the natural system. However, for day time N_2O production, only the $\delta^{15}N$ value should be considered, since the model was unable to recreate the day time $\delta^{18}O$ field data.

5.5.4 Daytime N_2O Production Pathways

Since the dissolved N_2O concentrations measured at the downstream location are significantly greater than upstream of the WWTPs, and cannot be explained by the input from the WWTP effluent alone, significant daytime N_2O production must have occurred in the study reach of the Grand River. There is evidence that denitrification occurred continuously in the river sediments. Denitrification can only occur in anoxic zones or microsites. The elevated CH_4 concentration during the day (minimum concentration of 20,000% saturation) indicated that there were anoxic zones within the river sediments, even when DO concentrations were high. Also, the N_2 concentration remained supersaturated above the concentration expected from the diel temperature variation at the sampling location. Since N_2 is the final product of denitrification, these observations indicated that anoxic conditions existed in the river sediments and denitrification was actively occurring under these conditions.

The amount of N_2O produced by denitrification in the river sediments likely varied in response to the DO concentration. When the DO concentration in the river was high, the anoxic zone would have retreated deeper within the sediments, slowing the rate of NO_3^- diffusion into the active denitrification zone, and reducing the amount of N_2O produced. Also, a deep active denitrification zone would slow the diffusion of N_2O out of the sediments, providing more time for N_2O to be further reduced to N_2 and reducing the total amount of N_2O released. When the DO concentration began to fall in the late afternoon and evening, the anoxic zone would move closer to the sediment surface, increasing the amount of N_2O produced and released.

The daytime concentrations of DO, NO_3^-, N_2 and CH_4 were similar upstream and downstream of the WWTPs (Table 5.2). Therefore, it is likely that the N_2O production rates through sediment denitrification were similar at these two locations; however the daytime N_2O concentration was much higher at the downstream site (Table 5.2). N_2O derived from WWTP effluent likely accounts for a maximum of 30% of the daytime excess dissolved N_2O observed at the downstream site. N_2O derived from sediment denitrification would only account for an additional 7% of the daytime excess N_2O if the day time denitrification rates are similar upstream and downstream of the WWTPs. Although additional input of organic matter from the WWTP and decaying plant matter may enhance anoxic conditions and denitrification in the sediments at the downstream site, the similar daytime CH_4 and N_2 concentrations at the upstream and downstream locations indicate that this was not an important factor. Therefore, an additional process is responsible for the elevated daytime N_2O concentrations at the downstream site.

Since nitrification was actively occurring during the day, it represents an additional pathway for N_2O production. Models developed to simulate N_2O production in the natural environment have indicated that generally the amount of N_2O produced through nitrification is low compared to the total amount of nitrogen processed. For example, the PnET-N-DNDC model was developed to simulate N_2O production in forest soils (Li et al. 2000). In this model, the N_2O production rate in nitrification is only 0.06% of the gross nitrification rate. Other models, such as RIVERSTRAHLER, used in the Lower Seine River and estuary have indicated that the nitrification N_2O production rate may be as high as 1-2% of the gross nitrification rate (Garnier et al. 2007). However, the RIVERSTRAHLER model suggests that N_2O production through nitrification only

reaches the maximum rate through the nitrifier-denitrification pathway, when DO concentrations are below 1.5 mg/L, and nitrite (NO_2^-) concentrations are greater than 1-4 mg N/L. Although daytime DO concentrations were much greater than 1.5 mg/L at the downstream location, it is possible that low DO concentrations were present at the sediment/water interface. NO_2^- concentrations were not measured in this study, but since it is an intermediate in both nitrification and denitrification, it may have been present in significant concentrations at the sediment / water interface. The excess daytime dissolved N_2O that cannot be attributed to WWTP effluent or sediment denitrification sources is approximately 55 to 80 nmol/L. Assuming that most of the nitrification and N_2O production occurs immediately downstream of the WWTP outfall, this corresponds to approximately 0.28% to 0.42% of the total NH_4^+ nitrogen converted to NO_3^- at the peak nitrification rate. These rates are less than the maximum nitrification N_2O production rates described by the RIVERSTRAHLER model (Garnier et al. 2007), and may be consistent with production through nitrification or the nitrifier-denitrification pathway.

The $\delta^{15}N$ of N_2O produced during the day (determined with the SIDNO model $\delta^{15}N$ = -22‰) is consistent with N_2O production through nitrification or nitrifier-denitrification. Using published enrichment factors and the observed day time range for $\delta^{15}N$ of NH_4^+, the $\delta^{15}N$ of N_2O produced through nitrification or nitrifier-denitrification would be expected to range from -23‰ to -5‰ (Sutka et al. 2006, Yoshida 1988), but may be as low as -87‰ (Perez et al. 2006). However, this result cannot be used to rule out N_2O production through sediment denitrification. Using published enrichment factors, the $\delta^{15}N$ of N_2O produced through denitrification would be expected to range

from -40‰ to -5‰ (Perez et al. 2006, Menyailo and Hungate 2006, Wada et al. 1991, Schumidt and Voekelius 1989, Mariotti et al. 1981, 1982).

The day time drop in $\delta^{18}O$ values is likely an indicator of N_2O production through nitrification or nitrifier-denitrification. Other studies have shown that the $\delta^{18}O$ of N_2O produced through nitrification has a similar value to ambient molecular oxygen (Perez et al. 2006, Yoshinari & Wahlen 1985). The $\delta^{18}O$ values for DO were observed to vary widely during the day, ranging from 8.3‰ at the maximum DO concentration, to 25.2‰ as the DO concentration decreased in the late afternoon and evening. This would account for the day time variation in $\delta^{18}O$ of N_2O and suggest that nitrification or nitrifier-denitrification is the dominant N_2O production process during the day.

5.5.5 Night-time N_2O Production

During the night period, when the DO concentration was very low, the N_2O production rate and concentration increased dramatically at the downstream location. The isotopic composition of N_2O produced at night was different than during the day (Figures 5.5, 5.6) indicating that the dominant production pathway was also different than during the day.

When the DO concentration dropped below 1.5 mg/L, the denitrification rate increased dramatically, as indicated by the rapid increase in N_2O and N_2 concentrations. As the DO concentration fell, the river sediments became more anoxic, and it is likely that the entire sediment layer, including the sediment / water interface was completely anoxic. This would have allowed N_2O production from denitrification to proceed at a high rate.

It is possible that denitrification occurred not only within the river sediments, but within the water column when the DO concentration was very low at night. Since N_2O production through denitrification in the water column is not limited by the diffusion of NO_3^- into the river sediments, its onset has the potential to produce a rapid change in the dissolved N_2O concentration. It is difficult to distinguish between denitrification in the water column and in the sediments on the basis of the measured N_2O, NO_3^- and N_2 concentrations alone. However, denitrification activity was likely higher in the sediments than in the water column, due to the greater number of denitrifying organisms that would have been present in the sediments and sediment surface.

The N_2O concentration began to fall shortly before sunrise while the DO concentration was low and the denitrification rate was expected to remain high. This is potentially due to the consumption of extracellular N_2O through reduction to N_2. However, the results of the stable isotope analysis of dissolved N_2O rules out this possibility. Other studies have shown that N_2O reduction causes a relative enrichment of $\delta^{18}O$ compared to $\delta^{15}N$ in the residual N_2O (Vieten et al. 2007, Menyailo & Hungate 2006, Mandernack et al. 2000), however, this enrichment was not seen in the dissolved N_2O as the concentration fell. Therefore, the drop in N_2O production when the DO concentration was at its lowest was likely a reduction in the N_2O:N_2 ratio of the denitrification products. More anoxic redox conditions induce a drop in the N_2O:N_2 ratio. If more N_2O is reduced to N_2 without first being released from the microbial cells during denitrification, it is likely that there is no relative enrichment related to this process. Therefore, the $\delta^{15}N$ and $\delta^{18}O$ – N_2O data supports the hypothesis that the drop in N_2O

concentration was due to a reduction in the ratio of N_2O:N_2 released during denitrification, rather than a reduction in extracellular N_2O to N_2.

The very large increase in the N_2 concentration measured at night is consistent with an increase in the denitrification rate when the DO concentration was low. However, the amount of NO_3^- that would be consumed to produce the observed N_2 increase from the daytime minimum to the night time maximum is approximately 3.5 mg N/L, which is more than the maximum NO_3^- concentration measured in the river. Therefore, the measured night time N_2 concentrations may have been elevated by entrapped air bubbles during sampling, and may not be representative of the actual N_2 concentrations in the river. A better estimate of the night time denitrification rate can be calculated using the N_2O concentrations, since entrapped air in the sample bottles would not cause a significant change in the measured concentration. The maximum N_2O concentration at night was 640 nmol N_2O/L, which is equivalent to approximately 0.02 mg N/L. Using the RIVERSTRAHLER model, Garnier et al. (2007) determined that the N_2O:N_2 production ratio for denitrification in the Seine River ranged between 1:10 and 1:5. If it can be assumed that the N_2O:N_2 ratios are similar in the Grand River, this relates to a maximum 0.2 mg N/L of NO_3^- consumed during maximum denitrification. Therefore, the drop in NO_3^- concentration observed downstream of the WWTPs at night resulted from the lack of NO_3^- production through nitrification, rather than from increased consumption through denitrification.

The high denitrification rates at night do not appear to cause an increase in the $\delta^{15}N$ and $\delta^{18}O$ values of the NO_3^- measured in the river. Using enrichment factors determined by Mengis et al. (1999), the consumption of 0.2 mg N/L NO_3^- should have

increased the NO_3^- $\delta^{15}N$ by approximately 4.3‰, and the $\delta^{18}O$ by approximately 2.8‰. However, if most of the denitrification occurred in the sediments, it would be limited by the diffusion of NO_3^- into the active zone. Any NO_3^- in the active zone of the sediments would be completely consumed, and since there is no residual, sediment denitrification would likely not cause an increase in the $\delta^{15}N$ and $\delta^{18}O$ values of NO_3^- in the water column. Therefore, since $\delta^{15}N$ and $\delta^{18}O$ of NO_3^- did not increase at night, this likely indicates most of the denitrification likely occurred in the sediments or at the sediment / water interface, rather than in the water column.

Nitrification activity during the night was minimal, and was likely not a significant source of N_2O production when DO concentrations were low. At night, when DO concentrations were less than 15 % saturation, it was likely that the entire sediment layer, including the sediment / water interface, was completely anoxic. Most nitrifying organisms downstream of the WWTPs are likely attached to the sediment surface. Since water column NH_4^+ concentrations are significant only in the short reach downstream (within approximately 10 km) of the WWTPs, nitrifying organisms would likely not survive in the water column, as they would be quickly carried away from the NH_4^+ substrate source. Therefore, the nitrifiying organisms were likely under completely anoxic conditions during the night period, and nitrification activity would cease until DO concentrations increased again shortly after sunrise.

Other observations are also consistent with a cessation of nitrification activity during the night period. As the DO concentration fell, the NO_3^- concentration measured at the downstream location also fell to the background concentration measured at the upstream site. Also, during the night, $\delta^{15}N$ values for both NO_3^- and NH_4^+ became less

positive. If NO_3^- was no longer being produced from nitrification of a high $\delta^{15}N$ NH_4^+ substrate, both the concentration and $\delta^{15}N$ of NO_3^- would have decreased. The decrease in $\delta^{15}N$ NH_4^+ is also consistent with a lack of nitrification at night.

The diel variation in nitrogen cycling processes can be summarized by a conceptual model (Figure 5.8).The dominant processes responsible for N_2O production in the Grand River downstream from the WWTPs varied in response to the diel DO concentration change. When DO concentrations were high, N_2O was produced mainly through nitrification or nitrifier-denitrification, and to a lesser extent by denitrification in the river sediment. During the night, when DO concentrations were low, denitrification was the dominant N_2O production pathway, occurring in the sediments and at the sediment / water interface.

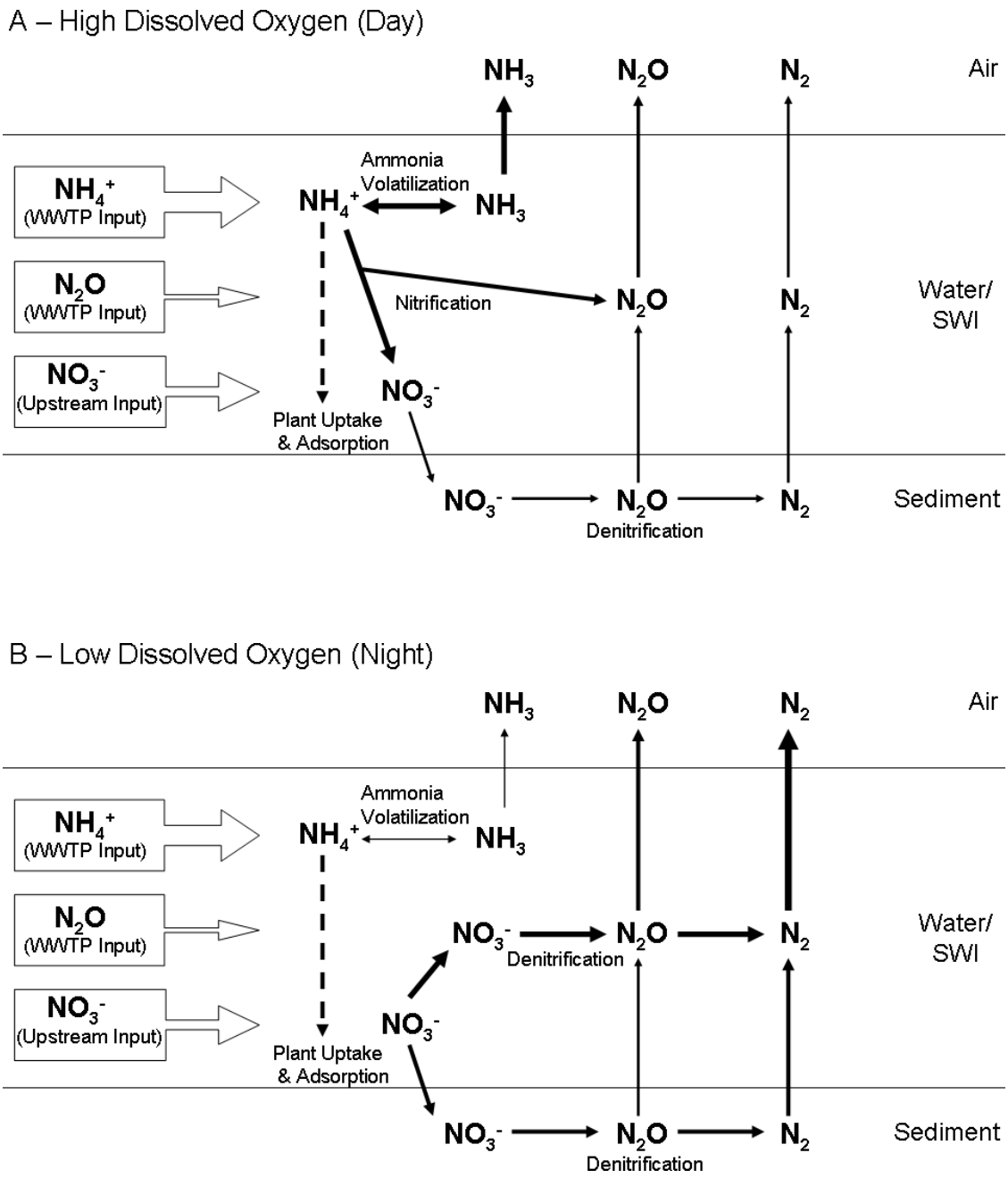

Figure 5.8: Conceptual model of the diel variability of nitrogen cycling in the Grand River. The major nitrogen transformations are thought to occur either in the sediments, in the water column, or at the sediment water interface (SWI). A – Nitrogen cycling during periods of high dissolved oxygen concentrations, typically during the day due to photosynthesis. B – Nitrogen cycling during periods of low dissolved oxygen, typically at night due to high respiration and a lack of photosynthesis. The thickness of the arrows represents the relative important of each pathway or source.

5.5.6 Implications

This study is one of the first to measure $\delta^{15}N$ and $\delta^{18}O$ of dissolved N_2O produced in a river. Boontanon et al (2000) measured $\delta^{15}N$ –N_2O ranging from -3.8‰ to 15.6‰ and $\delta^{18}O$ ranging from 36.6‰ to 63.8‰ in the Bang Nara River in Thailand, while the $\delta^{15}N$ and $\delta^{18}O$ of N_2O produced in the Grand River was generally more negative. The $\delta^{15}N$ and $\delta^{18}O$ values for emitted N_2O can be calculated for both rivers (equations 5.1 – 5.6, Figure 5.9). The $\delta^{15}N$ and $\delta^{18}O$ values for emitted N_2O from the Bang Nara River were calculated using N_2O % saturation values inferred from the data published by Boontanon et al. (2000). The flux weighted average for N_2O produced in the Grand River was -21.6‰ and 24.8‰ for $\delta^{15}N$ and $\delta^{18}O$, respectively. The flux weighted average for N_2O produced in the Bang Nara River (Boontanon et al. 2000) is more positive for $\delta^{15}N$ and $\delta^{18}O$ (0.1‰ and 41.1‰, respectively). It is not clear if this difference is a reflection of a difference in the N_2O production pathways between these two rivers (i.e. the dominance of nitrification, denitrification or other processes such as anamox), or if there are other factors involved. For example, the isotopic composition of the substrates (NO_3^- and NH_4^+) were not measured by Boontanon et al. (2000), so it is not possible to directly compare enrichment factors for N_2O production. The values for the Grand River are influenced by the contribution of WWTP derived N_2O, which had a isotopic composition that was much different than the values for in-river N_2O production determined using the SIDNO model (average $\delta^{15}N$ =4.4‰, average $\delta^{18}O$ =15.2‰, n = 4 , measured at the Kitchener WWTP). However, the large difference in $\delta^{15}N$ and $\delta^{18}O$ of N_2O between these two studies suggests that there is likely a large range of the isotopic composition of

N_2O produced in rivers worldwide, and much more work is necessary to fully characterize the composition of N_2O produced in these environments.

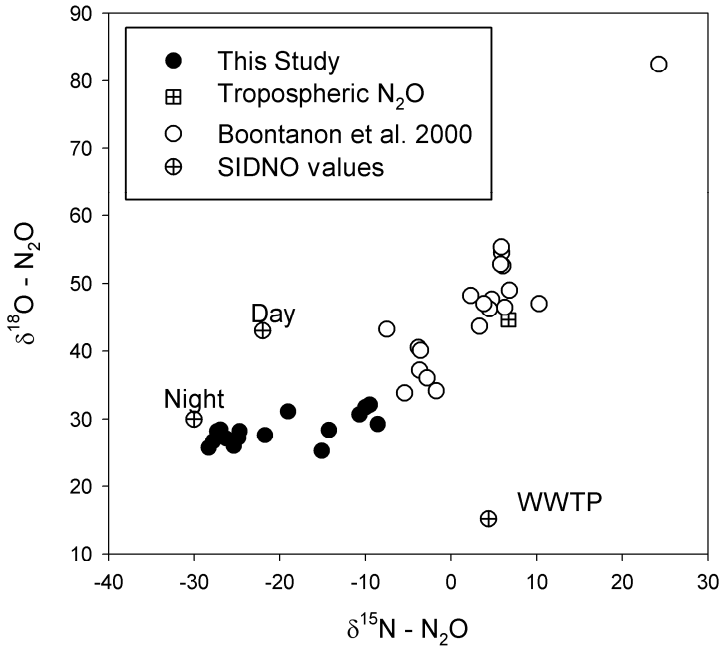

Figure 5.9: Calculated values for $\delta^{15}N$ and $\delta^{18}O$ of emitted N_2O from the Grand River compared to the data of Boontanon et al (2000). Values for day time and night time N_2O production determined using the SIDNO model are also shown, along with the average value for WWTP derived N_2O. The value for tropospheric N_2O was determined by Kaiser et al. (2003).

Since denitrification was the dominant N_2O production process during the night, the SIDNO model output can be used to determine apparent *in-situ* enrichment factors for N_2O production through denitrification in a river environment. Most of the published enrichment factors for these processes are based on laboratory culture experiments (e.g. Sutka et al. 2006, Toyoda et al. 2005, Casciotti et al. 2002), and may not be representative of N_2O production in the natural environment. Other studies have shown that only approximately 0.25% of the total microbial population in freshwater environments can be grown in laboratory cultures (Amann et al 1995). But by comparing

the model output for $\delta^{15}N$ and $\delta^{18}O$ of N_2O produced in the river to the measured $\delta^{15}N$ and $\delta^{18}O$ of the NO_3^- precursor, it is possible to infer the apparent in-situ enrichment factors for denitrification in the Grand River. During the night, the measured $\delta^{15}N$ for NO_3^- ranged between 0.8‰ and 4.4‰. The measured $\delta^{18}O$ for NO_3^- ranged between -3.2‰ and -1.4‰. Using the best fit values for $\delta^{15}N$ and $\delta^{18}O$ of N_2O produced through denitrification, a range of ε values can be calculated for ^{15}N and ^{18}O. For N_2O production through denitrification, $\varepsilon\ ^{15}N$ ranged between -34.4‰ to -30.8‰, and $\varepsilon\ ^{18}O$ ranged between 31.4‰ to 33.2‰.

The apparent nitrogen enrichment factors are more negative than those typically seen for denitrification in published literature. Although several laboratory incubation studies have measured $\varepsilon\ ^{15}N$ values for denitrification greater than -30‰ (Tilsner et al. 2003, Perez et al. 2006, Sutka et al. 2006, Toyoda et al. 2005, and Yoshida et al. 1988), $\varepsilon\ ^{15}N$ values for denitrification in many other studies have generally been smaller (typically ranging from -30‰ to -10‰, Menyailo & Hungate 2006, Wada et al. 1991, Barford et al. 1999, Schumidt and Voekelius 1989). The apparent $\varepsilon\ ^{18}O$ values for denitrification are more positive than most published values, though Casciotti et al. (2002) measured a $\varepsilon\ ^{18}O$ value of 40‰ for denitrification in a laboratory culture. It should be noted that the apparent enrichment factors measured in the Grand River are could be affected by N_2O consumption by extracellular reduction to N_2, this would cause the apparent enrichment factors to be more positive than the true values. In addition, most laboratory culture experiments inhibit the reduction of N_2O to N_2, which would change the observed enrichment factor.

The SIDNO results can also be used to calculate enrichment factors for N_2O produced through nitrification during the day, however, this calculated value is likely influenced by the contribution of N_2O from denitrification in the river sediments. The $\delta^{15}N$ of N_2O produced during the day was approximately -22‰, and the $\delta^{15}N$ of NH_4^+ in the WWTP effluent ranged from 4.1‰ to 16.0‰. Therefore, the apparent in-situ enrichment factor for nitrification ($\varepsilon\ ^{15}N$) ranged between -26‰ to -38‰. This value is less negative than most published values available in the literature (-112‰ to -35‰, Perez et al. 2006, Sutka et al. 2006, Yoshida 1988).

The results of this study also have implications for other studies that are aimed at the assessment of water quality. Most often, routine sampling of rivers for water quality monitoring is conducted during the day. However, the results presented here clearly indicate that this may often be inadequate to accurately characterize the concentrations of several important compounds. For example, the Canadian Water Quality Guideline for un-ionized ammonia (NH_3) is 19 μg/L (CCME 2007). Under the conditions observed during the sampling period (pH range 7.7 to 8.7, temperature range 25.3°C to 27.6°C), this limit corresponds to NH_4^+ concentrations ranging from 0.01 to 0.6 mg N/L. Our results indicate that these limits are consistently exceeded in the Grand River at the sampling location. However, since nitrification rates are typically greatest during the day when DO concentrations are highest, the concentration of NH_4^+ could fall below the threshold value during the day when NH_4^+ concentrations are low, and exceed the limit at night when the NH_4^+ concentration rises. Routine daytime water quality sampling would not capture this variability.

This study also has implications for studies of greenhouse gas emissions. Concentrations of N_2O and CH_4 in the Grand River are much higher at night. Greenhouse gas emissions from the Grand River would be significantly underestimated if only daytime concentrations were used. The opposite trend was seen by Harrison et al (2005) who found that the emission of N_2O from a subtropical eutrophic stream was much less at night than during the day. Our results also differ from that of Clough et al (2007) who did not observe a significant diel change in N_2O emission. In rivers with a large diel variation in DO concentrations, diel sampling is necessary to properly characterize nitrogen cycling and greenhouse gas production.

5.6 Summary & Conclusions

This study is one of the first to characterize the isotopic composition of N_2O produced in a river, and the only study to measure the diel variability in $\delta^{15}N$ and $\delta^{18}O$ of riverine N_2O. N_2O produced during the day was isotopically distinct from N_2O produced at night, indicating a diel shift in the dominant N_2O production pathways. Using the SIDNO model, it was possible to determine the isotopic composition of N_2O produced in the river, as the measured dissolved values were influenced by gas exchange with tropospheric N_2O and the contribution of N_2O derived from WWTP effluent. Using the model, it was determined that the N_2O produced in the river during the day (dominated by nitrification or nitrifier-denitrification) had a $\delta^{15}N$ of approximately -22‰, and a $\delta^{18}O$ of approximately 43‰. At night, the N_2O production rate was much greater than during the day, and was likely dominated by denitrification. The $\delta^{15}N$ of N_2O produced at night was approximately -30‰, while the $\delta^{18}O$ was approximately 30‰.

The results of this study indicate that the nitrogen cycling processes in the Grand River are linked to diel variations in DO concentration. Other studies have also observed a link between riverine nitrogen cycling and diel variations in DO concentration. Harrison et al. (2005) observed a diel shift in nitrogen cycling processes in a canal in the Yaqui Valley, Mexico. However, in contrast to the Grand River, Harrison et al. (2005) observed that denitrification peaked early at night but then ceased, due to the total consumption of NO_3^-. In the Grand River, denitrification and N_2O production occurred at a high rate throughout the night, indicating that the DO concentration did not drop sufficiently to cause the total denitrification of all the NO_3^- in the water column and sediments.

Another study on the LII River in New Zealand (Clough et al. 2007) also observed diel changes in N_2O production in response to changes in DO concentration. However, the diel range of DO concentration was much greater in the Grand River than was observed in the LII River (Clough et al. 2007). This related to a greater diel response in nitrogen cycling in the Grand River as compared to the LII River. The results of these studies clearly indicate that riverine nitrogen cycling responds to diel variation in DO concentration. Diel shifts in riverine nitrogen cycling are highly sensitive to the magnitude of the diel DO concentration range.

The results of this study indicate that the isotopic analysis of N_2O can provide additional information not available from concentration data alone. Although the isotopic enrichment factors for nitrification and denitrification often overlap, making a clear interpretation difficult, a change in the isotopic composition of produced N_2O is a conclusive indicator that the dominant production pathways have also changed. Also, the

$\delta^{18}O$ of N_2O may be a useful indicator for nitrification in environments with a strong diel variation in $\delta^{18}O$ of DO, since the $\delta^{18}O$ of N_2O produced through nitrification will respond to this variation. Additionally, the isotopic analysis of N_2O provides information regarding the importance of extracellular consumption of N_2O, allowing the relative importance of this pathway to be determined. The isotopic analysis of N_2O will prove valuable in future studies of nitrogen cycling and N_2O production in aquatic environments.

Chapter 6:

Stable Isotope Ratios of Nitrous Oxide Emissions from the Grand River, Ontario, Canada

6.1 Introduction

Nitrous oxide (N_2O) is a powerful greenhouse gas, approximately 310 times more potent than CO_2 on a 100-year timescale (Denman et al 2007). The concentration of N_2O in the atmosphere has steadily risen over the last 250 years (Denman et al 2007), and currently the atmospheric concentration is 320 ppbv, increasing at a rate of 0.26%/year (Prinn et al 1990, Prinn et al 2000). N_2O is produced by microbial transformations of reactive nitrogen (nitrification & denitrification) in the environment. Due to artificial nitrogen fixation, the amount of reactive nitrogen in the environment has increased dramatically over the last 250 years, coinciding with an increase in N_2O production in the environment (Denman et al 2007).

Stable isotope analysis is a powerful tool that can provide a deeper understanding of sources and processes responsible for the production of N_2O. For example, several studies have used $\delta^{15}N$ and $\delta^{18}O$ analysis of N_2O to distinguish between nitrification and denitrification processes in the field (e.g. Bol et al. 2003, Perez et al 2001). Another use of stable isotope analysis of N_2O is the isotopic characterization of global N_2O sources and sinks, for the calculation of atmospheric N_2O budgets.

Rahn & Wahlen (2000) developed a simple model of the isotopic composition of atmospheric N_2O. If the stable isotope ratios of the major N_2O sources are known, it is possible to determine the relative contribution of these sources using their model. Rahn &

Wahlen determined that the difference between the preindustrial and modern values for tropospheric N_2O is approximately 1.9‰ and 2.4 ‰ for $\delta^{15}N$ and $\delta^{18}O$ respectively, with $\delta^{15}N$ decreasing by approximately 0.03‰/year. The most recent and thorough isotopic characterization of tropospheric N_2O places the current values at 6.72 (+/- 0.12) ‰ and 44.62 (+/- 0.21) ‰ for $\delta^{15}N$ and $\delta^{18}O$, respectively (Kaiser et al 2003). At this level of precision, it will be several years before a change in $\delta^{15}N$ and $\delta^{18}O$ of atmospheric N_2O will be detected. Since the work of Rahn & Wahlen (2000), many more studies have been conducted to characterize the isotopic ratios of N_2O emitted from both terrestrial and oceanic environments. The results of these studies are summarized in Figure 6.1.

The global isotopic model of atmospheric N_2O developed by Rahn & Wahlen (2000) only considered terrestrial and oceanic sources of N_2O. More recent work has suggested that rivers and estuaries are a major source of N_2O to the atmosphere. Kroeze et al (2005) and Nevison et al. (2004) estimate that rivers and estuaries contribute between 0.5 to 2.9 Tg N/year of N_2O production. This compares to an estimated total of 9.4 Tg N/year and 3.8 Tg N/year from soil and oceanic sources (Denman et al 2007).

Although this evidence suggests that rivers and estuaries are a significant global source of N_2O to the atmosphere, the isotopic composition of this N_2O is poorly constrained. To date, only one other published study has reported the $\delta^{15}N$ and $\delta^{18}O$ values for N_2O produced in a river (Boontanon et al 2000).

To further complicate matters, the isotopic composition of N_2O emitted to the atmosphere from rivers is not equal to the isotopic composition of dissolved N_2O, due to the equilibration with tropospheric N_2O in such systems (Chapter 4). Additionally, several studies have shown that the N_2O flux and N_2O production processes in rivers can

change dramatically over diel time periods, in response to changes in redox conditions brought on by diel variations in dissolved oxygen (DO) concentrations (Harrison et al 2005, Clough et al 2007, Chapter 5). For these reasons, the $\delta^{15}N$ and $\delta^{18}O$ values of N_2O emitted from rivers is particularly difficult to characterize.

The purpose of this study is to characterize the isotopic composition of N_2O emitted to the atmosphere from the Grand River, Ontario, Canada, and to provide insights into the processes responsible for the variability observed. It is expected that the isotopic signature of N_2O in river systems will vary spatially and temporally, on seasonal and diel timescales. This information will be invaluable for the refinement of the global N_2O isotopic budget (Rahn & Wahlen 2000), and will greatly improve the understanding of N_2O production in rivers.

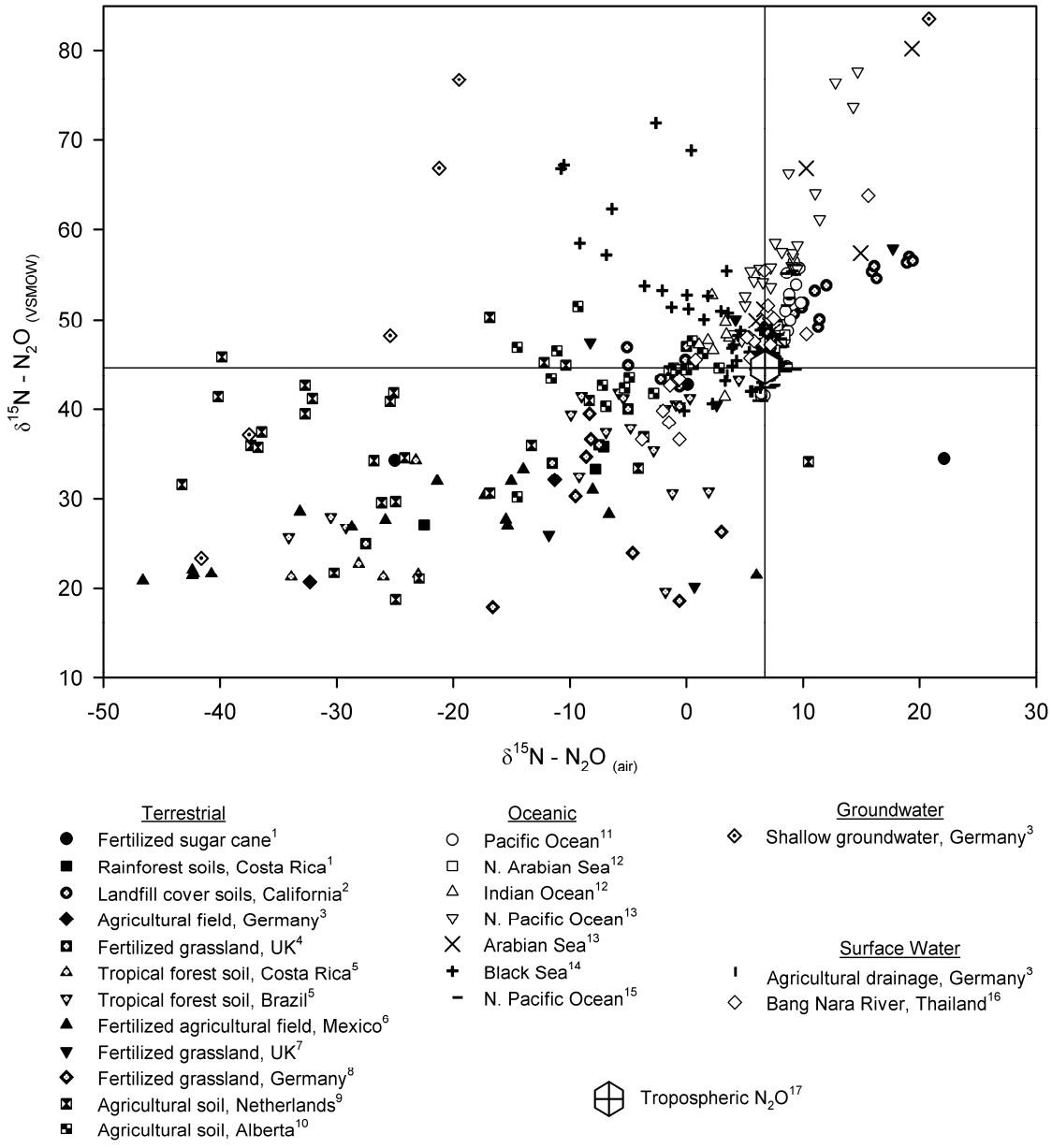

Figure 6.1: Summary of N_2O stable isotope data collected by various studies in terrestrial and aquatic environments. One point is an outlier, and did not fit on the scales of this plot (Shallow Groundwater, Germany[3] $\delta^{15}N = 86.1‰$, $\delta^{18}O = 89.8‰$). References: 1 – Kim & Craig (1993), 2 – Mandernack et al. (2000), 3 – Well et al. (2005), 4 – Yamulki et al. (2001), 5 – Perez et al. (2000), 6 – Perez et al. (2001), 7 – Bol et al. (2003), 8 – Tilsner et al (2003), 9 - Van Groenigen et al. (2005), 10 – Rock et al. (2007), 11 – Kim & Craig (1990), 12 – Naqvi et al (1998), 13 - Yoshanari et al (1997), 14 – Westley et al (2006), 15 - Dore et al. (1998), 16 – Boontanon et al. (2000), 17 – Kaiser et al. (2003)

6.2 Study Site

The Grand River is the largest river in southern Ontario, Canada. It is approximately 300 km long, and drains an area of 7000 km^2 into Lake Erie (Figure 6.2). In 2001, the population in the watershed was approximately 720 000, and is expected to increase by about 60% by 2031 (Ministry of Public Infrastructure Renewal 2006).

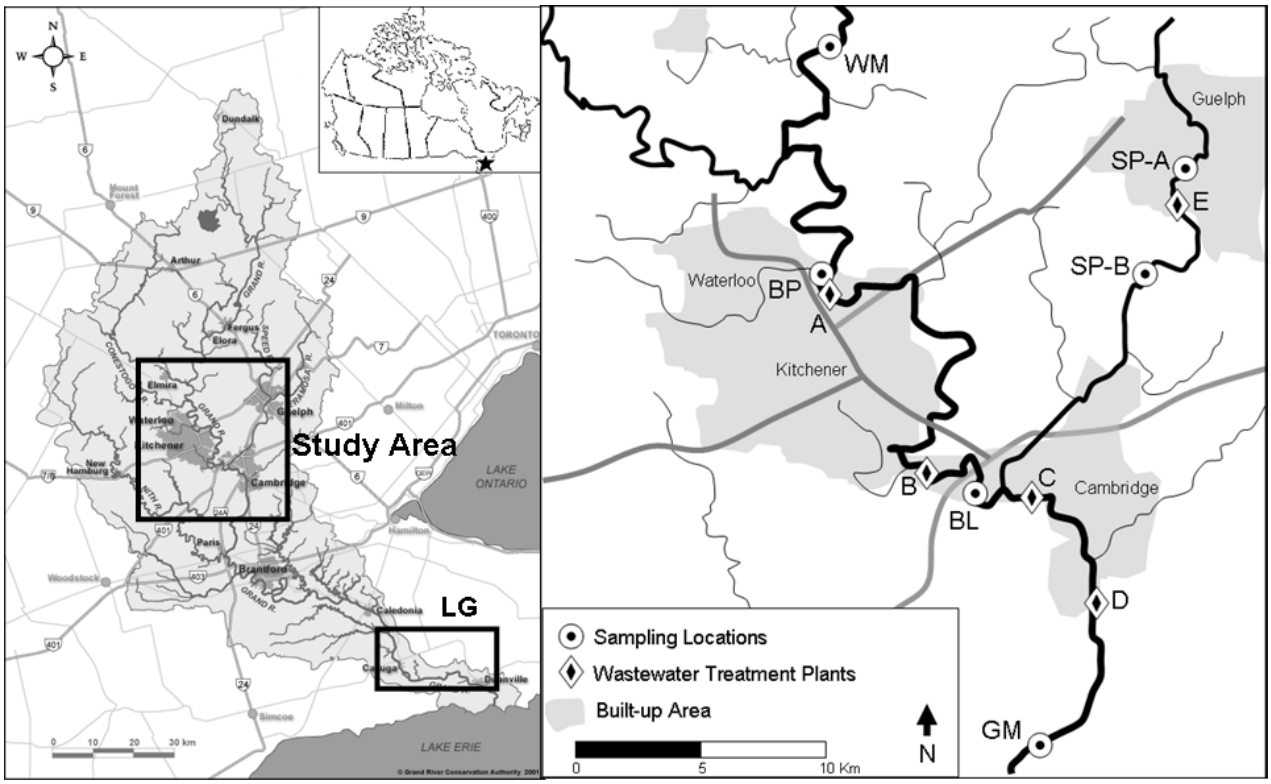

Figure 6.2: Map of the Grand River watershed and study area. River flow direction is generally north to south. Additional information about sampling points and wastewater treatment plants is given in Tables 6.1 & 6.2.

The Grand River is heavily impacted by both diffuse and point-source inputs of nitrogen. Agriculture is the primary land use in the watershed, and 26 wastewater treatment plants (WWTPs) currently discharge effluent to the Grand or its tributaries. The cities of Waterloo, Kitchener, Guelph and Cambridge form the urban centre of the watershed, and the WWTPs for these cities are the major source of municipal effluent to the river. Most of the sampling for this study was conducted at six major sampling points

in the central watershed, located upstream and downstream of these major WWTPs (Figure 6.2). Some additional data was collected from the lower reaches of the Grand River (LG - Figure 6.2), between the communities of York and Dunville. Information about the sampling locations and major WWTPs are summarized in Tables 6.1 & 6.2.

Table 6.1: Summary of sampling sites. Location names in the first column refer to labels in Figure 6.2.

Sampling Location	Watercourse	Geographical Coordinates	Description
WM	Grand River	43°35'07.77"N, 80°28'53.51"W	Upstream of urban centre
BP	Grand River	43°28'54.54"N, 80°28'53.32"W	Upstream of Waterloo and Kitchener WWTPs
BL	Grand River	43°23'07.80"N, 80°23'09.51"W	Downstream of Waterloo and Kitchener WWTPs
GM	Grand River	43°16'36.73"N, 80°20'47.15"W	Downstream of urban centre
SP-A	Speed River	43°32'04.47"N, 80°15'03.81"W	Upstream of Guelph WWTP
SP-B	Speed River	43°29'03.06"N, 80°16'54.16"W	Downstream of Guelph WWTP
LG	Grand River	43°01'18"N, 79°53'30"W to 42°54'7"N, 79°37'52"W	Low energy reaches of the Grand River, located between the communities of York and Dunville

Table 6.2: Nutrient loading from the major WWTPs in the Grand River watershed. Letters in the first column refer to labels in Figure 6.2. Data provided by NPRI (2007).

	WWTP	Mass Discharged through Effluent			
		NH_4^+ tonnes/yr	NO_3^- tonnes/yr	PO_4^{3-} tonnes/yr	Total N tonnes/yr
A	**Waterloo**	77.8	196.4	-	274.2
B	**Kitchener**	633.8	35.3	-	669.1
C	**Preston**	3.5	42.3	-	45.8
D	**Galt**	2.2	242	-	244.2
E	**Guelph**	6.3	1831	4.3	1837.3
(not shown)	**Brantford**	134.9	55.4	5.2	190.3
	Total	**858.5**	**2402.4**	**9.5**	**3260.9**

6.3 Methods

River water samples were collected periodically at the various sampling locations during the period of May 2006 to January 2008. Sampling at all locations (with the

exception of LG) was usually conducted every 2-3 weeks; however sampling was typically more intensive during the summer months. Sampling was also more intensive during and following high river flow periods (daily sampling during snowmelt and storm events), in order to capture the variability in N_2O fluxes associated with these hydrologic events.

Intensive diel sampling was conducted in June 2007 at four sites (BP, BL, SP-A, SP-B) over two separate 28 hour periods, with samples collected every 1.5 hours. Diel sampling was conducted at the BP and BL sites on June 26 – 27, 2007, and at the SP-A and SP-B sites on June 23 – 24, 2007. This diel sampling was conducted to characterize the changes in $\delta^{15}N$ and $\delta^{18}O$ of N_2O produced in the river in response to the diel dissolved oxygen (DO) cycles in the river at these locations. These four sites were chosen to contrast N_2O production upstream and downstream of the major WWTPs in the watershed (Figure 6.2, Table 6.2).

Samples for the measurement of dissolved N_2O concentration were collected in 50mL glass serum bottles (Wheaton # 223745), and capped with no headspace underwater with a red rubber stopper (Vaccutainer ™). Stoppers are baked at 60°C overnight before use to limit out gassing into the samples. Samples for the isotopic analysis of N_2O were collected in 500mL glass media bottles (Corning # 1395-500), and similarly capped underwater with no headspace using a black rubber lyophilization stopper (Wheaton # 224100-503). All samples were both preserved with saturated $HgCl_2$ solution (2mL solution / L sample) and kept on ice until they were transported back to the lab, typically within 4 hours of collection. Samples were kept in cold storage (4°C) until they were analyzed (typically within 2 days of collection).

Dissolved N_2O concentrations were determined using a headspace equilibration technique. A headspace was created in the sample bottles by injection of ultra-high purity helium using a syringe and hypodermic needle, while extracting sample water with a second syringe and needle. The samples were then placed on an orbital shaker for 1.5 hours to bring the dissolved phase into equilibrium with the headspace. N_2O concentration in the headspace was then determined using a Varian CP-3800, equipped with an ECD detector. The analytical error for dissolved N_2O concentration using this method is approximately ±5%.

Stable isotope ratios of dissolved N_2O were obtained using the purge and trap method described by Thuss et al (2008a). Briefly, dissolved N_2O is sparged from the water samples using a fast flowing stream of ultra-pure helium. Water vapour and CO_2 is stripped from the resulting gas mixture using a nafion membrane and chemical traps. N_2O is trapped cryogenically in a vial containing pyrex wool and glass beads in a liquid nitrogen bath. The extracted N_2O is then analyzed by CF-IRMS using a GV Trace-Gas preconcentrator system coupled with a GV Isoprime mass spectrometer. The analytical precision for both $\delta^{15}N$ and $\delta^{18}O$ is approximately ±0.5‰.

N_2O fluxes from the river to the atmosphere were calculated from the dissolved concentration using gas exchange coefficients determined with the PoRGy model (Venkiteswaran et al 2007). N_2O concentrations and flux rates for the Grand River during the study period are reported in more detail elsewhere (Rosamond 2008).

The isotopic ratios of the N_2O flux to the atmosphere were calculated using the isotopic and concentration data for dissolved N_2O, as described in Chapter 4. Since gas exchange is a two-way equilibrium process, there is a continuous invasion of

tropospheric N_2O into solution, even when the net N_2O flux is in the opposite direction. This calculation accounts for the isotopic effects of the isotopic equilibration with tropospheric N_2O, as well as the equilibrium and kinetic fractionation factors for N_2O gas exchange determined by Inoue & Mook (1994). The stable isotope ratios of the N_2O flux (R^{15}_{flux} and R^{18}_{flux}) are simply the ratios between the flux rates of the heavy and light isotopologues of N_2O:

$$R^{15}_{flux} = \frac{\text{Flux } {}^{15}\text{N}_2\text{O}}{\text{Flux } {}^{14}\text{N}_2\text{O}} = \frac{\text{Flux } {}^{15}\text{N}_2\text{O}}{\left(\text{Flux N}_2\text{O - Flux } {}^{15}\text{N}_2\text{O}\right)} \tag{6.1}$$

$$R^{18}_{flux} = \frac{\text{Flux N}_2{}^{18}\text{O}}{\text{Flux N}_2{}^{16}\text{O}} = \frac{\text{Flux N}_2{}^{18}\text{O}}{\left(\text{Flux N}_2\text{O - Flux N}_2{}^{18}\text{O}\right)} \tag{6.2}$$

The fluxes ($mol \cdot m^{-2} \cdot h^{-1}$) for bulk N_2O and the heavy isotopologues can be calculated as follows:

$$\text{Flux N}_2\text{O} = K\left(P(\text{N}_2\text{O})\text{K}_\text{h} - [\text{N}_2\text{O}]_{dissolved}\right) \tag{6.3}$$

$$\text{Flux } {}^{15}\text{N}_2\text{O} = K\left[\alpha^{15}_{in} P(\text{N}_2\text{O})\text{K}_\text{h}\left(\frac{R^{15}_{gas}}{1+R^{15}_{gas}}\right) - \alpha^{15}_{ev}[\text{N}_2\text{O}]_{dissolved}\left(\frac{R^{15}_{dissolved}}{1+R^{15}_{dissolved}}\right)\right] \tag{6.4}$$

$$\text{Flux N}_2{}^{18}\text{O} = K\left[\alpha^{18}_{in} P(\text{N}_2\text{O})\text{K}_\text{h}\left(\frac{R^{18}_{gas}}{1+R^{18}_{gas}}\right) - \alpha^{18}_{ev}[\text{N}_2\text{O}]_{dissolved}\left(\frac{R^{18}_{dissolved}}{1+R^{18}_{dissolved}}\right)\right] \tag{6.5}$$

Where $P(N_2O)$ is the partial pressure of tropospheric N_2O (atm - as determined by Prinn et al. 1990, Prinn et al. 2000), R^{15}_{gas} and R^{18}_{gas} are the isotopic ratios of tropospheric N_2O (as determined by Kaiser et al 2003), α^{15}_{in}, α^{18}_{in}, α^{15}_{ev}, and α^{18}_{ev} are the kinetic fractionation factors for N_2O gas exchange (as determined by Inoue & Mook 1994), and

$[N_2O]_{dissolved}$ is the dissolved concentration of N_2O ($mol \cdot m^{-3}$). K_h ($mol \cdot atm^{-1} \cdot m^{-3}$) is Henry's constant for N_2O, and can be calculated empirically as follows (adapted from Gevantman 2008):

$$K_h = 55394 \times e^{\left(-60.7467 + \frac{8882.8}{T} + 21.2531 \ln\frac{T}{100}\right)} \quad (6.6)$$

Where T is water temperature in K. Although the gas exchange coefficient ($K - m \cdot h^{-1}$) is unknown for equations 6.3 - 6.5, the isotopic ratios of the N_2O flux depend only on the relative flux rates between the major isotopologues, and the term is eliminated by substitution into equations 6.1 & 6.2.

The error associated with the calculated $\delta^{15}N$ and $\delta^{18}O$ values of the N_2O flux is greater than the error for $\delta^{15}N$ and $\delta^{18}O$ of dissolved N_2O, since the calculation also depends on the dissolved concentration which has an associated error value.

The error for the calculated isotopic ratios of the N_2O flux was calculated by varying the $\delta^{15}N$ and $\delta^{18}O$ values for dissolved N_2O by ±0.5‰, and the dissolved concentration values by ±5%. The maximum variation in the calculated values for $\delta^{15}N$ and $\delta^{18}O$ were taken as the error. For most data points, the error associated with this calculation was <2‰. Data points with an error greater than 5‰ were rejected.

To calculate the annual average isotopic composition of the bulk N_2O flux from the central Grand River, only data from 2007 were included in the analysis. The $\delta^{15}N$ and $\delta^{18}O$ data were weighted by flux rate and time. Flux rates for each data point were calculated using the dissolved N_2O concentration and representative gas exchange rates

calculated using the PoRGy gas exchange model (Rosamond et al 2008, Venkiteswaran et al 2007). The annual average isotopic composition of N_2O flux from the LG sites was not calculated due to insufficient data for this analysis.

6.4 Results

During the period from May 2006 to January 2008, 616 river samples were collected for dissolved N_2O concentration analysis (Figure 6.3). Of these samples, 268 were analyzed to determine the $\delta^{15}N$ and $\delta^{18}O$ of dissolved N_2O (Figure 6.4). In 40 of these samples, the dissolved N_2O concentration was too low to accurately calculate the isotopic composition of the N_2O flux, so it was possible to determine the $\delta^{15}N$ and $\delta^{18}O$ of the N_2O flux on only 228 samples (Figure 6.5). Generally, the calculated $\delta^{15}N$ and $\delta^{18}O$ values for the N_2O flux become less accurate as the concentration approaches 100% saturation. Typically, the rejected data points had concentrations that were less than 130% saturation. Therefore the rejected data points represented the lowest 15% of the measured N_2O concentrations, and the magnitude of the N_2O flux for these data points was insignificant.

There is a significant difference in $\delta^{15}N$ and $\delta^{18}O$ values for the dissolved N_2O and the N_2O flux to the atmosphere (Figure 6.6). The difference was most pronounced in samples with N_2O concentration less than 1000% saturation. The $\delta^{15}N$ and $\delta^{18}O$ values for dissolved N_2O range from -35.3 to 8.2‰ and 22.7 to 59.1‰, respectively. In contrast, the $\delta^{15}N$ and $\delta^{18}O$ values for the N_2O flux are more spread out, ranging from -57.4 to 8.7‰ and 11.3 to 77.1‰, respectively. This indicates that the isotopic composition of dissolved N_2O in the Grand River is largely controlled by the equilibration with

tropospheric N_2O, resulting in $\delta^{15}N$ and $\delta^{18}O$ values that approach the composition of tropospheric N_2O ($\delta^{15}N$ = 6.72 +/- 0.12‰ and $\delta^{18}O$ = 44.62 +/- 0.21‰; Kaiser et al 2003) as the concentration decreases. Since the isotopic composition of the N_2O emitted to the atmosphere (Figure 6.5) is most representative of the isotopic composition of N_2O produced in the river at steady state, (Chapter 4) the discussion in this chapter will focus on the calculated $\delta^{15}N$ and $\delta^{18}O$ values for the N_2O flux.

There is a large amount of spatial variation in the $\delta^{15}N$ and $\delta^{18}O$ – N_2O data collected from the Grand River. There is a clear difference in N_2O concentration and isotopic composition from upstream of the Waterloo and Kitchener WWTPs (WM & BP sites) compared to data collected immediately downstream (BL site). N_2O from the BL site is the most depleted in both ^{15}N and ^{18}O, with most of the flux values ranging from -30 to -10‰, and 20 to 30‰ for $\delta^{15}N$ and $\delta^{18}O$ (Table 6.3). The N_2O concentration is also the greatest at the BL site, with dissolved concentrations as high as 8,500% saturation (Figure 6.3, Table 6.3). These differences in N_2O concentration and isotopic composition are a result of nutrient input to the Grand River from the upstream WWTPs.

High nutrient concentrations downstream of the Waterloo and Kitchener WWTPs, cause heavy macrophyte growth in the river channel. Also, these treatment plants (especially the Kitchener WWTP, Table 6.2) release large amounts of NH_4^+ (Table 6.2), and rely on nitrification in the river oxidize the NH_4^+ to NO_3^-. Respiration and nitrification result in very low night-time concentrations of dissolved oxygen (DO) downstream of the Waterloo and Kitchener WWTPs, which stimulate high rates of N_2O production through denitrification (Chapter 5). The discharge of municipal WWTP

effluent into the Grand River therefore has a clear effect on the downstream nitrogen cycling and N_2O production.

The type of wastewater treatment and the quality of the effluent released to the river also has an effect on the isotopic composition and concentration of N_2O in the river. Although SP-B is also directly downstream of a major WWTP (Guelph), the N_2O isotopic composition and production rate at this location is very different than at BL (downstream of Waterloo and Kitchener WWTPs). While dissolved N_2O concentrations at BL reached a maximum of 8,500% saturation, the maximum concentration observed at SP-B was only 515 % saturation (Table 6.3). The isotopic composition of the N_2O flux at SP-B is also more enriched in ^{15}N and ^{18}O compared to BL (Table 6.3). While the nitrogen released by the Waterloo and Kitchener WWTPs is predominantly in the form of NH_4^+, the Guelph plant fully nitrifies the wastewater before it is released to the river, and NO_3^- is the predominant nitrogen species released. Therefore, the discharge of effluent from the Guelph WWTP likely does not stimulate nitrification in the river, though the release of NO_3^- has the potential to stimulate denitrification. However, the concentration of DO at SP-B does not fall below 4 mg/L, making very large increases in denitrification rate unlikely. Compared to the large difference in N_2O concentration and isotopic composition upstream and downstream of the Waterloo and Kitchener WWTPs (BP and BL), the concentration and isotopic composition of N_2O in the Speed River upstream and downstream of the Guelph WWTP (SP-A and SP-B) are quite similar (Table 6.3). Although the addition of NO_3^- and organic nitrogen from the Guelph WWTP has the potential to affect the downstream nitrogen cycling, there is no significant change in N_2O production.

Although GM is also located downstream of several major WWTPs (Figure 6.2), the N_2O concentrations (and thus N_2O production rates) are similar to the upstream sites (Figure 6.3). However, the isotopic composition of the N_2O flux is intermediate between the BL site and the rest of the upstream sites (Figure 6.5). Although the N_2O is similar to the upstream sites, the nitrogen source and N_2O production is influenced by the WWTPs upstream of this location. Previous work by the Grand River Conservation Authority has determined that there is significant groundwater discharge to the Grand River upstream of the GM site. The additional groundwater dilutes the nitrogen nutrients in the river, leading to an improvement in water quality. Macrophyte growth in the river channel at GM is much less than at BL, and thus the diel change in DO concentration is also much less at this location. Although the NO_3^- concentration at GM remain elevated with respect to the sites upstream of the WWTPs (WM and BP), the heavy NH_4^+ load from the Waterloo and Kitchener WWTPs is fully nitrified far upstream of the GM site. Therefore, effluent from these treatment plants does not affect N_2O production at this location to the same extent as the BL location.

The $\delta^{15}N$ and $\delta^{18}O$ values from the samples collected at the LG sites are the most positive compared to data collected at all other sites (Table 6.3). The isotopic composition of the N_2O flux from the LG sites is very similar to that of N_2O collected from oceanic waters (Figure 6.1). The gradient of the river is very low at the LG sites, and a small dam in Dunville, Ontario greatly increases river depth and hydraulic residence time throughout this reach. Since the river water is much deeper and more stagnant at these sites, dissolved N_2O remains in the water column relatively longer before it is released to the atmosphere through gas exchange. Therefore, there is a greater

potential for dissolved N_2O to be consumed through reduction to N_2 gas. Several studies have shown that $\delta^{18}O$ tends increase faster than $\delta^{15}N$ in residual N_2O during reduction to N_2 gas, and there is typically a 1:2 ratio for $\delta^{15}N$:$\delta^{18}O$ during this process (Vieten et al. 2007, Menyailo & Hungate 2006, Mandernack et al. 2000). The $\delta^{15}N$ and $\delta^{18}O$ values for the N_2O flux from the LG sites trends along this 1:2 line. Other studies that have measured the isotopic composition of N_2O from deep or stagnant water (oceanic studies, Figure 6.1, Green Lake – Wahlen & Yoshinari 1985, Bang Nara River – Boontanon et al 2000), have observed $\delta^{15}N$ and $\delta^{18}O$ values which are generally more positive compared to N_2O from terrestrial sources. It is likely that high $\delta^{15}N$ and $\delta^{18}O$ values are characteristic of dissolved N_2O in deep or stagnant water sites due to N_2O reduction to N_2.

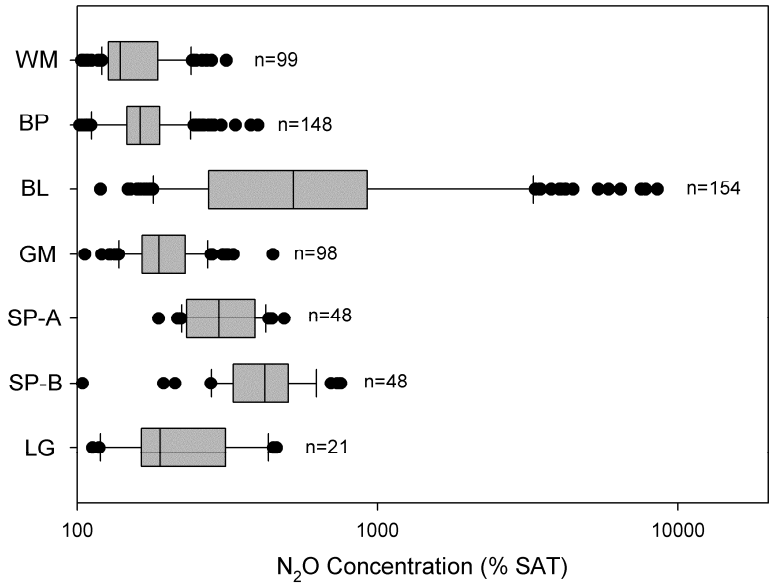

Figure 6.3: Dissolved N_2O concentrations measured at the seven sampling locations on the Grand and Speed Rivers during the study period. Bars represent median values, 10^{th}, 25^{th}, 75^{th}, and 90^{th} percentiles. Individual points represent outliers which fall outside the 10^{th} and 90^{th} percentiles. Note the log scale.

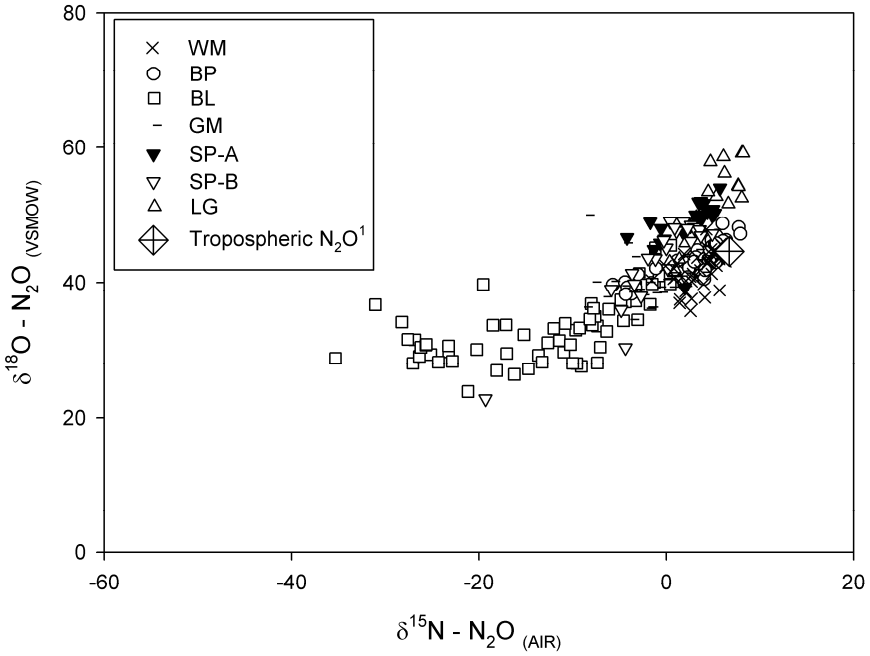

Figure 6.4: $\delta^{15}N$ and $\delta^{18}O$ values of dissolved N_2O measured at the seven sampling locations on the Grand and Speed Rivers during the study period. Analytical precision for $\delta^{15}N$ and $\delta^{18}O$ is approximately 0.5‰. [1](Kaiser et al 2003).

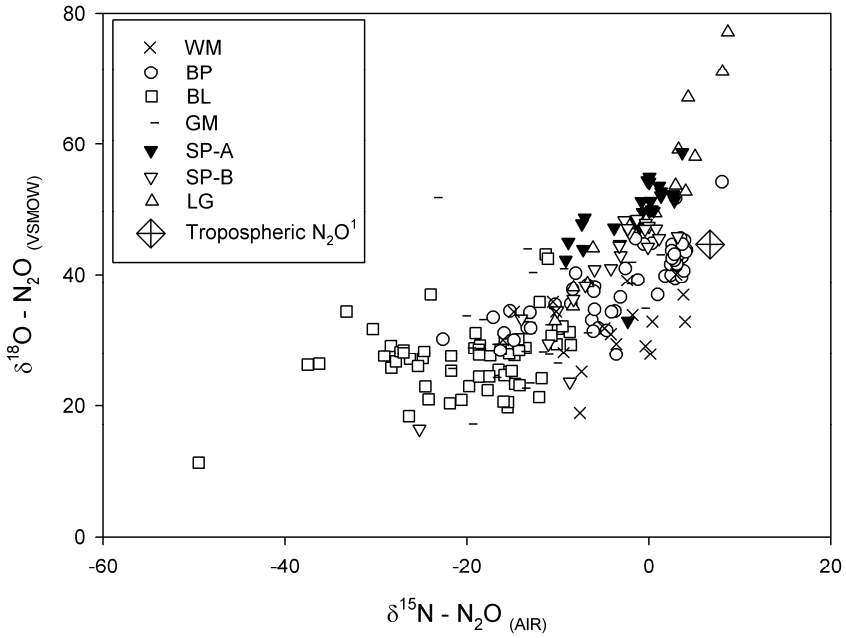

Figure 6.5: Calculated $\delta^{15}N$ and $\delta^{18}O$ values of the N_2O flux to the atmosphere from the seven sampling locations on the Grand and Speed Rivers during the study period. Values are calculated using equations 6.1-6.6, and the $\delta^{15}N$, $\delta^{18}O$ and concentration values of dissolved N_2O. Data points were rejected where the calculation error exceeded 5‰ for $\delta^{15}N$ or $\delta^{18}O$. The large cluster of BP points to the left of the tropospheric N_2O point were all collected during a 28 hour period [1](Kaiser et al 2003).

Table 6.3: Summary of dissolved N_2O concentration, and $\delta^{15}N$ and $\delta^{18}O$ values for dissolved and flux N_2O from the seven sampling locations on the Grand and Speed Rivers during the study period. Concentration data only includes samples for which $\delta^{15}N$ and $\delta^{18}O$ analysis was also conducted.

	Dissolved				Flux		
Sampling Location	**Concentration** (% saturation)	**$\delta^{15}N$** (‰)	**$\delta^{18}O$** (‰)	**n**	**$\delta^{15}N$** (‰)	**$\delta^{18}O$** (‰)	**n**
WM	105 to 115	-2 to 6	36 to 48	39	-18 to 8	11 to 53	29
BP	100 to 300	-35 to 2	24 to 46	68	-23 to 10	29 to 54	58
BL	120 to 8540	-6 to 9	23 to 49	68	-50 to -9	11 to 43	64
GM	105 to 330	-29 to 4	34 to 50	36	-24 to 1	17 to 52	29
SP-A	190 to 390	-4 to 6	39 to 54	26	-9 to 4	33 to 59	25
SP-B	105 to 515	-19 to 5	23 to 49	24	-25 to 3	16 to 9	23
LG	115 to 460	0 to 8	42 to 59	17	-10 to 9	33 to 82	13

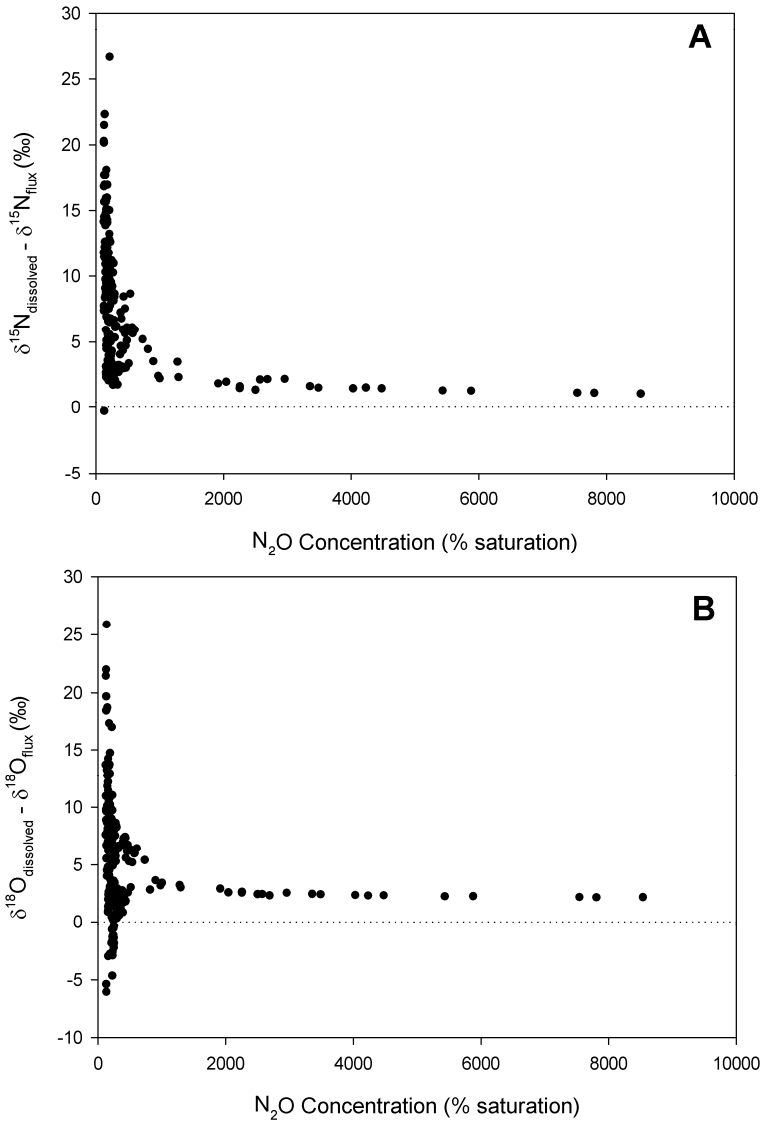

Figure 6.6: The difference in the isotopic composition of dissolved N_2O and calculated flux N_2O as a function of concentration. The difference is most pronounced when the concentration is less than 1000 % saturation. A – $\delta^{15}N_{dissolved} - \delta^{15}N_{flux}$ vs. concentration. B – $\delta^{18}O_{dissolved} - \delta^{18}O_{flux}$ vs. concentration.

6.4.1 Seasonal Variability

N_2O concentration and fluxes were generally much higher in the warmer months (May to October) compared to the colder months of the year (November to April) (Figure 6.7, Rosamond 2008). Since N_2O is produced as a result of biological processes, it is not

surprising that N_2O production rates are greater with increased water temperatures. Similarly, the $\delta^{15}N$ and $\delta^{18}O$ values of the N_2O flux to the atmosphere also vary seasonally.

Typically, there is a greater range of $\delta^{15}N$ and $\delta^{18}O$ values for N_2O produced during the warm months as compared to the cold months (Figures 6.8 & 6.9, Table 6.4). The difference in the $\delta^{15}N$ and $\delta^{18}O$ values of the N_2O flux between the various sampling locations is also most pronounced during the warm months (Figure 6.8, Table 6.4).

Generally, the N_2O flux is more depleted in ^{15}N and ^{18}O during the cold months of the year (November to April), and values are generally more consistent between the various sampling locations. The $\delta^{15}N$ of NO_3^- collected upstream and downstream of the major WWTPs at various times throughout the year was quite consistent, ranging between 7.4 and 11.2‰ (Table 6.5). Given that the isotopic composition of the nitrogen source is relatively constant throughout the year, the differences are a result of changes in isotopic enrichment factors for N_2O production only.

The NO_3^- concentration in the river is typically greater in the winter months as compared to the summer months. Since fractionation is expected to be greatest when the substrate is non limiting, the change in NO_3^- concentration does not explain the change in fractionation factors for N_2O production. Based on laboratory incubation experiments, fractionation factors for N_2O production are inversely proportional to the production rate when the substrate concentration is held constant (Mariotti et al. 1981, 1982). Since the N_2O production rate is lower during the cold months, this effect partially explains the lower $\delta^{15}N$ and $\delta^{18}O$ values.

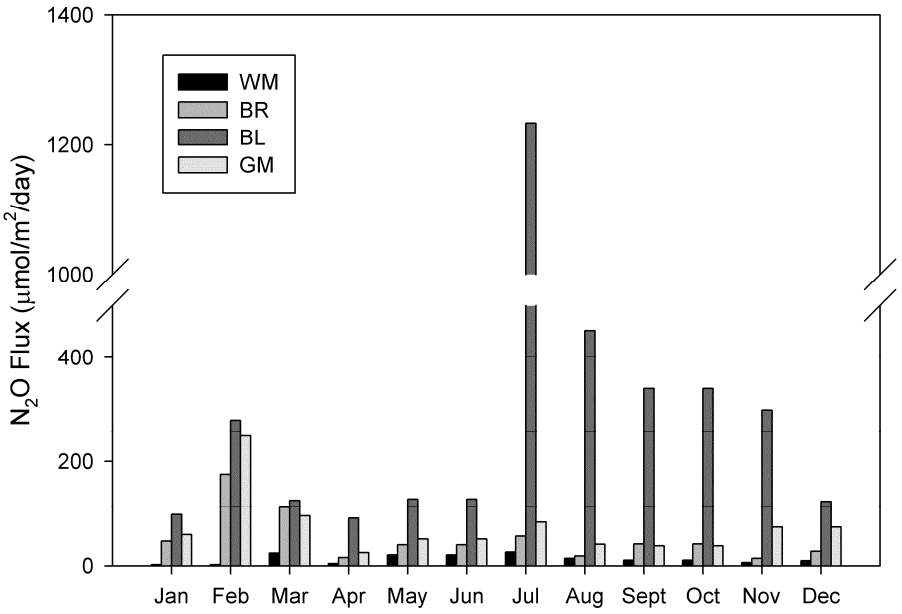

Figure 6.7: Average monthly N_2O flux rates from the four sampling locations in the central Grand River (Rosamond 2008). Fluxes are calculated using the concentration data and gas exchange rates obtained using the PoRGy model (Venkiteswaran et al 2007). Average monthly flux rates were not calculated for the SP-A, SP-B and LG sites due to insufficient data.

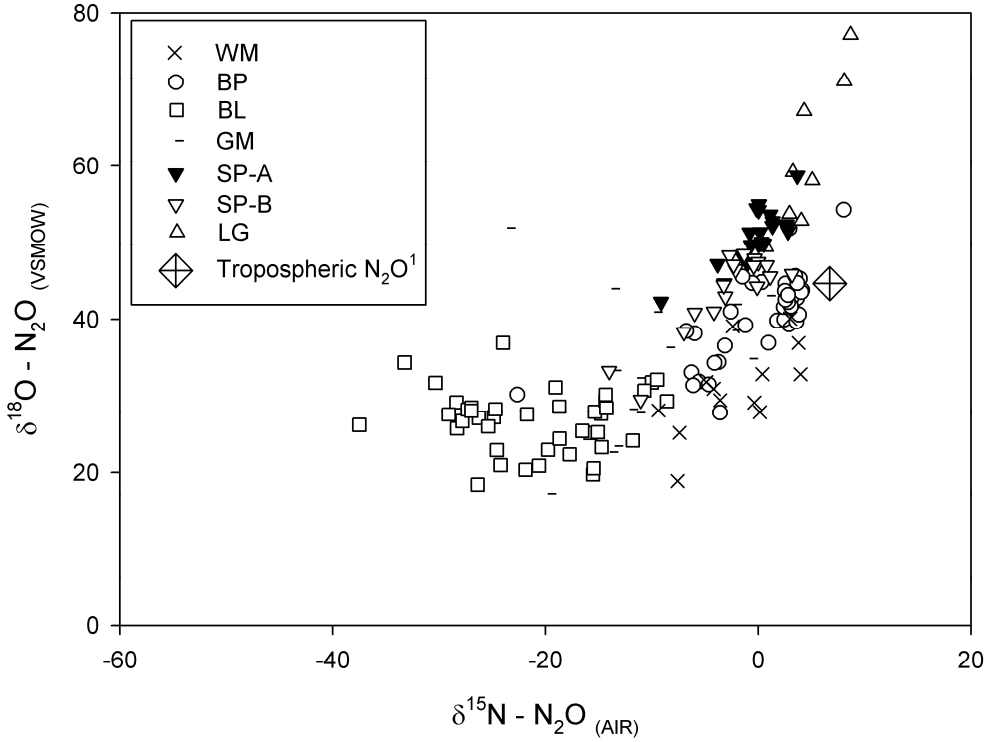

Figure 6.8: Calculated $\delta^{15}N$ and $\delta^{18}O$ values of the N_2O flux to the atmosphere from the seven sampling locations on the Grand and Speed Rivers for the period from May to October. These values are representative of N_2O produced during the warm months of the year. [1](Kaiser et al 2003).

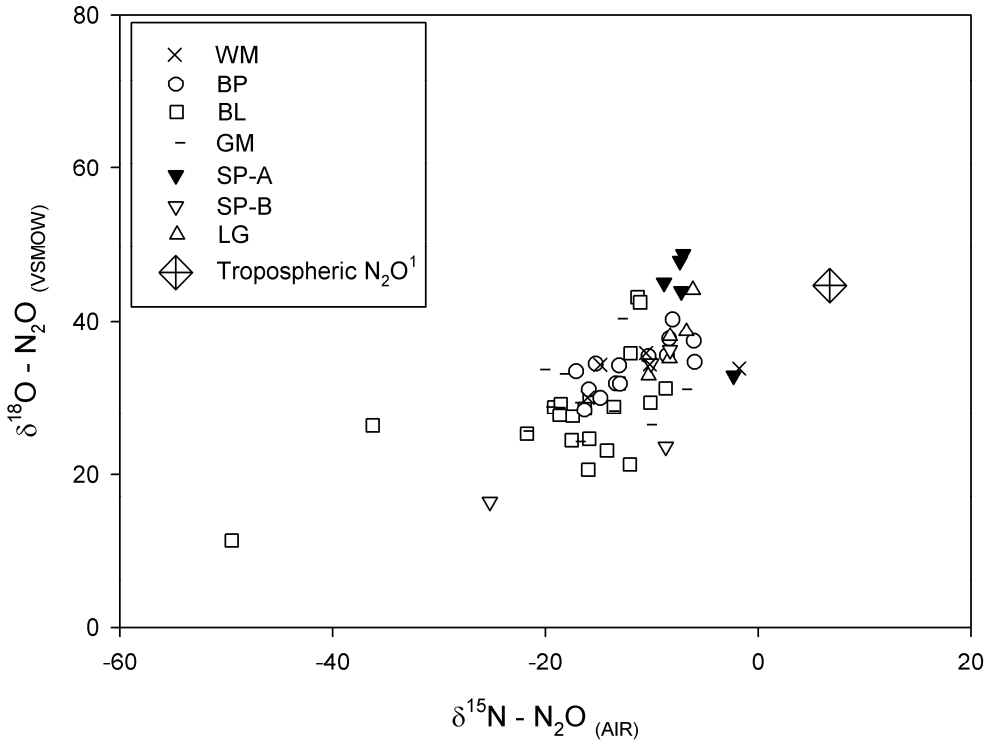

Figure 6.9: Calculated $\delta^{15}N$ and $\delta^{18}O$ values of the N_2O flux to the atmosphere from the seven sampling locations on the Grand and Speed Rivers for the period from November to April. These values are representative of N_2O produced during the cold months of the year. [1](Kaiser et al 2003).

Table 6.4: Summary of the calculated $\delta^{15}N$ and $\delta^{18}O$ values of the N_2O flux to the atmosphere from the seven sampling locations on the Grand and Speed Rivers for the summer and winter periods. Summer is defined as the period from May to October, and winter is defined as the period from November to April.

	Summer				Winter			
Sampling Location	**Concentration** (% saturation)	**$\delta^{15}N$** (‰)	**$\delta^{18}O$** (‰)	**n**	**Concentration** (% saturation)	**$\delta^{15}N$** (‰)	**$\delta^{18}O$** (‰)	**n**
WM	105 to 315	-9 to 4	19 to 40	13	105 to 165	-16 to -2	30 to 36	5
BP	100 to 300	-23 to 8	28 to 54	41	105 to 250	-17 to -6	28 to 40	14
BL	170 to 8540	-37 to -9	18 to 37	43	120 to 540	-49 to -9	11 to 43	21
GM	140 to 305	-24 to 1	17 to 52	15	105 to 270	-22 to -7	24 to 40	12
SP-A	185 to 255	-9 to 4	42 to 59	20	230 to 390	-9 to -2	33 to 49	5
SP-B	280 to 515	-14 to 3	29 to 48	19	105 to 610	-25 to -8	16 to 36	5
LG	110 to 460	1 to 9	49 to 77	8	160 to 190	-10 to -6	33 to 44	5

Table 6.5: A summary of the measured $\delta^{15}N$ values for NO_3^- in the Grand River, collected at various times throughout the year during the study period.

Sampling Location	$\delta^{15}N - NO_3^-$ (‰)			
	Average	Minimum	Maximum	n
BP	9.8	7.4	11.2	15
BL	9.3	7.4	11.2	12
GM	9.1	8.5	10.3	4
SP-B	8.7	-	-	1

6.4.2 Diel Variability

Previous work has shown that the production rate and isotopic composition of N_2O in the Grand River downstream of the Waterloo and Kitchener WWTPs (BL site) can vary greatly in response to diel changes in dissolved oxygen concentrations (Chapter 5). The results of diel sampling at three other sites (BP, SP-A, SP-B) in June 2007, indicate that these diel variations are present at other locations on the Grand River, but not to the same extent as at the BL site (Figure 6.10, 6.11).

As explained in Chapter 5, this diel variability is driven by changes in dissolved oxygen (DO) concentrations, which increase during the day due to photosynthesis, and decrease at night due to respiration (Figure 6.10). Since the N_2O production processes of nitrification and denitrification are highly sensitive to redox conditions (e.g. Harrison et al 2005), the relative importance of these processes for N_2O production is variable throughout the diel cycle. The diel DO concentration cycle is much more pronounced at BL than at the other three sites, leading to much greater variation in the rates of nitrification and denitrification at this location (Chapter 5). As a result, the diel variation

in NO_3^- and NH_4^+ concentration is much more pronounced at BL than the other sites (Figure 6.10).

In general, N_2O production is greatest during the night when DO concentrations are lowest (Figure 6.11). Since NH_4^+ is only present in significant concentrations (greater than 0.1 mg N/L) at the BL site, denitrification in the river sediments is likely the dominant N_2O production process at BP, SP-A and SP-B. Denitrification activity in the river sediments will increase in response to lower DO concentrations, though it is possible that the N_2O:N_2 ratio could decrease. However, these results indicate that the net N_2O production rate increases as the DO concentration decreases. Although previous research has shown that fractionation factors for N_2O production are inversely proportional to production rate (Mariotti et al. 1981, 1982), this effect is not seen at BP and SP-B, assuming that the $\delta^{15}N$ of NO_3^- is relatively constant (Table 6.6).

The gas exchange rate at SP-A is very high, due to a series of small dams located immediately upstream of the sampling location. For this reason, the DO concentration did not vary greatly over the diel cycle. As a result, the N_2O production rate and isotopic composition at SP-A remained relatively constant over the diel time period.

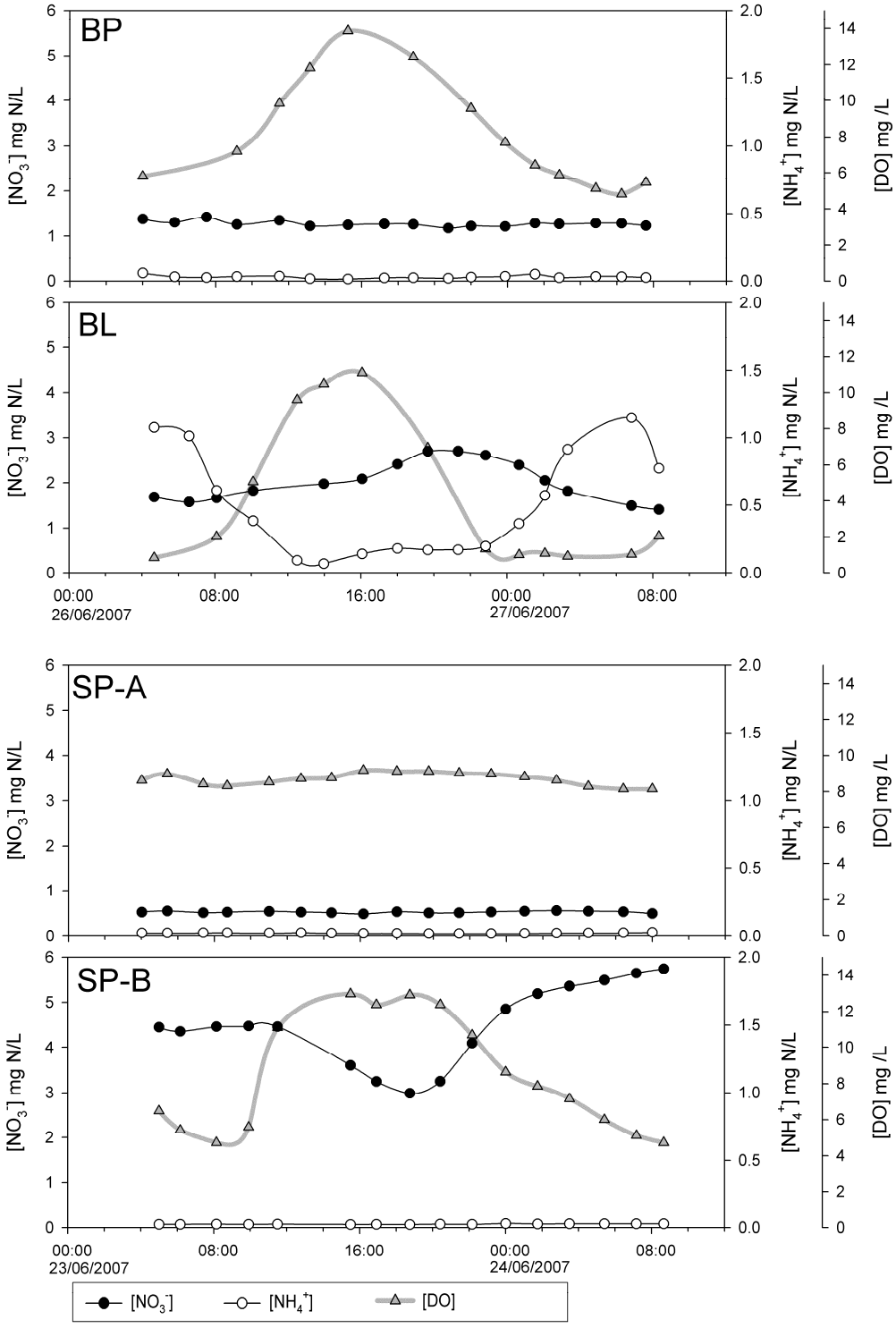

Figure 6.10: Diel variations in NO_3^-, NH_4^+ and DO concentration at four sampling locations measured in June 2007. Sampling at BP and BL was conducted over 28 hours from June 26 – 27, and sampling at SP-A and SP-B was conducted over 28 hours from June 23 – 24.

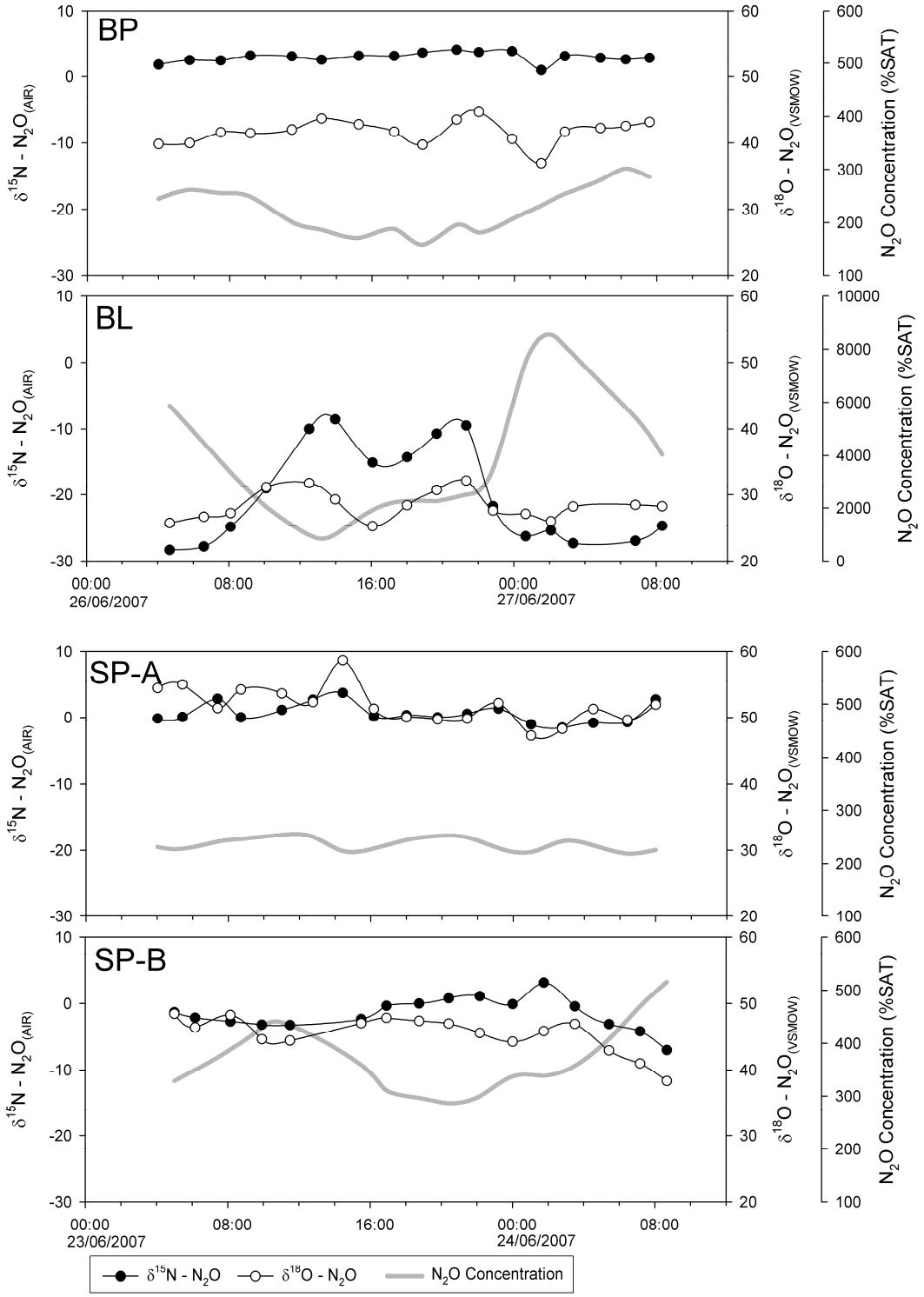

Figure 6.11: Diel variations in N_2O concentration and $\delta^{15}N$ and $\delta^{18}O$ values of the N_2O flux to the atmosphere at four sampling locations measured in June 2007. Sampling at BP and BL was conducted over 28 hours from June 26 – 27, and sampling at SP-A and SP-B was conducted over 28 hours from June 23 – 24. All vertical scales are the identical, except for the N_2O concentration scale for BL.

6.5 Disscussion

The annual average $\delta^{15}N$ and $\delta^{18}O$ values for WM, BP, GM, and SP-B are remarkably similar, ranging from -14‰ to -7‰ and 34.5‰ to 36.8‰, for $\delta^{15}N$ and $\delta^{18}O$ respectively (Table 6.6). These values are more negative with respect to $\delta^{15}N$ and $\delta^{18}O$ compared to published data from other aquatic environments (Figure 6.1). Although the average $\delta^{15}N$ value for SP-A is similar to the others, it is not clear why the $\delta^{18}O$ value is considerably higher (45.5‰). Since the $\delta^{18}O$ of N_2O produced through denitrification is largely controlled by oxygen exchange with environmental H_2O (Kool et al 2007), a small change in the extent of this exchange rate would have a great effect on the $\delta^{18}O$ of N_2O produced. Since different microbial species have been shown to facilitate oxygen exchange at greatly different rates (Kool et al. 2007), a difference in the microbial communities between locations would lead to a change in the rate of oxygen exchange. Alternatively, the higher $\delta^{18}O$ values could be a reflection of partial N_2O consumption in the river sediments (Vieten et al. 2007, Menyailo & Hungate 2006, Mandernack et al. 2000), however the $\delta^{15}N$ value for SP-A is not significantly greater than at the other locations.

As expected, the average isotopic composition of the N_2O flux from the BL site is significantly different than that from all the other locations. The $\delta^{15}N$ and $\delta^{18}O$ values for this site are heavily influenced by the night-time N_2O production during the warm summer months. The most depleted N_2O (both in ^{15}N and ^{18}O) at the BL site is produced during the summer nights when DO concentrations are low and N_2O production rates are highest. As explained in Chapter 5, N_2O production at BL at night likely occurs through denitrification in the sediments or at the sediment water interface, while during the day

most of the N_2O at BL is produced through nitrification, with sediment denitrification also contributing to N_2O production. Since N_2O at BP is also likely produced by denitrification in the sediments, and the $\delta^{15}N$ of NO_3^- is similar upstream and downstream of the WWTPs (Table 6.5), these results indicate that the fractionation factors for N_2O production through denitrification upstream of the WWTPs is different than downstream of the WWTPs This difference in enrichment factors is likely a result of a change in the microbial community responsible for denitrification upstream and downstream of the WWTPs.

The estimated total emission of N_2O to the atmosphere from the central Grand River was 15.5 tonnes in 2007. The annual average $\delta^{15}N$ and $\delta^{18}O$ values for N_2O emitted to the atmosphere from the central Grand River were -18.5‰ and 32.7‰ respectively. Since the total N_2O production in the Grand River is dominated by summertime production at the BL site (Figure 6.8), the total average isotopic composition of the N_2O flux from the Grand River most resembles that from the BL site. The flux and time weighted average values for $\delta^{15}N$ and $\delta^{18}O$ of N_2O produced in the Grand River are much more depleted than the values measured for N_2O in the Bang Nara River, Thailand (Boontanon et al 2000, Figure 6.12).

Table 6.6: Magnitude and isotopic composition of the N_2O flux to the atmosphere from the six major sampling locations. Only data collected for 2007 was included in this analysis.

Sampling Location	Surface area of Representative Reach (ha)	Total Annual N_2O Emission (tonnes)	$\delta^{15}N$ (‰)	$\delta^{18}O$ (‰)
WM	68	0.20	-11.3	36.8
BP	187.5	2.41	-7.0	36.6
BL	52.8	8.50	-26.3	29.3
GM	87.4	1.74	-14.0	34.5
SP-A	33.2	0.84	-6.7	45.5
SP-B	57.5	1.78	-7.5	35.5
Total	**486**	**15.5**	**-18.5**	**32.7**

Using only the available isotopic data for terrestrial and oceanic N_2O production, Rahn & Wahlen (2000) estimated that the $\delta^{15}N$ of tropospheric N_2O is decreasing by approximately 0.03‰ /year. However, due to the current limitations in precision of N_2O isotopic analysis, it will be several years before a clear trend can be directly observed (Kaiser et al. 2003). Since N_2O production in rivers was not accounted for in this calculation, this estimate may be greatly altered by including N_2O from this important source. However, using this very limited dataset, it is difficult to assess the impact of riverine N_2O production on the global isotopic budget of atmospheric N_2O.

If the global riverine N_2O production is similar in isotopic composition to the Bang Nara River, Thailand (Boontanon et al 2000), this source will have a very limited impact on the predicted negative trend for $\delta^{15}N$ of tropospheric N_2O (~0.03‰ / year Rahn & Wahlen 2000). However, if the average value obtained from the Grand River ($\delta^{15}N$ = -18.5, $\delta^{18}O$ = 32.7) is representative of global riverine N_2O production, $\delta^{15}N$ trend of tropospheric N_2O would be greater than that predicted by Rahn & Wahlen (2000). Once the true trend in the $\delta^{15}N$ and $\delta^{18}O$ of tropospheric N_2O is observed, the

isotopic composition of various global N_2O sources can be used to determine the relative significance of each source. Therefore, more work is needed to characterize the isotopic composition of riverine N_2O before the true isotopic contribution of this important source can be determined.

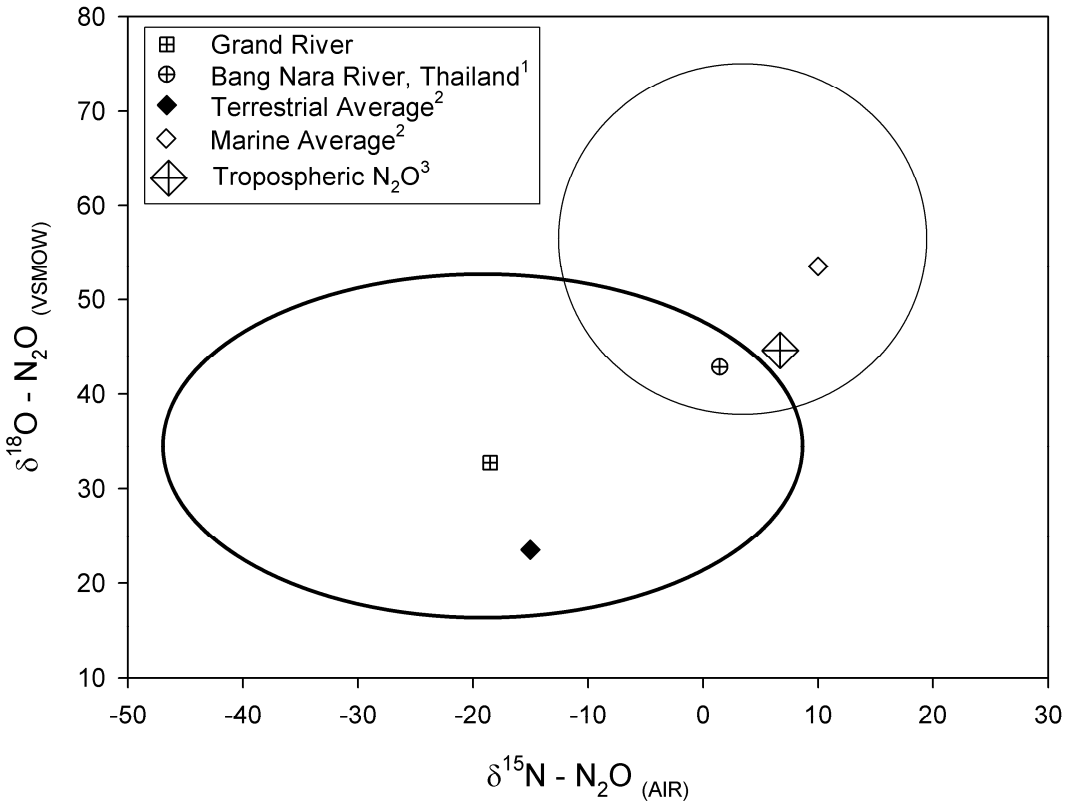

Figure 6.12: Flux and time weighted annual average $\delta^{15}N$ and $\delta^{18}O$ values of the N_2O flux for the Grand River compared to other published N_2O flux values. Only data collected for 2007 was included in this analysis. The average value for the Bang Nara River was calculated using the published $\delta^{15}N$, $\delta^{18}O$ and concentration values published by Boontanon et al 2000. The heavy and light outlined ovals represent the range of published data for terrestrial and oceanic environments from Figure 6.1, respectively. [1](Boontanon et al 2000), [2](Rahn & Wahlen 2000) [3](Kaiser et al 2003).

6.6 Conclusions

The $\delta^{15}N$ and $\delta^{18}O$ of N_2O emitted to the atmosphere from the Grand River is highly variable, with variability dependent on location with respect to nutrient sources such as WWTPs. It is possible to determine the composition of the bulk annual N_2O flux, by calculating the $\delta^{15}N$ and $\delta^{18}O$ of the N_2O flux from measured values for dissolved

N_2O concentration, $\delta^{15}N$ and $\delta^{18}O$. The isotopic composition of the bulk annual flux from the Grand River is significantly different than the only other reported value for riverine N_2O production (Boontanon et al 2000). If the isotopic composition of N_2O produced in the Grand River is representative of global riverine N_2O production, then Rahn & Wahlen (2000) likely have underestimated the trend for $\delta^{15}N$ of tropospheric N_2O. Due to the current analytical precision for $\delta^{15}N$ and $\delta^{18}O$ analysis of tropospheric N_2O (+/- 0.12‰ for $\delta^{15}N$ and +/- 0.21‰ for $\delta^{18}O$, Kaiser et al 2003), it will be several years before a clear trend can be detected. Additional research is needed to better characterize the isotopic composition of riverine N_2O production. This knowledge will enable researchers to better apportion global sources of N_2O and understand the production of this important greenhouse gas.

Chapter 7:

Summary of Conclusions

This project achieved several research objectives. The first was to develop an effective method to measure the stable isotope composition ($\delta^{15}N$ and $\delta^{18}O$) of dissolved N_2O. A new simplified method was developed for the isolation of dissolved N_2O. This technique involved purging dissolved N_2O from samples using an ultra pure helium stream, and cryogenic trapping the resulting N_2O in sample vials using a liquid nitrogen bath. Using this method, it is possible to analyze samples at concentrations as low as 6 nmol N_2O/L with a 20 minute processing time. Although other published studies have used online methods to measure the $\delta^{15}N$ and $\delta^{18}O$ of dissolved N_2O, this offline method allows for a greater sample throughput, and will allow researchers who do not have access to a dedicated mass spectrometer to collect and store dissolved N_2O for offsite isotopic analysis.

The second objective was to characterize the complex relationship between the $\delta^{15}N$ and $\delta^{18}O$ values for produced, dissolved and emitted N_2O in aquatic systems. Due to the kinetic and equilibrium isotope effects associated with gas exchange, as well as the equilibration with tropospheric N_2O, the isotopic composition of dissolved N_2O is not equal to that of the source N_2O, or that of N_2O emitted to the atmosphere in aqueous systems open to gas exchange. To provide insight into the relationship between the stable isotope compositions of source, dissolved and emitted N_2O, a simple box model was

created using Stella modelling software (SIDNO – **S**table **I**sotopes of **D**issolved **N**itrous **O**xide).

Using this model, it was found that when the residence time of dissolved N_2O is short compared to the period of variability, the isotopic composition of emitted N_2O is much more representative (compared to dissolved N_2O) of the isotopic composition of source N_2O. For a N_2O source with a constant $\delta^{15}N$ and $\delta^{18}O$, a simple change in production rate (and therefore dissolved concentration) can produce a change in the $\delta^{15}N$ and $\delta^{18}O$ values of dissolved N_2O, while the isotopic composition of the emitted N_2O will remain nearly constant. Also, under certain conditions, the $\delta^{15}N$ and $\delta^{18}O$ values of dissolved N_2O can remain nearly constant, even if the values for the source and emitted N_2O are changing dramatically.

Using a simple set of equations, it is possible to calculate the isotopic composition of N_2O emitted from an aquatic system if the concentration, $\delta^{15}N$ and $\delta^{18}O$ of dissolved N_2O are measured. The isotopic composition of emitted N_2O is a much more useful measurement than the isotopic composition of dissolved N_2O, both for inferring the $\delta^{15}N$ and $\delta^{18}O$ of the N_2O produced, as well as for global N_2O isotopic budgets. Therefore, it is recommended that the $\delta^{15}N$ and $\delta^{18}O$ of the emitted N_2O be calculated and reported for studies using stable isotope analysis of dissolved N_2O.

In future research, the SIDNO model should be improved by the addition of a term to account for the consumption of N_2O and reduction to N_2. This would allow for a more accurate understanding of the stable isotope dynamics of dissolved N_2O, especially in anoxic systems where N_2O consumption is an important process.

The third objective of this research project was to characterize the processes responsible for N_2O production in the Grand River. Previously published studies have shown that nitrogen cycle processes and N_2O production in rivers is strongly tied to diel changes in dissolved oxygen concentration. This link was confirmed in the Grand River by continuous sampling over a 28 hour period downstream of the major wastewater treatment plants.

It was found that nitrification or nitrifier-denitrification dominated N_2O production during the day when dissolved oxygen concentrations were high. Sediment denitrification likely also contributed to N_2O production during the day. Denitrification occurred at night when dissolved oxygen concentrations were low, producing N_2O at a much higher rate than during the day. The SIDNO model was used to determine the diel variation in the isotopic composition of N_2O production. N_2O produced during the day had a $\delta^{15}N$ value of -22‰ and a $\delta^{18}O$ value of 43‰. N_2O produced during the night had a $\delta^{15}N$ value of -30‰ and a $\delta^{18}O$ value of 30‰.

Using the $\delta^{15}N$ and $\delta^{18}O$ values for N_2O, NO_3^- and NH_4^+ in the river, apparent in-situ enrichment factors for N_2O production through nitrification and denitrification were calculated. For denitrification, the nitrogen enrichment factor ranged from -34‰ to -30.8‰, and the oxygen enrichment factor ranged from 31‰ to 33‰. The nitrogen enrichment factor for nitrification ranged between -50‰ to -46‰, though these values may be influenced by the contribution of N_2O from sediment denitrification. Since these enrichment factors are based on in-situ production, they are more representative of N_2O production than published enrichment factors obtained by laboratory cultures of single microbial species.

It is recommended that in future research, lab incubations of sediment and water from the Grand River be conducted to further investigate the relative importance of N_2O production in the sediments versus the water column. Isotopic data from these laboratory incubations could be used to further support the in-situ isotopic enrichment factors obtained using the SIDNO model.

This study fully characterized N_2O production in the Grand River downstream of the Waterloo and Kitchener WWTPs. Planned modifications to these treatment plants are expected to greatly improve the quality of effluent discharged to the Grand River within the next 10 years. It is recommended that further sampling be conducted after the improvements are completed in order to determine the importance of WWTP effluent quality on N_2O production and nitrogen cycling. The results of this research would have broad implications for river management and wastewater treatment in the future.

The final objective of this research project was to characterize the spatial and temporal variability of the isotopic composition of N_2O emitted from the Grand River. Although N_2O production in rivers accounts for a significant portion of the global N_2O budget, the isotopic composition of N_2O from this important source has not been well characterized. Only one other published study has measured $\delta^{15}N$ and $\delta^{18}O$ of N_2O produced in a river. The results of the present study indicate that the magnitude and isotopic composition of the N_2O flux to the atmosphere varies significantly both spatially and temporally in the Grand River.

Generally, N_2O fluxes are greatest immediately downstream of the major wastewater treatment plants. N_2O produced downstream of the Waterloo and Kitchener

WWTPs is more depleted in $\delta^{15}N$ and $\delta^{18}O$ compared to upstream locations. The Guelph WWTP does not have the same effect on downstream N_2O production. The major difference between the plants is that the Waterloo and Kitchener plants release large quantities of NH_4^+, while the Guelph plant only releases NO_3^-. These results indicate that the quality of wastewater effluent has a great effect on the downstream production of N_2O.

The $\delta^{15}N$ and $\delta^{18}O$ values of N_2O emitted from the sites on the lower Grand River were higher than any other location in the Grand River and were similar to the isotopic composition of N_2O produced in oceanic environments. The lower Grand River is deeper and slower moving than the other locations studied, and N_2O consumption is likely an important process in the lower reaches of the river. It is possible that high $\delta^{15}N$ and $\delta^{18}O$ values are characteristic of N_2O produced in deep water environments.

Overall, the magnitude and isotopic composition of the N_2O flux from the Grand River is dominated by night-time production downstream of the Waterloo and Kitchener WWTPs during the summer months. The flux and time weighted annual average isotopic composition of N_2O emitted from the Grand River was -18.5‰ and 32.7‰ for $\delta^{15}N$ and $\delta^{18}O$ respectively. This is significantly more depleted than N_2O from the Bang Nara River, Thailand (the only other published data for riverine N_2O production).

This study focused on N_2O production in the middle and lower reaches of the Grand River. Future research should investigate N_2O production and nitrogen cycling in the upper reaches and smaller tributaries in the Grand River watershed. Since the nitrogen sources and hydrologic conditions in these smaller watercourses are much different than that of the higher order reaches of the Grand River, it is expected that N_2O production

and nitrogen cycling would differ in these areas as well. Also, this study did not investigate N_2O production in the major reservoirs located within the Grand River watershed. The deep water and long hydraulic retention times in these reservoirs likely allows for denitrification and N_2O consumption to remove nitrogen from the system. Future research should examine the role of these reservoirs in nitrogen cycling in the Grand River watershed.

Currently, this study is the most thorough characterization of the $\delta^{15}N$ and $\delta^{18}O$ of N_2O produced in a river environment. However, further research is needed to characterize the isotopic composition of global riverine N_2O production. Current research indicates that approximately 25% of global anthropogenic N_2O production occurs in rivers, estuaries and near shore coastal environments (Denman et al 2007); however the isotopic composition of this important source is poorly constrained. The data presented here indicates that the isotopic composition of N_2O produced in river environments is highly variable, both spatially and temporally. The isotopic composition of riverine N_2O production is likely also influenced by other environmental factors such as climate, water quality, and hydrology. Future research into riverine N_2O production should focus on characterizing the isotopic composition of N_2O in rivers other than the Grand River, and should focus on developing links between environmental conditions and $\delta^{15}N$ and $\delta^{18}O$ of N_2O. This research is needed to accurately determine the effect of riverine N_2O production on the global atmospheric N_2O isotopic budget. If global riverine N_2O production is similar in isotopic composition to that from the Grand River, the negative trend for $\delta^{15}N$ and $\delta^{18}O$ of tropospheric N_2O will be significantly greater in magnitude than previously predicted. The thorough characterization of global riverine N_2O

production will allow for a more accurate understanding of the relative importance of global N_2O sources and sinks.

References

Ackerman, EA. (1941) The Koppen Classification of Climates in North America. *Geographical Review.* **31**(1): 105-111.

Aleem MIH, Hoch GE, Varner JE (1965) Water as the source of oxidant and reductant in bacterial chemosynthesis. *Proceedings of the National Academy of Sciences of the United States of America,* **54,** 869-873.

Amann, RI, Ludwig W, Schleifer K (1995) Phylogenetic identification and in situ detection of individual microbial cells without cultivation. *Microbiological reviews* **59**(1): 143-169

Andersson KK, Hooper AB (1983) O_2 and H_2O are each the source of one O in NO_2 produced from NH_3 by Nitrosomonas: ^{15}N evidence. *Federation of European Biochemical Societies Letters*. **164,** 236-240.

APHA (1995) Standard methods for the examination of water & wastewater. 19th edition. Washington, D.C. 4500-O C

Aravena R, Robertson WD (1998) Use of multiple isotope tracers to evaluate denitrification in ground water: Study of nitrate from a large-flux septic system plume. *Ground Water,* **36,** 975-982.

Barford CC, Montoya JP, Altabet MA, Mitchell R (1999) Steady-state nitrogen isotope effects of N_2 and N_2O production in Paracoccus denitrificans. *Applied and Environmental Microbiology*, **65,** 989-994.

Blackmer AM, Bremner JM (1977) Nitrogen Isotope discrimination in denitrification of nitrate in soils. *Soil Biology and Biochemistry*, **9,** 73-77.

Bollmann A, Conrad R (1997a) Acetylene blockage technique leads to underestimation

of denitrification rates in oxic soils due to scavenging of intermediate nitric oxide. *Soil Biology and Biochemistry* **29**(7):1067-1077

Bollmann A, Conrad R (1997b) Enhancement by acetylene of the decomposition of nitric oxide in soil. *Soil Biology and Biochemistry* **29**(7):1057-1066

Bol R, Toyoda S, Yamulki S, Hawkins JMB, Cardenas LM, Yoshida N. (2003) Dual isotope and isotopomer ratios of N_2O emitted from a temperate grassland soil after fertilizer application. *Rapid Communications in Mass Spectrometry* **17**:2550-2556

Boontanon N, Ueda, S, Kanatharana P, Wada E, (2000) Intramolecular stable isotope ratios of N_2O in the tropical swamp forest in Thailand. *Naturwissenschaften* **87**:188-192

Böttcher J, Strebel O, Voerkelius S, Schmidt HL (1990) Using isotope fractionation of nitrate-nitrogen and nitrate-oxygen for evaluation of microbial denitrification in a sandy aquifer. *Journal of Hydrology*, **114,** 413-424.

Bouwman, A. F., 1990. Exchange of greenhouse gases between terrestrial ecosystems and atmosphere. In: Bouwman, A. F. (Ed.), Soils and the Greenhouse Effect. Wiley, New York, pp. 61-127

Bremner, J.M. (1997) Sources of nitrous oxide in soils. *Nutrient Cycling in Agroecosystems* **49**: 7-16

Brenninkmeijer CAM. (1991) Robust, High-Efficiency, High-Capacity Cryogenic trap. *Analytical Chemistry* 1991; **63**(11): 1182.

Brenninkmeijer CAM Röckmann T. (1996) Russian Doll type cryogenic traps: Improved design and isotope separation effects. *Analytical Chemistry* **68**(17): 3050.

Brenninkmeijer CAM, Röckmann T (1999) Mass spectrometry of the intramolecular nitrogen isotope distribution of environmental nitrous oxide using fragment-ion analysis. *Rapid Communications in Mass Spectrometry* **13**:2028-2033

Cabello P, Roldan MD, Moreno-Vivian C (2004) Nitrate reduction and the nitrogen cycle in archaea. *Microbiology* **150**: 3527-3546

Casciotti KL, Sigman DM, Galanter Hastings M, Böhlke JK, Hilkert A (2002) Measurement of the oxygen isotopic composition of nitrate in seawater and freshwater using the denitrifier method. *Analytical Chemistry* **74**:4905-4912

Cey EE, Rudolph DL, Aravena R, Parkin G (1999) Role of the riparian zone in controlling the distribution and fate of agricultural nitrogen near a small stream in southern Ontario. *Journal of Contaminant Hydrology,* **37,** 45-67.

Clough TJ, Bertram JE, Sherlock RR, Leonard RL, Nowicki BL, (2006) Comparison of measured and EF5-r-derived N_2O fluxes from a spring-fed river. *Global Change Biology* **12**:352-363

Clough T, Buckthought LE, Kelliher FM, Sherlock RR, (2007) Diurnal fluctuations of dissolved nitrous oxide (N_2O) concentrations and estimates of N_2O emissions from a spring-fed river: implications for IPCC methodology. *Global Change Biology* **13**:1-12

Cho CM, Yan T, Liu X, Wu L, Zhou J, Stein LY (2006) Transcriptome of a *Nitrosomonas europaea* mutant with a disrupted nitrite reductase gene (*nirK*) *Applied and Environmental Microbiology* **72**(6): 4450-4454

Cole JJ, Caraco NF, (2001) Emissions of nitrous oxide (N_2O) from a tidal, freshwater river, the Hudson River, New York. *Environmental Science & Technology* **35**(6):991-996

Coplen TB, Böhlke JK, Casciotti KL (2004) Using dual-bacterial denitrification to improve $\delta^{15}N$ determinations of nitrates containing mass-independent ^{17}O. *Rapid Communications in Mass Spectrometery* **18**:245-250

Denman KL, Brasseur G, Chidthaisong A, Ciais P, Cox PM, Dickinson RE, Hauglustaine D, Heinze C, Holland E, Jacob D, Lohmann U, Ramachandran S, da Silva Dias PL, Wofsy SC. (2007) In *Climate Change 2007: The Physical Science Basis. Contribution of Working Group I to the Fourth Assessment Report of the Intergovernmental Panel on Climate Change,* Soloman S, Qin D, Manning M, Chen Z, Marquis M, Averyt KB, Tignor M (eds). Cambridge University Press.: New York,; 143-145, 544 - 546

Dore JE, Popp BN, Karl DM, Sansone FJ. (1998) A large source of atmospheric nitrous oxide from subtropical North Pacific surface waters. *Nature* **396**: 63.

Dumont E, Harrison JA, Kroeze C, Bakker EJ, Seitzinger SP, (2005) Global distribution and sources of dissolved inorganic nitrogen export to the coastal zone: Results from a spatially explicit, global model. *Global Biogeochemical Cycles* **19**, GB4S02, doi:10.1029/2005GB002488

Environment Canada (2004) Canadian Climate Normals 1971 – 2000, Climate records for Waterloo – Wellington Airport. [Accessed May 22, 2008]. http://www.climate.weatheroffice.ec.gc.ca/climate_normals/results_e.html?Province=ONT%20&StationName=&SearchType=&LocateBy=Province&Proximity=25&ProximityFrom=City&StationNumber=&IDType=MSC&CityName=&ParkName=&LatitudeDegrees=&LatitudeMinutes=&LongitudeDegrees=&LongitudeMinutes=&NormalsClass=A&SelNormals=&StnId=4832&

Firestone MK, Davidson EA (1989) Microbiological basis of NO and N_2O production and consumption in soil. In: *Exchange of Trace Gases between Terrestrial Ecosystems and the Atmosphere* (eds Andreae MO, Schimel DS), pp. 7-21. John Wiley & Sons Ltd., Chichester.

Garnier, J Cébron A, Tallec, G, Billen G, Sebilo M, Martinez A, (2006) Nitrogen behavior and nitrous oxide emission in the tidal Seine River estuary (France) as nfluenced by human activities in the upstream watershed. *Biogeochemistry* **77**:305-326

Garnier, J, Billen G, Cébron A, (2007) Modelling nitrogen transformations in the lower Seine river and estuary (France): impact of wastewater release on oxygenation and N_2O emission. *Hydrobiologia* **588**:291-302

Gruber N, Galloway JN (2008) An Earth-system perspective of the global nitrogen cycle. *Nature* **451**:293-296

Gevantman, LH (2007) “Solubility of Selected Gases in Water” In *CRC Handbook of Chemistry and Physics, 88th Edition (Internet Version 2008)*, Lide DR. (ed.) CRC Press / Taylor and Francis.: Boca Raton, FL, 2007

Harrington, J.B. (1987), Climate Change: A Review of Causes. *Canadian Journal of Forestry Resources* **17**: 1313-1339

Harrison JA, Matson PA, Fendorf SE, (2005) Effects of a diel oxygen cycle on nitrogen transformations and greenhouse gas emissions in a eutrophied subtropical stream. *Aquatic Sciences* **67**(3):308-315, doi:10.1007/s00027-005-0776-3

Hayatsu M, Tago K, Saito M (2008) Various players in the nitrogen cycle: Diversity and functions of the microorganisms involved in nitrification and denitrification. *Soil Science and Plant Nutrition* **54**: 33-45

Hollocher TC, Tate ME, Nicholas DJD (1981) Oxidation of Ammonia by Nitrosomonas europaea: Definitive ^{18}O-Tracer evidence that hydroxylamine formation involves a monooxygenase. The *Journal of Biological Chemistry,* **256,** 10834-10836.

Hollocher TC (1984) Source of the oxygen atoms of nitrate in the oxidation of nitrite by Nitrobacter agilis and evidence against a P-O-N anhydride mechanism in oxidative phosphorylation. *Archives of Biochemistry and Biophysics*, **233,** 721-727.

HYDAT (2005) National Water Data Archive, Water Survey of Canada, Environment Canada. http://www.wsc.ec.gc.ca/products/hydat/main_e.cfm?cname=hydat_e.cfm [Accessed May 22, 2008]

Inoue HY, Mook WG, (1994) Equilibrium and kinetic nitrogen and oxygen isotope fractionations between dissolved and gaseous N_2O. *Chemical Geology (Isotope Geosciences Section)* **113**:135-148

Iribar, A, Sánchez-Pérez, JM, Lyautey E, Garabétian F (2008) Differentiated free-living and sediment-attached bacterial community structure inside and outside denitrification hotspots in the river-groundwater interface. *Hydrobiologia* **598**:109-121

Kaiser, J. (2002) Stable isotope investigations of atmospheric nitrous oxide. PhD Dissertation, Johannes Gutenberg-Universität, Mainz

Kaiser J, Rockmann T, Brenninkmeijer CAM, (2003) Complete and accurate mass spectrometric isotope analysis of tropospheric nitrous oxide. *Journal of Geophysical Research* **108**(D15):4476, doi:10.1029/2003JD003613

Kemp MJ, Dodds WK, (2002) Comparisons of nitrification and denitrification in prairie and agriculturally influenced streams. *Ecological Applications* **12**(4):998-1009

Kendall C (1998) Chapter 16: Tracing nitrogen sources and cycling in catchments. *In:* Isotope tracers in catchment hydrology (eds Kendall C, McDonnell JJ), pp. 519-576. Elsevier Science BV, Amsterdam.

Kendall, C., Aravena, R. (2000) Nitrate isotopes in groundwater systems. In *Environmental Tracers in Subsurface Hydrology*. Cook, P., Herczeg, A.L. (eds). Kluwer Academic Publishers: Massachusetts, pp 261-297.

Kim KR, Craig H. (1990) Two-isotope characterization of N_2O in the Pacific Ocean and constraints on its origin in deep water. *Nature* **347**: 58

Kim KR, Craig H. (1993) Nitrogen-15 and Oxygen-18 Characteristics of nitrous oxide: A global perspective. *Science* **262**(5141): 1855.

Kool DM, Wrage N, Oenema O, Dolfing J, Van Groenigen JW (2007) Oxygen exchange between (de)nitrification intermediates and H_2O and its implications for source determination of NO_3^- and N_2O: a review. *Rapid Communications in Mass Spectrometry* **21**: 3569-3578

Kroeze C, Dumont E, Seitzinger SP (2005) New estimates of global emissions of N_2O from rivers and estuaries. *Environmental Sciences* **2**(2-3): 159-165

Kumar, S, Nicholas DJD, Williams EH (1983) Definitive ^{15}N NMR evidence that water serves as a source of 'O' during nitrite oxidation by Nitrobacter agilis. *Federation of European Biochemical Societies Letters*, **152,** 71-74.

Laursen AE, Seitzinger SP, (2002) Measurement of denitrification in rivers: an integrated, whole reach approach. *Hydrobiologia.* **485**:67-81

Laursen AE, Seitzinger SP (2004) Diurnal patterns of denitrification, oxygen consumption and nitrous oxide production in rivers measured at the whole-reach scale. *Freshwater Biology* **49**:1448-1458

Lide DR (ed.) (2008) "Vapour Pressure of Fluids at Temperatures Below 300K" In *CRC Handbook of Chemistry and Physics, 88th Edition (Internet Version 2008)*, CRC Press / Taylor and Francis.: Boca Raton, FL, 2007

Lide, D.R., Frederiskse, H.P.R. (eds.) (1995) *CRC Handbook of Chemistry and Physics, 76th Edition*. CRC Press, Inc, Boca Raton, FL

Mandernack KW, Rahn T, Kinney C, Wahlen M. (2000) The biogeochemical controls of the $\delta^{15}N$ and $\delta^{18}O$ of N_2O produced in landfill cover soils. *Journal of Geophysical Research*; **105**(D14):17709

Mariotti A, Germon JC, Hubert P, Kaiser P, Letolle R, Tardieux A, Tardieux P (1981) Experimental determination of nitrogen kinetic isotope fractionation: Some principles; illustrations for the denitrification and nitrification processes. *Plant Soil*, **62,** 413-430.

Mariotti A, Germon JC, Leclerc A (1982) Nitrogen isotope fractionation associated with the $NO_2^- \rightarrow N_2O$ step of denitrification in soils. *Canadian Journal of Soil Science*, **62,** 227-241.

Mariotti A, Landreau A, Simon B (1988) ^{15}N isotope biogeochemistry and natural denitrification process in groundwater: application to the chalk aquifer of northern France. *Geochimica et Cosmochimica Acta*, **52,** 1869-1878.

McKenney DJ, Wang SW, Drury CF (1997) Reaction of nitric oxide with acetylene and oxygen: Implications for denitrification assays. *Soil Science Society of America Journal* **61**: 1370-1375

McMahon PB, Dennehy KF (1999) N_2O emissions from a nitrogen-enriched river. *Environmental Science & Technology* **33**:21-25

Mengis M, Schiff SL, Harris M, English MC, Aravena R, Elgood RJ, MacLean A (1999) Multiple geochemical and isotopic approaches for assessing ground water NO_3^- elimination in a riparian zone. *Ground Water*, **37,** 448-457.

Menyailo OV, Hungate BA (2006) Stable isotope discrimination during soil denitrification: Production and consumption of nitrous oxide. *Global Biogeochemical Cycles*, **20 (GB3025),** doi:10.1029/2005GB002527.

Ministry of Public Infrastructure Renewal (2006) Places to Grow: Growth Plan for the Greater Golden Horseshoe, Ontario Provincial Government

Montzka SA, Butler JH, Elkins JW, Thompson TM, Clarke AD, Lock LT (1999) Present and Future Trends in the Atmospheric Burden of Ozone – Depleting Halogens. *Nature* **398:** 690-694

Murray M (2008) Evaluating the isotopic fingerprint of wastewater treatment plant nitrogen and its evolution in the Grand River. *Honours BSc Thesis*, University of Waterloo, Waterloo, Ontario Canada

Naqvi SWA, Yoshinari T, Jayakumar DA, Altabet MA, Narvekar PV, Devol AH, Brandes JA, Codispoti LA. (1998) Budgetary and biogeochemical implications of N_2O isotope signatures in the Arabian Sea. *Nature* **394**: 462-465

Nevison C, Lueker T, Weiss RF (2004) Quantifying the nitrous oxide source from coastal upwelling. *Global Biogeochemical Cycles* **18**: GB1018, doi:10.1029/2003GB002110

NPRI (2007). National Pollutant Release Inventory, Environment Canada http://www.ec.gc.ca/pdb/npri/npri_home_e.cfm. [Accessed May 22, 2008]

Ostrom, N. E., M. E. Russ, B. N. Popp, T. M. Rust, and D. M. Karl, Mechanisms of N2O production in the subtropical North Pacific based on determinations of the isotopic abundances of N2O and O2, Chemosphere Global Change Sci., 2, 281– 290, 2000

Pérez T, Trumbore SE, Tyler SC, Davidson EA, Keller M, de Camargo PB (2000) Isotopic variability of N_2O emissions from tropical forest soils. *Global Biogeochemical Cycles*, **14,** 525-535.

Pérez T, Trumbore SE, Tyler SC, Matson PA, Ortiz-Monasterio I, Rahn T, Griffith DWT (2001) Identifying the agricultural imprint on the global N_2O budget using stable isotopes. *Journal of Geophysical Research* **106**(D9):9869-9878

Pérez T, Garcia-Montiel D, Trumbore S, Tyler S, De Camargo P, Moreira M, Piccolo M, Cerri C (2006) Nitrous oxide nitrification and denitrification ^{15}N enrichment factors from Amazon forest soils. *Ecological applications*, **16,** 2153-2167.

Popp BN, Westley MB, Toyoda S, Miwa T, Dore JE, Yoshida N, Rust TM, Sansone FJ, Russ ME, Ostrom NE, Ostrom PH. (2002) Nitrogen and oxygen isotopomeric constraints on the origins and sea-to-air flux of N_2O in the oligotrophic subtropical North Pacific gyre. *Global Biogeochemical Cycles* **16**(4): 1064. doi:10.1029/2001GB001806

Prinn, R.G., R.F. Weiss, P.J. Fraser, P.G. Simmonds, D.M. Cunnold, F.N. Alyea, S. O'Doherty, P. Salameh, B.R. Miller, J. Huang, R.H.J. Wang, D.E. Hartley, C. Harth, L.P. Steele, G. Sturrock, P.M. Midgely, and A. McCulloch. (2000) A history of chemically and radiatively important gases in air deduced from ALE/GAGE/AGAGE. *Journal of Geophysical Research* **105**: 17751-17792

Prinn, R.G., D.M. Cunnold, R. Rasmussen, P.G. Simmonds, F.N. Alyea, A. Crawford, P.J. Fraser, and R. Rosen, (1990) Atmospheric emissions and trends of nitrous oxide deduced from ten years of ALE-GAGE data, *Journal of Geophysical Research* **95:** 18369-18385

Rahn T, Wahlen M (2000) A reassessment of the global isotopic budget of atmospheric nitrous oxide. *Global Biogeochemical Cycles* **14**(2): 537-543

Robertson WD, Schiff SL. (2008) Persistent elevated nitrate in a riparian zone aquifer. *Journal of Environmental Quality* **37**:669-679 doi:10.2134/jeq2007.0102

Rock L, Ellert BH, Mayer B, Norman AL (2007) Isotopic composition of trophospheric and soil N_2O from successive depths of agricultural plots with contrasting crops and nitrogen amendments. *Journal of Geophysical Research* **112**, D18303, doi:10.1029/2006JD008330

Rosamond MR (2008) Nitrogen cycling in Canadian rivers: Temporal and spatial variability in N2O fluxes, production, and isotopic enrichment factors. Ph.D. Thesis, University of Waterloo (In-Progress).

Sander, R. (1999) *Compilation of Henry's Law Constants for Inorganic and Organic Species of Potential Importance in Environmental Chemistry,* Air Chemistry Department, Max-Planck Institute of Chemistry, Germany. http://www.mpch-mainz.mpg.de/~sander/res/henry.html [Accessed May 22, 2008].

Sansone FJ, Popp BN, Rust TM. (1997) Stable carbon isotopic analysis of low-level methane in water and gas. *Analytical Chemistry* **69**: 40.

Schumidt HL, Voerkelius S (1989) *Origin and isotope effects of oxygen in compounds of the nitrogen cycle*. Proceedings of the 5th Working Meeting on Isotopes in Nature, Leipzich, pp. 613-624.

Sebilo M, Billen G, Mayer B, Billiou D, Grably M, Garnier J, Mariotti A (2006) Assessing nitrification and denitrification in the Seine River and Estuary using chemical and isotopic techniques. *Ecosystems* **9**:564-577

Shearer GB, Kohl D (1986) N_2-fixation in field settings: estimations based on natural ^{15}N abundance. *Australian Journal of Plant Physiology*, **13,** 699-756.

Smith RL, Howes BL, Duff JH (1991) Denitrification in nitrate-contaminated groundwater: Occurrence in steep vertical geochemical gradients. *Geochimica et Cosmochimica Acta*, **55,** 1815-1825.

Spoelstra J, Schiff SL, Jeffries DS, Semkin RG (2004) Effect of storage on the isotopic composition of nitrate in bulk precipitation. *Environmental Science Technology* **38**:4723-4727

Spoelstra, J., Murray, M. and Elgood, R.J. (2006) A simplified diffusion method for $\delta^{15}N$ analysis of NH_4^+. Environmental Geochemistry Lab Technical Procedure 20. Department of Earth and Environmental Sciences, University of Waterloo. 10 pp.

Sprent, J.I. (1987). The ecology of the nitrogen cycle. Cambridge University Press, New York

Stein LY, Yung YL (2003) Production, Isotopic Composition, and Atmospheric Fate of Biologically Produced Nitrous Oxide. *Annual Reviews of Earth and Planetary Science* **31**:329-356

Sutka RL, Ostrom NE, Ostrom PH, Gandhi H, Breznak JA (2003) Nitrogen isotopomer site preference of N_2O produced by *Nitrosomonas europaea* and *Methylococcus capsulatus* Bath. *Rapid Communications in Mass Spectrometry*, **17,** 738-745.

Sutka RL, Ostrom NE, Ostrom PH, Gandhi H, Breznak JA (2004) Erratum: Nitrogen isotopomer site preference of N_2O produced by Nitrosomonas europaea and Methylococcus capsulatus Bath. *Rapid Communications in Mass spectrometry*, **18,** 1411-1412.

Sutka RL, Ostrom NE, Ostrom PH, Breznak JA, Gandhi H, Pitt AJ, Li F (2006) Distinguishing nitrous oxide production from nitrification and denitrification on the basis of isotopomer abundances. *Applied and Environmental Microbiology*, **72,** 638-644.

Thornber CS, DiMilla PD, Nixon SW, McKinney RA (2008) Natural and anthropogenic nitrogen uptake by bloom-forming macroalgae. *Marine Pollution Bulletin* **56**:261-269

Tilsner J, Wrage N, Lauf J, Gebauer G (2003) Emissions of gaseous nitrogen oxides from an extensively managed grassland in NE Bavaria, Germany. II. Stable isotope natural abundance of N_2O. *Biogeochemistry*, **63,** 249-267.

Tsunogai U, Tadasuke K, Hirota A, Ohkubo SB, Komatsu DD, Nakagawa F (2008) Sensitive determinations of stable nitrogen isotopic composition of organic nitrogen though chemical conversion into N_2O *Rapid Communications in Mass Spectrometry* **22**:345-354

Tsunogai U, Yoshida N, Ishibashi J, Gamo T (2000) Carbon isotopic distribution of methane in deep-sea hydrothermal plume, Myojin Knoll Caldera, Izu-Bonin arc: Implications for microbial methane oxidation in the oceans and applications to heat flux estimation

Toyoda, S, Yoshida, N (1999) Determination of nitrogen isotopomers of nitrous oxide on a modified isotope ratio mass spectrometer. *Analytical Chemistry* **71**:4711-4718

Toyoda S, Mutobe H, Yamagishi H, Yoshida N, Tanji Y (2005) Fractionation of N_2O isotopomers during production by denitrifier. *Soil Biology & Biochemistry*, **37,** 1535-1545.

Van Groenigen JW, Zwart KB, Harris D, van Kessel C (2005) Vertical gradients of $\delta^{15}N$ and $\delta^{18}O$ in soil atmospheric N_2O – temporal dynamics in a sandy soil. *Rapid Communications in Mass Spectrometry* **19**: 1289-1295

Venkiteswaran JJ, Wassenaar LI, Schiff SL, (2007) Dynamics of dissolved oxygen isotopic ratios: a transient model to quantify primary production, community respiration, and air-water exchange in aquatic ecosystems. *Oecologia* **153**:385-398

Venter JC, Remington K, Heidelberg JF, Halpern AL, Rusch D, Eisen JA, Wu D, Paulsen I, Nelson KE, Nelson W, Fouts DE, Levy S, Knap AH, Lomas MW, Nealson K, White O, Peterson J, Hoffman J, Parsons R, Baden-Tillson H, Pfannkoch C, Rogers Y, Smith H (2004) Environmental genome shotgun sequencing of the Sargasso Sea. *Science* **304**: 66-74

Vieten B, Blunier T, Neftel A, Alewell C, Conen F (2007) Fractionation factors for stable isotopes of N and O during N_2O reduction in soil depend on reaction rate constant. *Rapid Communications in Mass Spectrometry*, **21,** 846-850.

Wada E, Yoshida N, Yoshioka T, Yoh M, Kabaya Y (1991) ^{15}N abundance of N_2O in aquatic ecosystems with emphasis on denitrification. In: *Cycling of Reduced Gases in the Hydrosphere* (eds Adams DD, Seitzinger SP, Crill PM), pp. 115-124. E. Schweizerbart'sche Verlagsbuchhandlung, Stuttgart, Germany.

Wada E. Ueda S. (1996) Carbon, nitrogen and oxygen isotope ratios of CH_4 and N_2O on soil ecosystems. In *Mass Spectrometry of Soils*, Boutton, T.W., Yamasaki, S. (eds.). Marcel Dekker, Inc.: New York, 1996; 177-204

Wahlen M, Yoshinari T. (1985a) Oxygen isotope ratios in N_2O from different environments. *Nature* **313**: 780.

Wahlen M, Yoshinari T. (1985b) Oxygen isotope ratios in N_2O from nitrification at a wastewater treatment facility. *Nature* **317**:349 – 350

Well R, Flessa H, Jaradat F, Toyoda S, Yoshida N (2005) Measurement of isotopomers signatures of N_2O in groundwater. *Journal of Geophysical Research* **110**: G02006, doi:10.1029/2005JG000044

Werner R, Brand WA. (2001) Referencing strategies and techniques in stable isotope ratio analysis. *Rapid Communications in Mass Spectrometry* **15**:501-519

Westley, M. B., H. Yamagishi, B. N. Popp, and N. Yoshida (2006),Nitrous oxide cycling in the Black Sea inferred from stable isotope and isotopomer distributions, Deep Sea Res., Part, 53, 1802, doi:10.1016/j.dsr2.2006.03.012

Yamulki S, Toyoda S, Yoshida N, Veldkamp E, Grant B, Bol R (2001) Diurnal fluxes and the isotopomers ratios of N_2O in a temperate grassland following urine amendment. *Rapid Communications in Mass Spectrometry* **15**:1263-1269

Yoshida N (1984) *Nitrogen isotope studies on the geochemical cycle of nitrous oxide*. Thesis, Tokyo Institute of Technology, Tokyo, 184 pp.

Yoshida N (1988) ^{15}N-depleted N_2O as a product of nitrification. *Nature*, **335,** 528-529.

Yoshinari T, Altabet MA, Naqvi SWA, Codispoti L, Jayakumar A, Kuhland M, Devol A. (1997) Nitrogen and oxygen isotopic composition of N_2O from suboxic waters of the eastern tropical North Pacific and the Arabian Sea – measurement by continuous flow isotope ratio monitoring. *Marine Chemistry* **56**: 253.

Zafiriou OC. (1990) Laughing Gas From Leaky Pipes. *Nature* **347:** 15.